



Universitetet
i Stavanger

FACULTY OF SCIENCE AND TECHNOLOGY

MASTER'S THESIS

Study programme/specialisation: MSc in Petroleum Engineering / Drilling	Spring semester, 2017 Open
Author: Eirik Aas Lind
Supervisor: Kjell Kåre Fjelde	
Title of master's thesis: Simulation and Modelling of Injectivity during Pressurized Mud Cap Drilling with the AUSMV Numerical Scheme	
Credits: 30	
Keywords: Pressurized Mud Cap Drilling (PMCD) Injection Bullheading AUSMV simulation	Number of pages: 79 + supplemental material/other: 21 Stavanger, 15.06.2017

Acknowledgement

I would like to thank my supervisor Kjell Kåre Fjelde for all the time, guidance and the positive mindset, which made working on this thesis a very exciting and enjoyable experience.

I would also like to thank my aunt, Synnøve Lind Rygh for giving good advice and for taking her time to help me.

And at last I would like to thank my family for all their support during my work on this thesis, and through these 5 years of study.

Stavanger, June 2017

Eirik Aas Lind

Abstract

Operation and drilling in highly fractured carbonate formations are associated with several challenges. Some of the main challenges include large/total losses of drilling fluids, loss of hydrostatic pressure and gas influxes. One of the modern drilling technologies that provides a solution, is Pressurized Mud Cap Drilling (PMCD). The main principle of PMCD is to drill with a cheap sacrificial fluid that is forced into the fractured formation along with all cuttings. Nothing is circulated back to surface. The annulus is filled with a fluid designed to cause underbalanced pressure, which encourages influx of gas. When the pressure at the surface rises to a certain level due to gas migration, bullheading is used to force the kick back down into the formation.

To help get a greater understanding of the pressure development before and during PMCD bullheading, computing software is used to model and simulate such complex flow scenarios. In the past, work has been done to implement a PMCD bullheading operation into a numerical scheme, which allowed for simulation and analysis. The model used is a transient model, which uses the numerical procedure of the AUSMV scheme to solve conservation equations from the drift flux model. MatLab computing software is used to perform the calculations, and the model is written in matlab programming language. The goal of this thesis is to continue building on the previous model, and increase the realism of the simulations.

The previous version of the PMCD bullheading code, had shortcomings with regards to injectivity. Pressure development through time did not account for formation injectivity, and bottomhole injection pressure was fixed to an assumed value. During bullheading, all fluids were assumed to be injected without any resistivity from the formation. Also, during gas migration in the shut-in well, the model did not allow any fluids to flow back into the formation as the pressure increased in the bottom. In this thesis, the Injectivity Index model is implemented into the model to solve these two problems.

The injectivity model was simulated and tested with two different methods of implementation, through the boundary cell fluxes, and through the source term of the partial differential equations. Tests were also done to see effects from different degree of injectivity. Compared to the original pressure plots, the new results showed a much more realistic pressure development, both during bullheading and during gas

migration in shut-in well. The results also showed that the pressure development in the well is highly dependent on the injectivity of the formation. For simulation with injection through the bottom cell, the difference between the boundary cell flux method, and the source term method were insignificant. However, the source term method has an advantage, since it allows us to place the injection zone in any cell through the well. One problem was encountered though, for a high number of cells in the discretization, the pressure started to oscillate during the first half of the bullheading procedure, even though the timestep was adjusted. This was not solved, and needs further investigation.

The Production Index (PI) model was also used in an experimental test, where the goal was to see if the gas kick could be taken through the model. Previously the kick was forced into the bottom of the well by a fixed rate. The results showed that a much smaller amount of gas was taken into the well. It is much harder to control how much gas that is taken, since it not only depends on the PI-value but also the pressure difference between the reservoir and the well, which varies through time.

Some additional research was done to boundary treatment of slope limiters and pressure calculation. The original model came with two ways of doing the boundary cell calculation of slope limiters, one that extrapolated the values from the closest neighbor cell and one that fixed them to zero. The results showed minimal difference between the two slope limiter methods. Similar for pressure calculation in the boundary cells, there was two ways of doing it, one that extrapolated from the closest neighbor cell and one that calculated the pressure based on physical values. For the bottomhole pressure the results were very similar, but some difference was seen in the surface pressure.

Table of Contents

Acknowledgement	iii
Abstract	v
Table of Contents	vii
Table of Figures	x
List of Tables	xii
1. Introduction	1
2. Bullheading	3
2.1 Introduction to Bullheading	3
2.2 Bullheading during Well Control	4
2.3 Bullheading during Production or Intervention	5
2.4 Disadvantages of Bullheading	5
3. Managed Pressure Drilling and Pressurized Mud Cap Drilling	6
3.1 Managed Pressure Drilling	6
3.1.1 <i>Conventional Drilling</i>	6
3.1.2 <i>Underbalanced Drilling</i>	6
3.1.3 <i>Managed Pressure Drilling</i>	7
3.1.4 <i>Variations of the MPD technology</i>	9
3.2 Pressurized Mud Cap Drilling	10
3.2.1 <i>Mud Cap Drilling</i>	10
3.2.2 <i>Principle of PMCD</i>	11
3.2.3 <i>PMCD Fluids</i>	12
3.2.4 <i>PMCD Preparation and Operation</i>	14
3.2.5 <i>Advantages, Disadvantages and Challenges of PMCD</i>	14
3.2.6 <i>Carbonate Drilling with Pressurized Mud Cap Drilling</i>	16
3.3 PMCD Field Cases and Other PMCD Studies.	17
3.3.1 <i>East Malaysia PMCD [26]</i>	17
3.3.2 <i>Combining PMCD and Early Kick Detection Techniques for Fractured Formations Overlying a High Pressure Reservoir in Offshore Kalimantan [6]</i>	18
3.3.3 <i>Prediction Model for Gas Migration in Well During PMCD Operation[5]</i>	19

4. The Transient Flow Model.....	21
4.1 The Two-Phase Model.....	21
4.2 Closure Laws	22
4.3 The AUSMV Scheme	24
4.4 Boundary Conditions	28
4.5 Slope Limiters.....	30
5. Injectivity Modelling	31
5.1 Water Injection Wells	32
5.1.1 Pore Plugging.....	33
5.1.2 Temperature Effects.....	34
5.2 Production Index.....	34
5.3 Assumptions for Highly Fractured Injection	37
6. Implementation and Simulation of Injectivity Model in MATLAB	38
6.1 Matlab Code Configuration	39
6.2 Case 1 - Injection Model During Bullheading in Boundary Conditions	41
6.2.1 Case 1 - Implementation and Preparation	41
6.2.2 Case 1 - Simulation Results	44
6.3 Case 2 – Flowback to Reservoir During Kick Rise in Boundary Conditions .	47
6.3.1 Case 2 - Implementation and Preparation	47
6.3.2 Case 2 - Simulation Results	48
6.4 Case 3 – Injection Model During Bullheading in Source Term.	51
6.4.1 Case 3 - Implementation and Preparation	51
6.4.2 Case 3 - Simulation Results	53
6.5 Case 4 – Flowback to Reservoir During Kick Rise in Source Term.	55
6.5.1 Case 4 - Implementation and Preparation	55
6.5.2 Case 4 - Simulation Results	55
6.6 Case 5 –Taking the Kick with The Injectivity Model.	58
6.6.1 Case 5 - Implementation and Preparation	58
6.6.2 Case 5 - Simulation Results	59
6.7 Case 6 – Effect of Different Boundary Conditions for Slope Limiters	62
6.7.1 Case 6 - Implementation and Preparation	62
6.7.2 Case 6 - Simulation Results	64

6.8 Case 7 – Effect of Different Boundary Conditions for Inlet Pressure	66
6.8.1 Case 7 - Implementation and Preparation	66
6.8.2 Case 7 - Simulation Results	66
7. Observations, Conclusions and Future Work.....	68
7.1 Observations	68
7.2 Conclusions.....	73
7.3 The Main Findings.....	75
7.4 Future Work.....	Feil! Bokmerke er ikke definert.
8. References.....	77
9. Appendix.....	80

Table of Figures

Figure 1 - Circulation Method and Bullheading Method [2].....	3
Figure 2 - Bullheading to Kill Gas Production Well [1]	5
Figure 3 - Drilling Window for MPD, UBD and Conventional Drilling[14].....	7
Figure 4 - Conventional Drilling vs MPD, well depth pressure profiles [17]	8
Figure 5 - MPD Variables and Methods [3]	9
Figure 6 - Mud Cap Drilling Illustration [4].....	11
Figure 7 - Pressurized Mud Cap Drilling Illustration [4]	12
Figure 8 - Rotating Control Device Body, Latch and Bearing Assembly [6]	13
Figure 9 - Highly Fractured Carbonate Formations [Photograph by K.K. Fjelde, Billefjorden, Svalbard]	16
Figure 10 - Flow Diagram of a Combined PMCD and EKD Setup [6]	19
Figure 11 - Illustration of the Well Discretization with the Virtual Cell [5].....	19
Figure 12 - Update of discretized variables [29]	27
Figure 13 - Slope Limiter Concept [8]	30
Figure 14 - Water/CO ₂ Injection Well Example[31]	32
Figure 15 - Injection Rate and Pressure vs Time [32].....	33
Figure 16 - Decline in productivity index at higher flow rates [8].....	36
Figure 17- Bottom Hole Pressure vs Time for Original Model.....	41
Figure 18 - Bottom Hole Pressure vs Time for Case 1	44
Figure 19 - Surface Pressure vs Time for Case 1	45
Figure 20 - Bottom Hole Pressure vs Time for Different Injectivities for Case 1.....	45
Figure 21 - Surface Pressure vs Time for Different Injectivities for Case 1	46
Figure 22 - Gas Volume Fraction vs Depth for Case 1	46
Figure 23 - Surface Pressure vs Time for Case 2	48
Figure 24 - Bottom Hole Pressure vs Time for Case 2.....	48
Figure 25 - Bottom Hole Pressure vs Time for Different Injectivities for Case 2.....	49
Figure 26 - Surface Pressure vs Time for Different Injectivities for Case 2	49
Figure 27 - Liquid Velocity vs Depth for Case 2	50
Figure 28 - Gas Volume Fraction vs Depth.....	50
Figure 29 - Physical Difference Between Source Term and Boundary Flux Injection in Bottom Cell.....	51
Figure 30- Bottom Hole Pressure vs Time for Case 3.....	53

Figure 31 - Surface Pressure vs Time for Case 3	53
Figure 32 - Bottom Hole Pressure vs Time for Case 3.....	54
Figure 33 - Surface Pressure vs Time for Case 3	54
Figure 34 - Bottom Hole Pressure vs Time for Case 4.....	56
Figure 35 - Surface Pressure vs Time for Case 4	56
Figure 36 - Bottom Hole Pressure vs Time for Different Injectivities for Case 4.....	57
Figure 37 - Surface Pressure vs Time for Different Injectivities for Case 4	57
Figure 38 - Gas Mass vs Time for Case 5	59
Figure 39 - Bottom Hole Pressure vs Time for Case 5.....	60
Figure 40 - Gas Volume vs Time for Case 5	60
Figure 41 - Surface Pressure vs Time for Case 5	61
Figure 42 – Bottom Hole Pressure vs Time for Case 6	64
Figure 43 – Bottom Hole Pressure vs Time for Case 6	64
Figure 44 – Bottom Hole Pressure vs Time for Case 6	65
Figure 45 – Bottom Hole Pressure vs Time for Case 6	65
Figure 46 – Surface Pressure vs Time for case 7.....	67
Figure 47 – Bottom Hole Pressure vs Time for Case 7	67

List of Tables

Table 1 - Fluid Data [22]	14
Table 2 - Well Geometry Data.....	39
Table 3 - Fluid Data.....	39
Table 4 - Well Discretization.....	39
Table 5- Inlet Fluid Rates	40
Table 6 - Time vs Well Conditions.....	40
Table 7 - Values Used to Estimate Injectivity Index in Case 1	42
Table 8 - Injection Index Interpolation.....	43
Table 9 - Different Values of Injectivity Used in Simulation	44
Table 10 - Values Used to Estimate Injectivity Index in Case 3	51
Table 11 - Values Used to Estimate Injectivity Index in Case 4.....	55
Table 12 - Values Used to Estimate Production Index in Case 5.....	58
Table 13 - Slope Limiter Condition vs Number of Boxes and Timestep.....	63

1. Introduction

The world's demand for energy and the goal of becoming more cost-efficient pushes the petroleum industry into development of new and better technologies. When it comes to drilling, recent technology within the concept of Managed Pressure Drilling (MPD) becomes increasingly more relevant. Being able to successfully carry out drilling operations in highly fractured carbonate reservoirs is a major challenge, and one of the MPD technologies that has proven itself effective to accomplish this, is Pressurized Mud Cap Drilling (PMCD)[7]. Carbonate reservoirs contain over half of the world's discovered hydrocarbon reserves, and these formations are associated with many challenges for the drillers. Some of the challenges can for instance be problems with drill-fluid losses, gas migration and damage to the reservoirs. The PMCD technology allows such formations to be drilled in a safe and cost-efficient manner.

To help get a greater understanding of complex flow scenarios and to plan drilling operations, computing software is used to model and simulate. Work has previously been done to implement the physics of bullheading in a PMCD operation, into a model, so that different operation scenarios can be simulated[8, 9]. The model used is a combination of the drift flux model and a numerical scheme called the AUSMV-scheme[10], and MatLab programming software is used to execute the calculations of the model.

The main objective of this thesis is to increase the accuracy of the PMCD bullheading simulations done with the AUSMV model, by improving the downhole boundary condition treatment. This will be done by adding an injection model. A survey will be done to find such a model, implement it into the code and test it. The current state of the model does not consider how different degree of injectivity in the formation affects the pressure in the well. With PMCD, a gas influx, commonly referred to as a kick, is not circulated out of the system, but instead bullheaded back down into the formation. We will also consider how to include injectivity of liquid during the closed-in period where the gas migrates and pressure increases. This was done in [5], using another numerical way of doing it. Because kick scenarios come with a degree of risk to safety, understanding how the kick affects the pressure in the system is important.

Some work will also be done to see how different boundary treatment of variables in the system affects the simulation results. There are two different boundary treatments

of slope limiters that will be tested, one where boundary values are set to 0 and one where they are interpolated from closest neighbor cell. The boundary calculation of pressure also has two different methods that will be tested, one where the pressure is calculated from physical properties of the fluids and the well, and one where the pressure is extrapolated.

The structure of the work in this thesis is as follows:

- First a theoretical introduction to bullheading, Managed Pressure Drilling and Pressurized Mud Cap Drilling.
- The transient model is presented, which includes an explanation of the drift flux model and the AUSMV scheme.
- Theory related to injection is discussed. Also, the injectivity index model is presented. Assumptions for use of the injectivity index in the transient model is made.
- Implementation of the Injectivity Index model is done in the boundary conditions of the code, for bullheading and shut-in well gas migration. The simulation results are also presented. (Case 1 and 2)
- Implementation of the Injectivity Index model in the source term is done, for both the bullheading phase and the shut-in well gas migration phase. Simulation results is presented. (Case 3 and 4)
- The Productivity Index model is implemented into the source term, with the goal of taking the kick through the model and simulation results is presented. (Case 5)
- Simulation is done for the two different boundary treatments of slope limiters. (Case 6)
- The two different boundary pressure calculation methods are implemented and simulated for. (Case 7)
- All results are discussed and conclusions is made.
- Suggestions for future work.

2. Bullheading

2.1 Introduction to Bullheading

When conventional methods of handling well control problems no longer are possible, bullheading is an alternative technique. Bullheading is an operation where liquids are pumped into the well without circulating back to surface. Circulation down the well can be done through annulus, the drillpipe or through both simultaneously. The goal is most commonly to force undesired and hazardous influx fluids back into the formation. Bullheading is used in several different scenarios, such as an option during well control, during production/intervention or during managed pressure drilling, which will be covered more deeply in the next chapter. [2, 8]

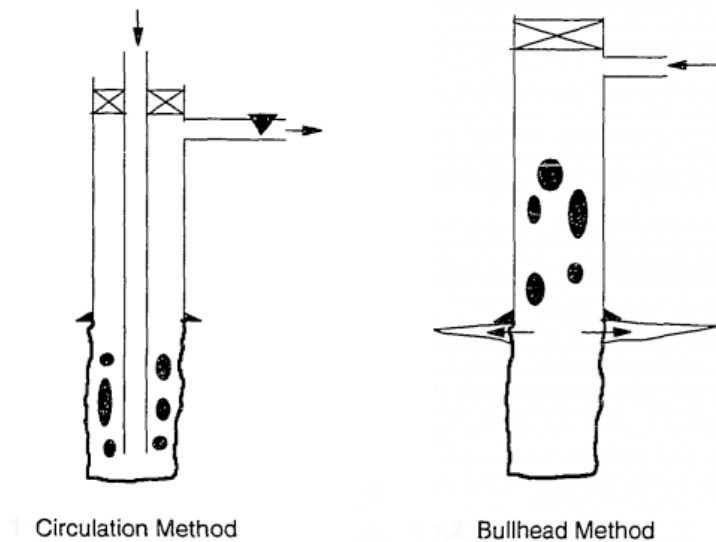


Figure 1 - Circulation Method and Bullheading Method [2]

When choosing to use the bullheading method, several factors must be considered as they directly affect the chances of the operation being successful [11]:

- Reservoir permeability – The permeability of the reservoir affects the time it takes to pump fluids into it. In some scenarios, the formation must be fractured to successfully inject the fluids. It also impacts the pressure in the well.
- Surface equipment – The pressure tolerance of the equipment is a safety concern, and must be able to withstand the highest possible pressure

encountered during the bullheading. This equipment includes BOP, wellhead, casing, etc.

- Influx fluid - It is easier to inject a gas back into the formation, than a liquid (such as oil or water). The viscosity of the fluid is also an important parameter, as high viscosity fluids is harder to inject[12].

2.2 Bullheading during Well Control

If the hydrostatic pressure acting on the bottom hole in the well becomes lower than the formation pressure, a fluid influx will occur. This is called a kick. The difference in density between the drilling fluid and the formation fluid will cause the kick to migrate through the well, to the surface. Once a kick has occurred, several well control methods can be used to regain control of the well, depending on the situation. Well control has the purpose of accomplishing the following[2]:

1. Regain well control.
2. Prevent further fluid influx.
3. Remove the kick from the well.
4. Increase drill fluid hydrostatic pressure.

The two most common ways of handling a kick is by using:

1. The Driller's Method
2. Wait and Weight method

Both mentioned methods above rely on being able to circulate up through annulus. There are situations during drilling where either of the two methods are not applicable, such as [2]:

- Plugged bit or drillstring prevents conventional circulation up annulus.
- Hazardous influx fluids, such as hydrogen sulfide.
- Rig not capable of handle the high volume of influx fluid at the surface.
- Excessive pressures at the surface or the casing shoe which poses a risk of blowout.

Before a well control bullheading procedure can be carried out, the surface pressure limitation of the surface equipment must be determined, the pressure which will fracture the formation must be calculated and a bullheading pressure chart must be made, showing the number of strokes pumped vs. pumping pressure.

The first that is done when the bullheading procedure starts, is to bring the pump to a low speed to overcome the surface pressure. Then the pump rate is increased gradually to target pump rate, while carefully monitoring the well pressure. It is important to not exceed equipment pressure safety limits [11, 12].

2.3 Bullheading during Production or Intervention

If it's not possible to do well intervention in a live well by using conventional methods, such as wireline and coiled tubing, the well must be killed. The production well is then full of hydrocarbons which must be forced back down into the formation. Bullheading can be used to do this. When this is done, seawater is used first, before it is replaced with kill pill and a heavy kill fluid. The kill pill is there to block the pores of the formation so that minimal amounts of brine contaminates the reservoir. The tubing must be filled with a kill fluid of density high enough to create sufficient hydrostatic pressure to keep the hydrocarbons out[1]. Figure below shows bullheading of a gas production well:

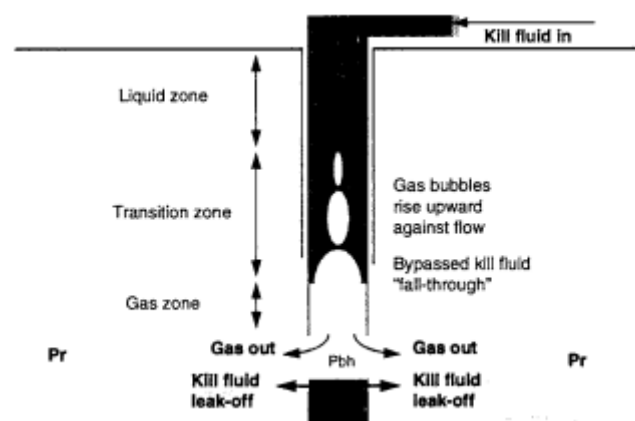


Figure 2 - Bullheading to Kill Gas Production Well [1]

2.4 Disadvantages of Bullheading

Because bullheading challenges the safety of the casings and the wellhead, misapplication of the technique may result in worsening the problem. Many wells have been lost by inappropriate selection of bullheading kill fluids [13]. It is important to note that when bullheading, the kill fluid will always exit at the weakest point in the well which might not be the source of the kick [12]. This can be a disadvantage as it poses a risk of fracturing formation along the open hole section of the well, and causing an underground blowout. Another disadvantage is possible damage to surface equipment, as it must withstand the large pressures encountered through the operation.

3. Managed Pressure Drilling and Pressurized Mud Cap Drilling

3.1 Managed Pressure Drilling

This section will briefly go through the three major ways of performing a drilling operation, and the differences between them. The focus is to get a good understanding of what Managed Pressure Drilling is and what is separating it from the other common techniques as explained in paper[14].

3.1.1 Conventional Drilling

The oldest of the technologies is called conventional drilling and is most often done by using an overbalanced pressure. This is defined as a state where the pressure in the well is greater than the pore pressure in the formation. The bottomhole pressure is mostly controlled by the drilling mud density and by adjusting the flowrate. The well pressure state can then be described by the function[15]:

$$P_{BH} = P_{Hyd} + \Delta P_{friction} \quad (1)$$

Where P_{BH} is bottomhole pressure, P_{Hyd} is the hydrostatic pressure and $\Delta P_{friction}$ is the pressure created by the annular flow friction. Conventional drilling is done with an open system, which means the circulation loop is open to atmosphere pressure.

3.1.2 Underbalanced Drilling

Another way of performing a drilling operation is through Underbalanced Drilling (UBD). In an underbalanced operation, the hydrostatic fluid pressure is set to be low than the reservoir pressure, with the intention of causing influx of formation fluids and production while drilling.

$$P_{Res} > P_{Hyd} \quad (2)$$

Underbalanced drilling will enhance the reservoir productivity by causing less damage to the reservoir formation. A high overpressure may cause physical migration of in-situ fines and clays, and influx of solids present in the drilling mud into the formation matrix[16].

3.1.3 Managed Pressure Drilling

Drilling in harsh environments with higher probability for problems and non-productive time (NPT) has led to development of a new generation of drilling technology which makes these wells possible and economical to drill. Some of the problems MPD has been developed to handle is problems related to loss of circulation, stuck pipes, wellbore instability and well control incidents. This is often seen in wells where the margin between pore pressure and fracture gradient is very narrow. Instead of having an open circulation with atmospheric backpressure, a closed loop is created which allows the drillers to control the surface backpressure. This is controlled by taking the return fluid through a choke that can be adjusted. The International Associations of Drilling Contractors (IADC) have defined Managed Pressure Drillings as “*an adaptive drilling process used to more precisely control the annular pressure profile throughout the wellbore.*” Also defined are the objectives of MPD: “*to ascertain the downhole pressure environment limits and to manage the annular hydraulic pressure profile accordingly*”[15].

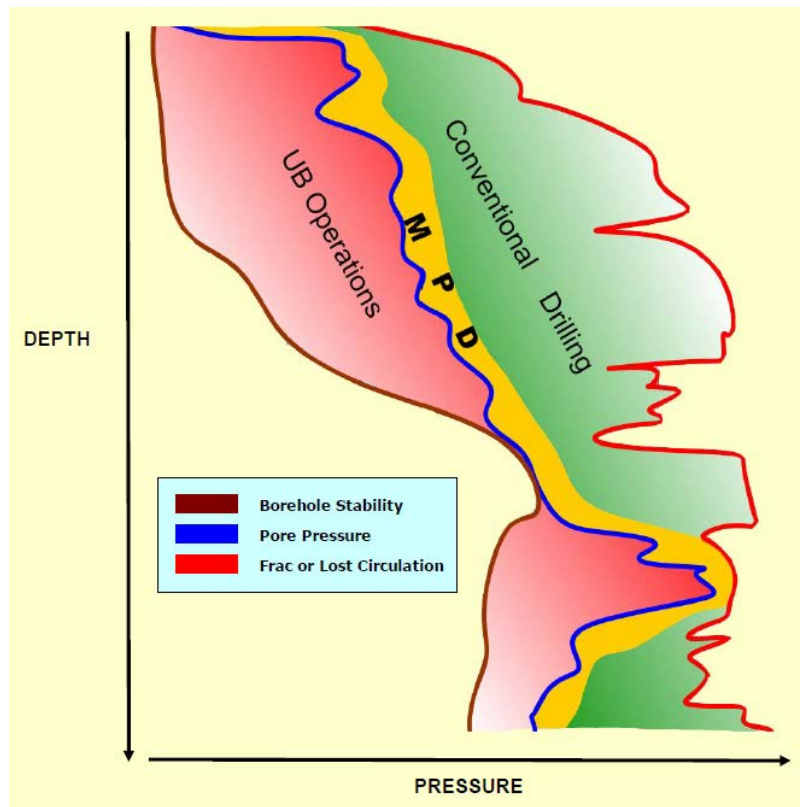


Figure 3 - Drilling Window for MPD, UBD and Conventional Drilling[14]

Figure 3 above shows the drilling pressure windows that is used by the different methods. The advantage of MPD is clearly illustrated in the challenging interval where fracture/lost circulation pressure is very close to pore pressure.

By adjusting the surface backpressure during circulation, it is possible to change the equivalent circulating density. Once target ECD is obtained the bottom-hole will stabilize at the desired pressure. This is done by continuously determining the downhole pressure of the well which is being drilled. A general MPD operation can be described by the formula[15]:

$$P_{BH} = P_{Hyd} + \Delta P_{friction} + Backpressure \quad (3)$$

The difference between conventional drilling and managed pressure drilling, with regards to pressure vs depth plot, is shown in figure X below:

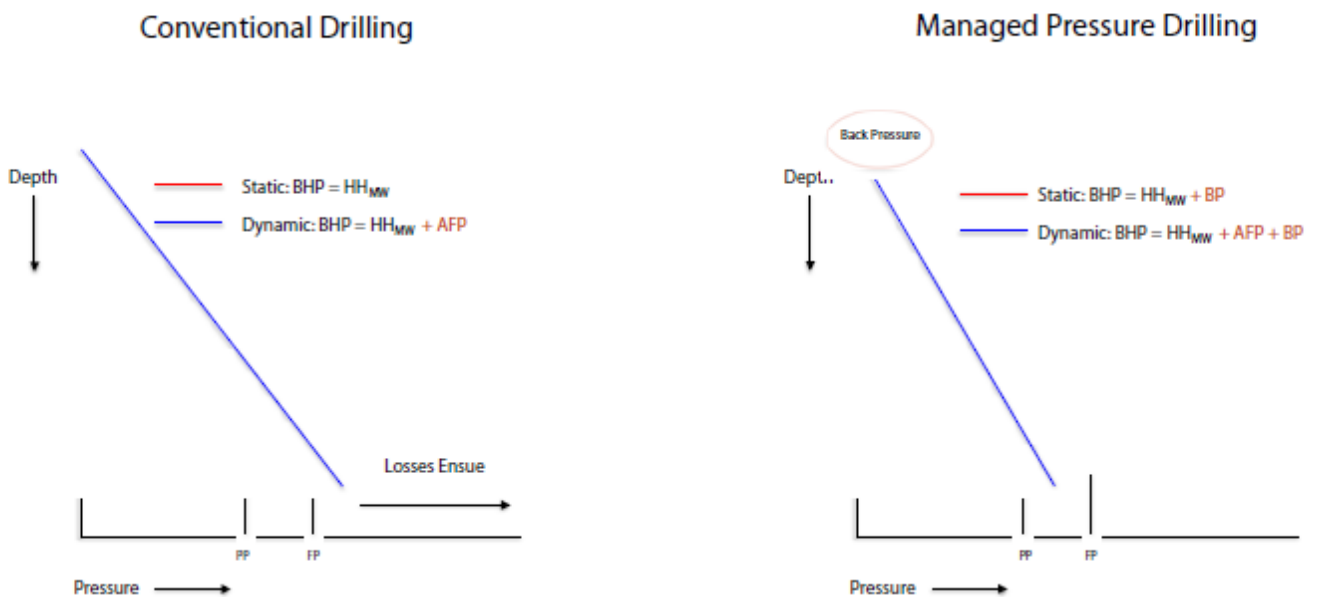


Figure 4 - Conventional Drilling vs MPD, well depth pressure profiles [17]

The surface backpressure can be manipulated as necessary to avoid reservoir influx, and to avoid loss of drilling fluid into the formation. This can also be used to avoid downhole pressure variations when the mud pumps are started. When the pumps start, the applied backpressure is reduced proportionally to the increase in friction circulation pressure in the annulus of the well. The same applies when the pumps are

stopped [17]. It is also possible to maintain the same pressure during circulation and connections using a backpressure pump to ensure circulation across the choke.

3.1.4 Variations of the MPD technology

MPD covers a wide range of different variations of the technology with different advantages and disadvantages. Some of the main variations include[15]

- Pressurized Mud Cap Drilling (PMCD)
- Constant Bottomhole Pressure (CBHP)
- Dual Gradient (DG)

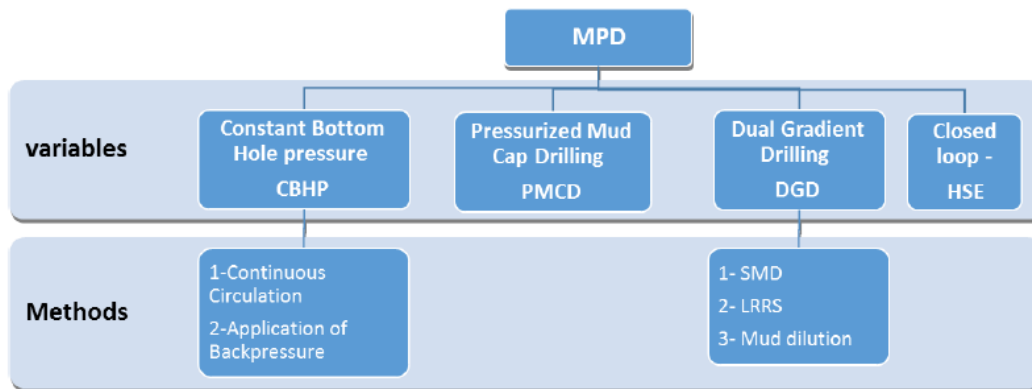


Figure 5 - MPD Variables and Methods [3]

Pressurized Mud Cap Drilling is important for this thesis and will be explained more in detail in the next subchapter. With Constant Bottomhole Pressure drilling the goal is keeping a constant pressure at the bottom of the well during drill pipe connections. In this system, a choke adds the backpressure, and during connections a backpressure pump circulates fluid across the choke to increase the choke pressure and compensate to the lost friction in the well when the main pumps are stopped.

3.2 Pressurized Mud Cap Drilling

Of the many variations of MPD technologies, Pressurized Mud Cap Drilling is important for this thesis. IADC has defined PMCD as a variation of MPD which involves “*drilling with no returns to surface where an annulus fluid column, assisted by surface pressure, is maintained above a formation that is capable of accepting fluid and cuttings.*” [6] The PMCD drilling technique has been developed to deal with challenging high-pressure and highly fractured formations, with sour reservoirs containing hazardous gases such as H₂S. Solving the challenge of handling drilling of high fractured formations is desired due to the high production potential of such formations. Some of the major problems when drilling highly fractured formations include loss of drilling fluids, safety related to kick situations and how to avoid causing unnecessary damage to relatively unstable formations [18]. PMCD is an extension of the Mud Cap Drilling (MCD) technique, which was taken into use to handle highly fractured reservoir with presence of sour gases[19]. With mud cap drilling, the fluid losses are accepted, but the nonproductive downtime is avoided.

3.2.1 Mud Cap Drilling

The main principle of MCD is to replace conventional drilling mud with a sacrificial fluid, which is pumped down the drillstring and into the formation. The annulus is filled with a mud cap fluid, which could be either seawater or viscous mud. This way all cuttings is carried by the sacrificial fluid into the formation and nothing returns to surface[19]. The figure below illustrates a MCD operation. When conventional drilling losses exceed 50% of circulation rate, MCD is usually taken into use[18]. To control the bottomhole pressure, pumping cap fluid down annulus might be necessary, and to balance the reservoir pressure, heavy weighted mud is used. When drilling then continues and the mud weight is increased again, even more losses will occur due to the increase in overpressure higher up in the well. This overbalance is one of the main disadvantages with floating mud cap drilling, as it will cause increasingly higher loss rates as the drilling continues. The cost of supplying such an operation with substantial amounts of heavy drilling fluids are enormous[6].

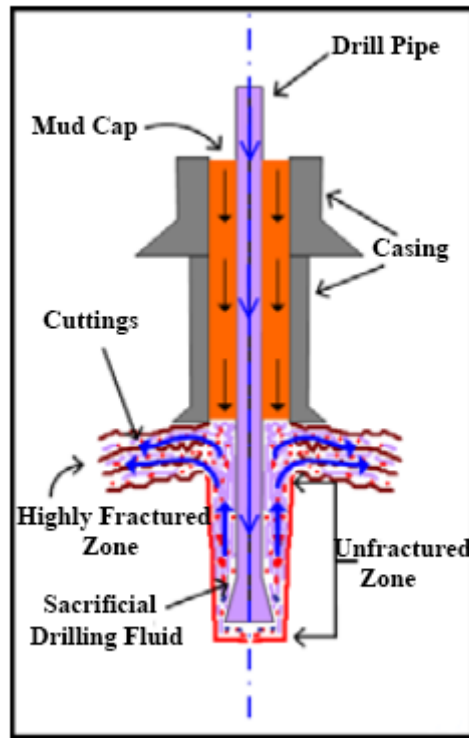


Figure 6 - Mud Cap Drilling Illustration [4]

3.2.2 Principle of PMCD

To deal with the problems related to Mud Cap Drilling, Pressurized Mud Cap Drilling was developed. One of the challenges for ordinary MCD was to simultaneously balance the pressure at several fractures with significant vertical distance. With PMCD it is possible to operate in thick fractured formations. The main principles of PMCD is similar to MCD, but with some differences.[20] The idea is to have a mud column in annulus, which is lighter than required to balance the formation pressure. Annulus is sealed on top with a Rotating Control Device (RCD). This creates an underpressure, and without circulation all formation fluids would be produced into the well. Another drilling fluid is pumped down the rotating drillstring and all cuttings is circulated into the fractured formation. The circulation from the drillstring into the formation makes it much harder for the kick to enter the well, as the gas is pushed back into the formation. The surface pressure in annulus is monitored and is used as an indicator of what is going on at the bottom of the well. When a gas kick eventually enters the well, the surface pressure rises as the gas migrates and replaces the fluids in the well. The pressure increases until a predetermined level, and the annulus fluid

is bullheaded down into the formation[20]. This cycle can be repeated several times. Figure 7 below illustrates the main principle of PMCD:

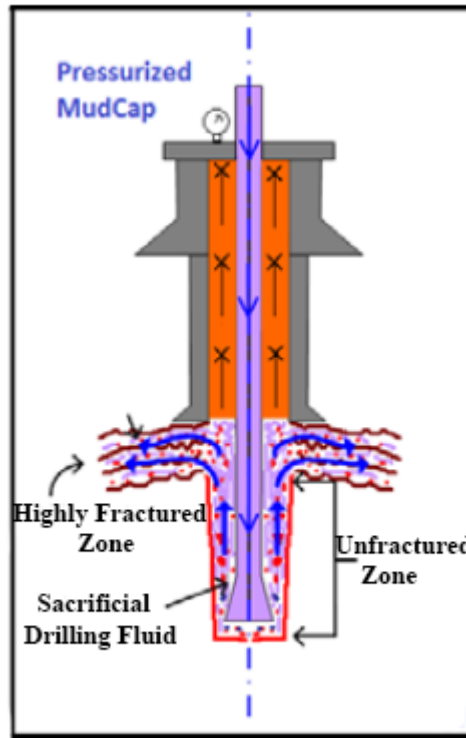


Figure 7 - Pressurized Mud Cap Drilling Illustration [4]

3.2.3 PMCD Fluids

Sacrificial fluid (SAC) is pumped down the drillstring, and circulated into the formation, bringing along all cuttings. As the name tells, a sacrificial fluid is not expected to be recovered, and thus makes access to large quantities of SAC necessary. That is why the SAC is mainly composed of freshwater [21]. Simultaneously a Light Annular Mud (LAM) is held in the annulus. The LAM is designed to create a hydrostatic fluid column with lower pressure than the formation pressure, thus creating an underbalanced situation[19]. This is the main difference between MCD and PMCD. By introducing a new piece of equipment, a Rotating Control Device (RCD), it is possible to create the necessary backpressure in the annular column by closing the well. This changes the flow loop from an open to atmosphere flow system, to a closed system. Gas that enters annulus will cause annular pressure to rise, and when it reaches a given level, the gas is bullheaded back down into the formation. LAM is used to bullhead, and thus causing some LAM to be lost into the formation.



Figure 8 - Rotating Control Device Body, Latch and Bearing Assembly [6]

Paper [18] has requirements for an ideal capmud:

- Non-damaging to formation matrix.
- No reactions with reservoir fluids that generates emulsions that damages or blocks the formation.
- High rheology in downhole to avoid mixing with reservoir fluid.
- Must be mixable in high volumes.
- Low cost.

A field case described in paper [22] gives an example of the cost difference between two LAM compositions. Three wells were drilled. One well (well G) was drilled using synthetic olefin-based mud (SBM), and the two others (well H and I) was drilled with a water based mud (WBM), a simplified formulation of polymeric aqueous fluid. Only well G and well H had a section drilled using PMCD. Well G was drilled 70m using PMCD, with a total loss of 778 bbl of SBM LAM. Well H was drilled 83m with PMCD and the total losses of WBM LAM was 2730 bbl. Conventional MPD was also used during the operation, with a 2416 bbl loss for well G and a 5275 bbl loss for well H. All data is given in table below:

	Well G	Well H
Length drilled with MPD (m)	89	134
LAM losses during MPD (bbl)	2416	5275
Length drilled with PMCD (m)	70	83
LAM losses during PMCD (bbl)	778	2730
Total LAM loss (bbl)	3194	8005
Total cost (mud treatment and fabrication)	\$900.000	\$180.000

Table 1 - Fluid Data [22]

The cost difference between the two LAMs is significant, especially considering the much larger volumes used of WBM. One reason for the larger use of WBM was due to the higher gas migration velocity in aqueous fluids, so a higher pump rate was necessary to bullhead the kick. Either way, compared for the cost of mud treatment and fabrication, the difference is huge. This is a reason why LAM mud must be designed properly, to avoid large unnecessary costs.

3.2.4 PMCD Preparation and Operation

Training, planning and preparation is important to successfully perform a PMCD operation. Paper [23] presents a three-level training program for PMCD operation, which helps to do a safe and efficient operation.

1. Level one training – Learning what PMCD is and the necessary equipment. Informing the workers that an unfamiliar operation is about to happen.
2. Level two training – Procedure specific training with instruction of all responsibilities. Also training in different scenarios and contingency actions that may be encountered.
3. Level three training – Inspection of all PMCD flow lines and valves, and review of the actions to be done when the first loss situation happens.

3.2.5 Advantages, Disadvantages and Challenges of PMCD

The main advantages and disadvantages are presented in [24], are already mentioned, but here is an overview.

Advantages[24]:

- Allows drilling through severe/total loss formation in a safe and efficient manner.

- Much lower cost compared to conventional drilling techniques, related to both fluids and non-productive time.
- Prevents damage to the reservoir from LCM, gunk and cement.
- No gas is circulated to surface, which makes H₂S encounters much safer.

Disadvantages[24]:

- No returns to surface, includes no cuttings from the formation. This means less samples and data for the geologists.
- PMCD requires substantial amounts of fluid, which can be a cost issue. This is why proper fluid design of LAM is important[22].

Because a PMCD operation is very different from conventional drilling techniques, it comes with several challenges. Operation planning, expertise, strategies, fluid selection and equipment, are all critical factors to a PMCD operation[23]. Reference [23] outlines some of the main PMCD challenges:

- Related to geology and geophysics, finding the top of carbonate formations is a challenge and estimating the reservoir pressure. Currently the best practices to estimate formation position is by using near bit Gamma Ray.
- Designing a LAM which is both easily made, effective and with relative low cost. This is a challenge when creating a LAM management plan. Fluid logistics is also something which must be considered, since switching between conventional drilling and PMCD will require different types of mud. A good Pit and Fluids Management plan is important.
- With regards to rig equipment, it can be a challenge to operate within the safe pressure limitations. Annular pressures can get high, and also certain LAM mud designs can result in high friction pressure when bullheading.

3.2.6 Carbonate Drilling with Pressurized Mud Cap Drilling

A key factor in a successful PMCD operation is the formations capability of taking the fluids and the cuttings. Because the majority of hydrocarbon reserves in the world is located in carbonate reservoirs, and many carbonate formations is highly fractured, carbonates are of interest when it comes to PMCD[23]. Conventional operation in fractured carbonates is often associated with significant or total fluid losses, and with huge risks of influx of formation gases into the wellbore[15]. Carbonates can either be weathered or naturally fractured, with flow paths large enough to freely pass drill mud and plugging material. In such formations, losses will occur with a bottomhole pressure equal or lower than the pore pressure, not at the fracture pressure. With small fractures it is possible to plug them with either the drill cuttings or by adding plugging material in drilling fluid[7].

Carbonate rocks are a type of sedimentary rock and is largely made up of two types of rock, Limestones and Dolostones. 10-15% of all sedimentary rocks are carbonate rocks. Limestones are mainly composed of calcite (CaCO_3), and dolostones are mostly composed of dolomite ($\text{CaMg}(\text{CO}_3)_2$). The main characterization of carbonate rocks is the presence of CO_3 . Due to the carbonate minerals solvability in acidic waters they often are characterized by high porosity and permeability [25]. Carbonate formations is also known for having large cave and channel systems, commonly referred to as karst. When karst is present in the formation they will be cause huge fluid losses. In the picture below, highly fractured carbonate formation is shown. The darker spots in the picture illustrates karst channels and caves.



Figure 9 - Highly Fractured Carbonate Formations [Photograph by K.K. Fjelde, Billefjorden, Svalbard]

3.3 PMCD Field Cases and Other PMCD Studies.

To get a more complete view of how typical PMCD operations is carried out and improved on, this subchapter will briefly describe some field cases and other studies.

3.3.1 East Malaysia PMCD [26]

Paper [26] presents a field case from East Malaysia, where two wells were drilled, a main well and a sidetrack from the main. Problems with lost circulation was encountered and PMCD was unsuccessfully attempted. After 4 years a new operation was planned, this time with a PMCD specialist. The PMCD team helped plan all aspects of the new operation, including well design, completion, choice of fluids and drilling procedures. The mistakes done from the previous attempt was analyzed and precautionary steps was planned to avoid the same mistakes. Procedures upon entering loss zones was to fill annulus with Drill Weight Mud(DWM) until the loss rates was evaluated. Then the well would be evaluated for PMCD suitability. When PMCD was applied the second time, several stages of the operation were handled differently. Some of the key points was:

- The hole was kept full when total losses was encountered, without stopping the mud pumps. Annulus was continuously filled with DWM.
- In the first attempt, they tried to circulate out gas using drillers method. This time no attempts were done to shut in the well and circulate gas out.
- LCM was not used the second time, due to its lack of ability to plug and stop losses in the carbonate formation.
- Gas kick migration was handled with injection of LAM at high flowrates. Previously they were unable to lower the annulus surface pressure, even during bullheading.
- They did not bleed off pressure at the surface during the operation, as it would only induce more gas migration.

With the improved PMCD decision making a section of 430 m was successfully drilled, with an increase in drilling efficiency from 5.6 m/day to 60.6 m/day. For a more detailed description of the operation with all important discussions, see the referenced paper.

3.3.2 Combining PMCD and Early Kick Detection Techniques for Fractured Formations Overlying a High Pressure Reservoir in Offshore Kalimantan [6]

Paper [6] describes a case where a well was successfully drilled in offshore Kalimantan, Indonesia, by using a synergized PMCD and Early Kick Detection (EKD) setup. The well had a high-pressure gas reservoir, below a zone with high circulation loss formations. To solve the problems, two key components were used, a RCD and a Coriolis mass flow meter (CMF). Because of the high-pressure gas reservoir and the overlying fractured formation, the operation was exposed for several well control situations. Therefore, PMCD was taken into use. They also had problems when entering the high pressurized gas reservoir, with regards to monitoring of the gas influxes. To correctly monitor the flow rate with high accuracy in a closed-loop system, they used CMF in a system called Early Kick Detection (EKD). Being able to identify kick and loss when it begins and volumes are still small, gives the drillers a huge advantage and increases the chance of successfully handling the situation.

EKD works in a closed-loop system, provided by an RCD, which makes switching between PMCD and EKD easier. When using EKD, all flow out is measured by the CMD and compared to the flow in. Any gain or loss will then be displayed clearly to the drillers. The EKD system has several advantages:

- Early kick and loss detection.
- Indication of gas migration to surface.
- Monitor surface leaks and pipe washouts.
- Identification of wellbore breathing or ballooning.

By combining the two methods on the same MPD setup they could successfully use PMCD to drill through the fractured high loss zone, and quickly switch to EKD mode to drill through the high-pressure reservoir. Figure 10 below shows how four different drilling modes are connected in one setup, conventional drilling, closed-loop circulation drilling mode, PMCD and EKD.

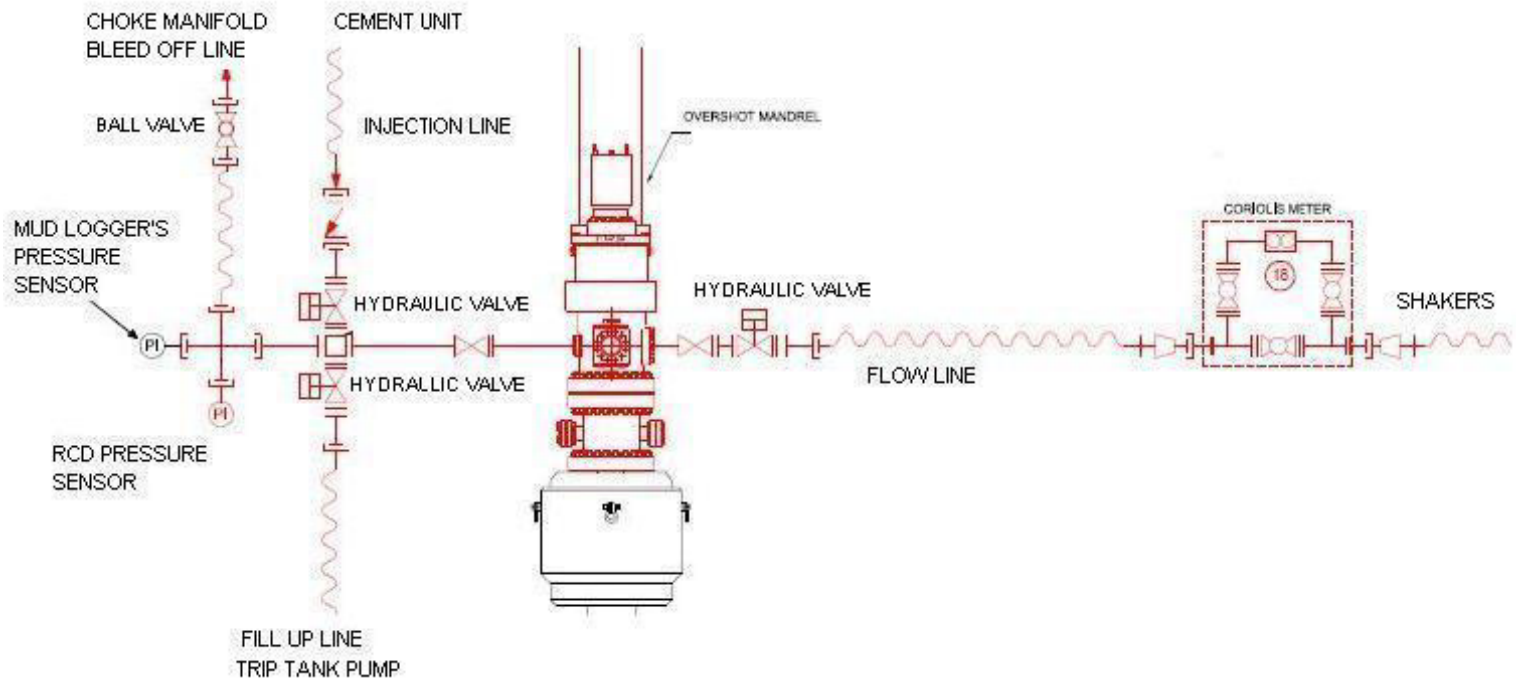


Figure 10 - Flow Diagram of a Combined PMCD and EKD Setup [6]

3.3.3 Prediction Model for Gas Migration in Well During PMCD Operation[5]

Paper [5] presents a solution to model fluid losses through fractures and production from the reservoir. In the paper, they are comparing PMCD simulation data from the software OLGA with data from a modified version of the AUSMV scheme. The OLGA software acts as a reference to the industry, and makes it possible to validate the modified model. The AUSMV model works by discretizing the well into a specific number of cells and give each cell its own set of variables, which is updated through

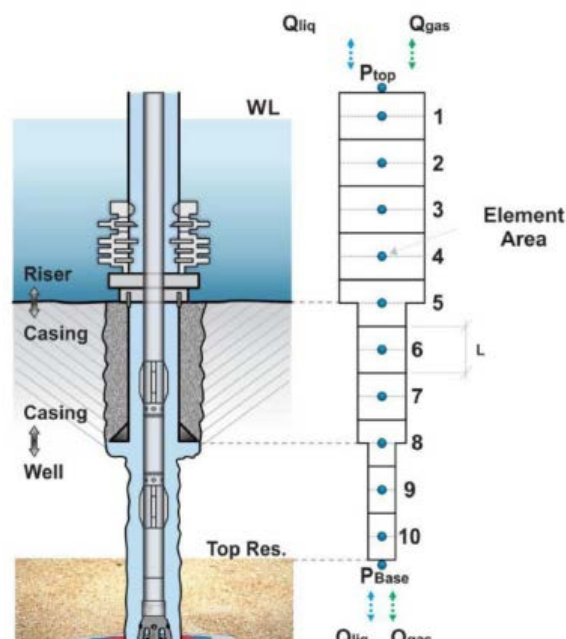


Figure 11 - Illustration of the Well Discretization with the Virtual Cell [5]

time to simulate changes. More details on how the AUSMV scheme works is presented in chapter 4. When performing PMCD, influxes of gas and migration of gas to surface is expected. This migration will cause an increase in the bottomhole pressure, which again will force fluids into the formation if high enough. To simulate this crossflow, they created a new virtual cell outside the well discretization cells, which represents the interaction between the reservoir and the fractured zone. Being able to simulate this crossflow is important to predict the correct pressure development in the well. If fluids are allowed to enter the formation, the pressure buildup will be lower compared to what it would be, if the fluids are not allowed to enter the formation. Comparing the simulation results with the data from OLGA showed a good match, and they found the new modified model capable of successfully simulating a PMCD well control scenario, with gas migration in a closed well. They also proposed another way of doing this for future studies, namely using the source term from the partial differential equation to handle the injection and production from the reservoir. This is something we will try to accomplish later in this thesis.

4. The Transient Flow Model

This chapter will introduce and explain the transient flow model used to perform the necessary simulations for this thesis. The code is a combination of the two-phase drift flux model and the numerical AUSMV scheme. The model has many uses, mostly for analyzing dynamic transient flow systems and phenomena which occurs during hydrocarbon transport in such systems. In this thesis, it will be used to perform simulation and plotting of a kick and bullheading scenario during a PMCD operation. Suggestions for improvements in the code will be implemented and tested later in the thesis. All information presented in this chapter is taken from papers [27] and [28], [10].

The Advection Upstream Splitting Method with Velocity splitting functions (AUSMV) is a hybrid scheme based on the Advection Upstream Splitting Method (AUSM) and the AUSM+ extension. These schemes combine the efficiency from the flux-vector splitting schemes (FVS) and the accuracy of the flux-difference splitting schemes (FDS) [28]. By extending these flux-splitting schemes, used for calculating Euler and Navier-Stokes equations, the resulting AUSMV scheme is obtained [10]. The AUSMV scheme, proposed by Evje and Fjelde (2001), is a one-dimensional, two-phase model which is capable of treating transitions from co-current to counter current flow and transitions from one-phase to two-phase flow [27]. It is also capable of handling contact discontinuities (mass fronts) and non-oscillatory approximations of acoustic waves [28].

4.1 The Two-Phase Model

The Drift Flux model in its full form is a two-phase model which handle mass, momentum and energy conservation for liquid and gas. It is defined for a one-dimensional system and predicts flow rate and pressure changes with good accuracy [10]. By adding together momentum and energy equations for liquid and gas, the resulting mixture momentum and energy equations are obtained. Source terms to handle effects such as mass transfer in and out of the system, friction and gravity is also necessary. The model is transient, which means it can express changes in the system over time. It is a hyperbolic model, at least in the physically reasonable region of the parameters [10].

By assuming constant temperatures in the system, isothermal flow, the two phase drift-flux model can be expressed with three conservation equations [27]:

1. Conservation of mass for liquid:

$$\frac{\partial}{\partial t} [A\alpha_l\rho_l] + \frac{\partial}{\partial x} [A\alpha_l\rho_lv_l] = A\Gamma_l \quad (4)$$

2. Conservation of mass for gas:

$$\frac{\partial}{\partial t} [A\alpha_g\rho_g] + \frac{\partial}{\partial x} [A\alpha_g\rho_gv_g] = A\Gamma_g \quad (5)$$

3. Conservation of mixture momentum:

$$\frac{\partial}{\partial t} [A(A\alpha_l\rho_l + A\alpha_g\rho_g)] + \frac{\partial}{\partial x} [A(A\alpha_l\rho_lv_l^2 + A\alpha_g\rho_gv_g^2)] + A\frac{\partial}{\partial x} p = -Aq \quad (6)$$

Where α_l and α_g are the liquid and gas fractions respectively, ρ_l and ρ_g are the densities and v_l and v_g are the phase velocities. Liquid and gas are hereby referred to by the index l and g respectively. A is the flow area cross section and p is the pressure.

4.2 Closure Laws

To solve all the unknowns in the drift-flux model, a set of closure laws is necessary and the number of closure laws must be equal to the number of unknowns in the equations. This will also require more assumptions to be made.

First, it is assumed no mass transfer between the liquid and gas phases:

$$\Gamma_l = \Gamma_g = 0 \quad (7)$$

It is also necessary to express the mixture properties of the two phases, which includes mixture density, viscosity and velocity.

$$\begin{aligned} \rho_{mix} &= \alpha_l\rho_l + \alpha_g\rho_g \\ \mu_{mix} &= \alpha_l\mu_l + \alpha_g\mu_g \\ v_{mix} &= \alpha_lv_l + \alpha_gv_g \end{aligned} \quad (8)$$

The two volume fractions can be written as:

$$\alpha_l + \alpha_g = 1. \quad (9)$$

Then the source term related to gravity and friction effects can be written:

$$q = F_g + F_w, \quad (10)$$

where the gravitational effects are calculated by

$$F_g = g(\rho_{mix}) \cos \theta, \quad (11)$$

and the frictional effects

$$F_w = \frac{2f v_{mix} \rho_{mix} \text{abs}(v_{mix})}{(d_{out} - d_{in})}. \quad (12)$$

In these expressions, θ is the inclination of the one-dimensional system, and g is the gravitational constant. The outer and inner diameter of the annular flow area is represented by d_{out} and d_{in} . To determine the friction factor f the Reynolds number must be calculated, since it depends on whether the flow is turbulent or laminar. The Reynolds number is calculated:

$$Re = \frac{\rho_{mix} \text{abs}(v_{mix})(d_{out} - d_{in})}{\mu_{mix}} \quad (13)$$

If the Reynolds number is below 2000, the flow is laminar, and the friction factor used is calculated:

$$f = 24/Re. \quad (14)$$

If the Reynolds number is over 3000 the flow is considered turbulent, and friction is calculated by:

$$f = 0.052 Re^{-0.19} \quad (15)$$

To ensure a smooth transition between the two flow regimes, interpolation is used between 2000 and 3000.

To describe the velocities of the fluids a gas slip law is also necessary:

$$v_g = K v_{mix} + S, \quad (16)$$

Where K and S is the flow parameters dependent on which kind of flow pattern that is present (bubble flow, slug flow, etc.). K is a coefficient and S is the slip velocity. When $K = 1.0$ and $S = 0$ we have a no slip scenario between the two fluids.

A simple model is used to calculate the liquid density:

$$\rho_l = \rho_{l,0} + \frac{p - p_{l,0}}{a_l^2}, \quad (17)$$

where a_l is the sound velocity in the liquid phase, and $p_{l,0}$ and $\rho_{l,0}$ are constant, based on the properties of the fluid. In the currently used two-phase model, these constants have been given the values: $a_l = 1500$ [m/s], $p_{l,0} = 1$ [bar] and $\rho_{l,0} = 1000$ [kg/m³]. To calculate the gas density the following expression is used, taken from a simplified ideal gas law:

$$\rho_g = \frac{p}{a_g^2}, \quad (18)$$

where a_g is the sound velocity in the gas phase, with an approximated value of $a_g = 316$ [m/s], and p is the pressure in the system.

4.3 The AUSMV Scheme

The main principle of this calculation method is to split the length of the flow system into a desired number of cells, called the discretization process. Then we can use the drift flux model and the AUSMV scheme to calculate all necessary flow properties in every cell. The number of cells, and the length of each timestep is dependent on each other, which is shown later. When all cells have been calculated, the time is updated, by adding one timestep, and all the same calculations are performed for the next time value. This means that the number of boxes and the length of the timestep decides how many calculations are performed. In this process, the AUSMV scheme is used for the numerical computations. The next section of this chapter shows how the drift flux model is combined with the AUSMV scheme, and how the AUSMV scheme is obtained. This is a general description of how the model is derived, and for further details and a more complete overview reference is made to the source material, [27] and [10].

By combining equation (4), (5) and (6) the drift flux model can be written in a vector form:

$$\partial_t \mathbf{w} + \partial_x F(\mathbf{w}) = G(\mathbf{w}) \quad (19)$$

Where

$$\mathbf{w} = \begin{pmatrix} \alpha_l \rho_l \\ \alpha_g \rho_g \\ \alpha_l \rho_l v_l + \alpha_g \rho_g v_g \end{pmatrix}, \quad F(\mathbf{w}) = \begin{pmatrix} \alpha_l \rho_l v_l \\ \alpha_g \rho_g v_g \\ \alpha_l \rho_l v_l^2 + \alpha_g \rho_g v_g^2 + p \end{pmatrix}, \quad G(\mathbf{w}) = \begin{pmatrix} 0 \\ 0 \\ -q \end{pmatrix} \quad (20)$$

From here, the flux component $F(\mathbf{w})$ can be split into a convective flux and a pressure flux:

$$F(\mathbf{w}) = F_c + F_p = \begin{pmatrix} \alpha_l \rho_l v_l \\ \alpha_g \rho_g v_g \\ \alpha_l \rho_l v_l^2 + \alpha_g \rho_g v_g^2 \end{pmatrix} + \begin{pmatrix} 0 \\ 0 \\ p \end{pmatrix} \quad (21)$$

The convective flux component can then be broken further down into two separate fluxes, one for liquid and one for gas:

$$F_c = F_{c,l} + F_{c,g} = \begin{pmatrix} \alpha_l \rho_l v_l \\ 0 \\ \alpha_l \rho_l v_l^2 \end{pmatrix} + \begin{pmatrix} 0 \\ \alpha_g \rho_g v_g \\ \alpha_g \rho_g v_g^2 \end{pmatrix} = \alpha_l \rho_l v_l \begin{pmatrix} 1 \\ 0 \\ v_l \end{pmatrix} + \alpha_g \rho_g v_g \begin{pmatrix} 0 \\ 1 \\ v_g \end{pmatrix} \quad (22)$$

The flux can then be expressed as:

$$F(\mathbf{w}) = \alpha_l \rho_l v_l \begin{pmatrix} 1 \\ 0 \\ v_l \end{pmatrix} + \alpha_g \rho_g v_g \begin{pmatrix} 0 \\ 1 \\ v_g \end{pmatrix} + \begin{pmatrix} 0 \\ 0 \\ p \end{pmatrix} \quad (23)$$

Now the convective liquid and gas flux, $F_{c,l}$ and $F_{c,g}$, is expressed for the left and right side of the cell section from the discretization. The AUSMV scheme is based on the hybrid flux-vector splitting scheme, the FVS scheme:

$$F_{j+1/2}^{FVS}(\mathbf{w}_L, \mathbf{w}_R) = (\alpha_l \rho_l)_L \Psi_{1,L}^+ + (\alpha_l \rho_l)_R \Psi_{1,R}^- + (\alpha_g \rho_g)_L \Psi_{g,L}^+ \\ + (\alpha_g \rho_g)_R \Psi_{g,R}^- + (F_p)_{j+1/2} \quad (24)$$

where

$$\Psi_{1,L}^+ = \Psi_1^+(v_{l,L}, c_{j+1/2}), \quad \Psi_{1,R}^- = \Psi_1^-(v_{l,R}, c_{j+1/2}) \quad (25)$$

and

$$\Psi_1^+(v, c) = V^+(v, c) \begin{pmatrix} 1 \\ 0 \\ v \end{pmatrix}, \quad \Psi_1^-(v, c) = V^-(v, c) \begin{pmatrix} 1 \\ 0 \\ v \end{pmatrix} \quad (26)$$

The same goes for the gas phase:

$$\Psi_{g,L}^+ = \Psi_g^+(v_{g,L}, c_{j+1/2}), \quad \Psi_{g,R}^- = \Psi_g^-(v_{g,R}, c_{j+1/2}) \quad (27)$$

where

$$\Psi_g^+(v, c) = V^+(v, c) \begin{pmatrix} 0 \\ 1 \\ v \end{pmatrix}, \quad \Psi_g^-(v, c) = V^-(v, c) \begin{pmatrix} 0 \\ 1 \\ v \end{pmatrix} \quad (28)$$

Also, the pressure flux component F_p is defined by the FVS discretization on the form:

$$p_{j+1/2} = P^+(v_L, c_{j+1/2}) p_L + P^-(v_R, c_{j+1/2}) p_R \quad (29)$$

Where the pressure splitting formulas P^+ and P^- is defined by:

$$P^\pm(v, c) = V^\pm(v, c) \cdot \begin{cases} \frac{1}{c} \left(\pm 2 - \frac{v}{c} \right), & \text{if } |v| \leq c \\ \frac{1}{v}, & \text{otherwise} \end{cases} \quad (30)$$

In all expressions above, the L and R index represent the left and right side of the cell, c is the common speed of sound in the cell interface and v is the mixture velocity.

Now comes the difference between the FVS scheme and the AUSMV scheme, the expression for the velocity splitting formulas V^+ and V^- . In the FVS scheme it is given as

$$V^\pm(v, c) = \begin{cases} \pm \frac{1}{4c} (v \pm c)^2, & \text{if } |v| \leq c \\ \frac{1}{2} (v \pm |v|), & \text{otherwise} \end{cases} \quad (31)$$

In the AUSMV scheme the velocity splitting formulas are replaced by a more general pair, which makes it capable of reproducing stationary contact discontinuities. As stated in reference paper [27], ‘‘One main drawback of the FVS scheme is the excessive numerical dissipation at volume contact discontinuities’’. The new velocity splitting formula is given:

$$\tilde{V}^\pm(v, c, \chi) = \begin{cases} \chi V^\pm(v, c) + (1 - \chi) \frac{v \pm |v|}{2}, & \text{if } |v| \leq c \\ \frac{1}{2} (v \pm |v|), & \text{otherwise} \end{cases} \quad (32)$$

A new parameter χ is included and it is expressed by:

$$\chi_L = \alpha_R, \quad \chi_R = \alpha_L \quad (33)$$

By using the new velocity splitting formula \tilde{V}^\pm , the AUSMV flux is introduced and referred to as $F_{j+1/2}^{AUSMV}$. It is used to create the following expression which calculates new variables for each timelevel:

$$U_j^{n+1} = U_j^n - \frac{\Delta t}{\Delta z} (F_{j+1/2}^{AUSMV} - F_{j-1/2}^{AUSMV})^n - \Delta t Q_j^n, \quad (34)$$

with

$$U = \begin{bmatrix} u_1 \\ u_2 \\ u_3 \end{bmatrix} = \begin{bmatrix} \alpha_l \rho_l \\ \alpha_g \rho_g \\ \alpha_l \rho_l v_l + \alpha_g \rho_g v_g \end{bmatrix}, \quad (35)$$

where the index n is the timestep and j is the cell number. The source term is represented by Q_j^n , and will be manipulated later in the thesis. In figure 12 below it is shown how each cell is calculated relative to the neighbor cells and the fluxes between.

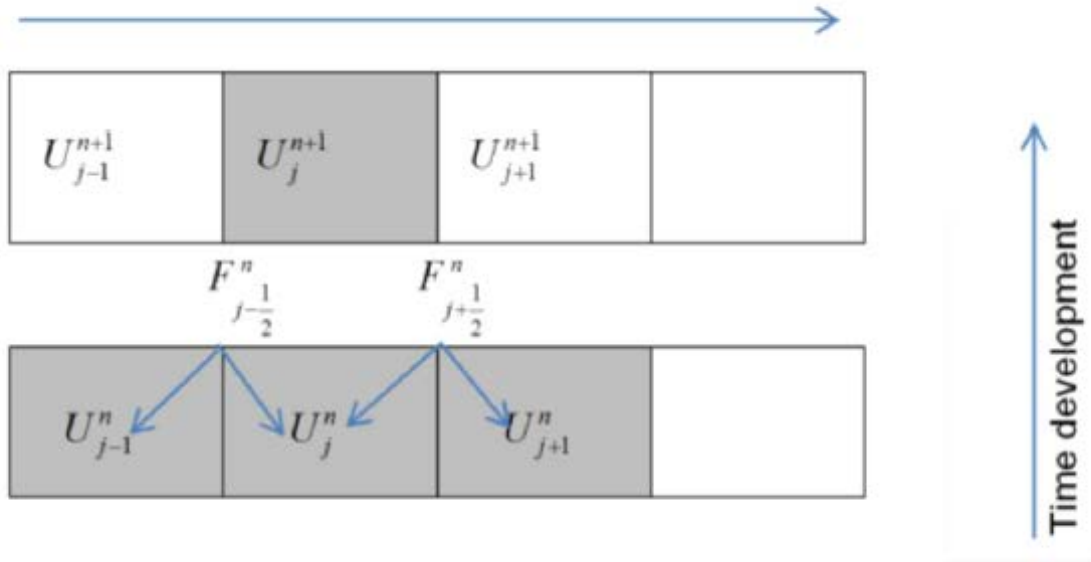


Figure 12 - Update of discretized variables [29]

The timestep Δt is calculated by:

$$\Delta t = CFL \frac{\Delta x}{\max(|\lambda_1|, |\lambda_2|, |\lambda_3|)}, \quad (36)$$

Where CFL represents a number between 0 and 1, which depends on the formulation of the scheme[29]. Of the three eigenvalues, λ_1 , λ_2 and λ_3 , the first and the third represents the pressure pulses propagating downstream and upstream. The second eigenvalue corresponds to the wave speed of the gas volume wave going downstream.

4.4 Boundary Conditions

In the boundary cells, the numerical fluxes in and out of the well cannot be defined by the scheme. The fluxes must be specified by using given information, for instance inlet mass flow rates and outlet pressure. The remaining information needed must be extrapolated or calculated based on the values in the boundary cells[8]. Different well conditions require different boundary treatment. Later in the thesis, changes will be made to the boundary conditions.

Open well conditions:

For an open well the mass and convective momentum fluxes at the inlet is known, but the inlet pressure must be determined. Currently there is presented two ways to handle the inlet boundary pressure. The first is defined in paper [8] where inlet pressure flux is calculated by this expression:

$$P_{inlet} = p(1) + \frac{\Delta z}{2} \rho_{mix} g \cos \theta + \frac{\Delta z}{2} \frac{\Delta p_{fric}}{\Delta z} \quad (37)$$

The second way is defined in paper [28]:

$$P_{inlet} = p(1) + 0.5(p(1) - p(2)) \quad (38)$$

At the outlet cell, all mass and convective momentum fluxes are extrapolated and the outlet pressure flux is set to atmospheric conditions.

Closed well conditions:

For a closed well scenario, both inlet and outlet mass and convective momentum fluxes are set to zero. The inlet pressure fluxes are calculated the same way as for open well conditions, and the outlet pressure flux is also presented in two variants. From paper [8] the expression is given as:

$$P_{outlet} = p(N) - \frac{\Delta z}{2} \rho_{mix} g \cos \theta - \frac{\Delta z}{2} \frac{\Delta p_{fric}}{\Delta z} \quad (39)$$

where N is the total number of segments from the discretization.

Another way to calculate outlet pressure is presented in [28]:

$$P_{outlet} = p(N) + 0.5(p(N) - p(N - 1)) \quad (40)$$

Bullheading conditions:

During bullheading it is assumed that the reservoir can take all bullheading fluids, and the pressure flux is set to a fixed value. In the given version of the code, this value is selected to be 200 bar. The convective pressure flux at the bottom is then given as:

$$F_p = \begin{pmatrix} 0 \\ 0 \\ 20000000 \end{pmatrix}$$

The mass and convective momentum fluxes are calculated by extrapolation at the bottom of the well, which is the inlet. At the top of the well, the outlet, the mass and convective momentum fluxes are defined by the selected bullheading rates. The positive direction of the well is upwards, hence the bullheading values must be negative. The pressure flux is calculated the same way as for closed well conditions, by using equation (40).

4.5 Slope Limiters

One unfavorable phenomena which occurred in the original version of the transient AUSMV model was numerical diffusion[8]. The disadvantage of numerical diffusion is that sharp physical interfaces, for instance between a one-phase flow region and a two-phase flow region, will be smoothed out. This can be avoided by upgrading the scheme from first order accuracy to second order, and is done by introducing a slope limiter concept. The principle is to avoid constant value of the variables through a cell, and instead use the slope limiters to calculate boundary values between the cells. If the boundary values are found, they can be used to calculate the numerical fluxes. The concept is illustrated in the figure below.

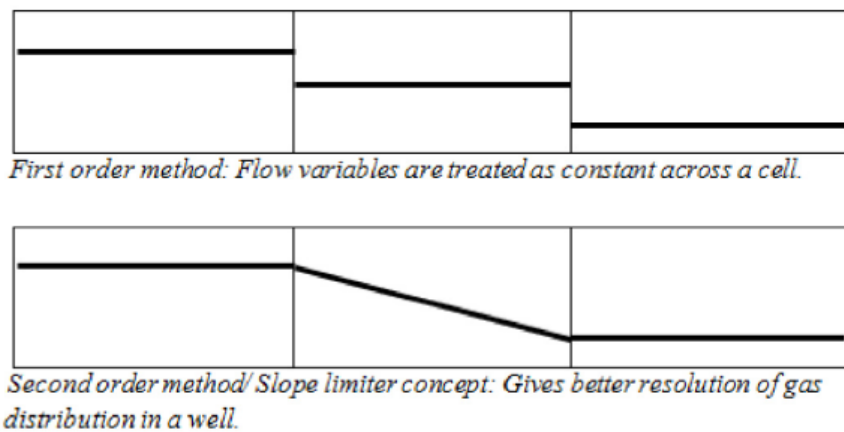


Figure 13 - Slope Limiter Concept [8]

One interesting point of discussion when it comes to the slope limiter concept, is the handling of the boundary cells. There are two ways to handle these cells, either extrapolate the value from the closest neighbor cell or have them set to zero. Later in the thesis, a couple of simulations is done where these two concepts are tested.

5. Injectivity Modelling

The main goal of this thesis is to carry on the work done earlier presented in paper [8], where the AUSMV scheme was adapted to simulate for bullheading during pressurized mud cap drilling. As stated in paper [8], one of the problems to be investigated further was with regard to formation injectivity and how it affects the pressure development during the operation. In the paper, this problem was solved by simply fixing the downhole pressure to a constant value through the bullheading, which is not realistic situation.

As briefly described earlier in the thesis, it is critical for the PMCD operation to have sufficient injectivity. If the formation has low permeability and there is a pressure buildup during the bullheading, fracturing of the formation may occur and damage the well.

To find an injection model which fits the transient model and can be used in the simulation scenario of interest, it is necessary to do research of both production wells and water injection wells and see how they handle it. The main goal in this chapter is to discuss different challenges related to injection, describe the injection process and the models found to describe the injection.

5.1 Water Injection Wells

There are several challenges related to water injection wells. Paper [30] presents the state of the art and challenges when it comes to geomechanically modeling of injector wells, and some of the points made will be briefly discussed in this subchapter. As this thesis discusses fluid injection as a part of bullheading, fluid injection is primarily used to sweep hydrocarbons at the end of a reservoirs life, and to extend the production. This is done by restoring the reservoir pressure. Fluid injection can also be used to dispose waste fluids.

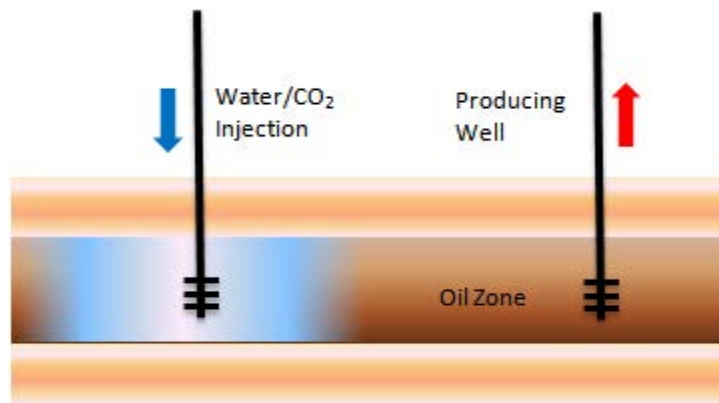


Figure 14 - Water/CO₂ Injection Well Example[31]

Waterflooding requires high injection rates and high sweep efficiency, and these two variables are dependent on each other, which makes achieving good injectivity an important goal for an Enhanced Oil Recovery (EOR) injection operation. There are several main causes of loss of injectivity in a formation:

- Pore plugging from solids and oil droplets
- Thermally induced failure, caused by temperature differences.
- Mechanical failure of formation due to pressure transients
- Channelization and liquefaction in poorly consolidated sands.

Changes in injectivity from the initial values due to any reason given above, will make it necessary to increase the injection pressure and the pump rate to maintain the same injection rate. With an increased injection pressure comes the risk of fracturing the wellbore formation. The figure below shows an example taken from [32] and

illustrates the injection rate development with an almost constant injection pressure. This is a field scenario from the Gulf of Mexico, and is a typical example of injection rates vs bottom hole pressure. Initially the injection performs at a high rate, above 6000 bbl/day, but suffers a rapid decrease over the next 100 days of operation. From day 100 until ca. day 250 the injection rate gradually decreases from 2000 bbl/day to 500 bbl, before it stabilizes. It must be noted that the mentioned scenario above describes a very different operation, compared to injection during a bullheading, with regards to the timescale. With such a long timescale, the well is experiencing a much higher degree of exposure to the threats which compromises the injectivity, and, as shown in the example, suffers from them. However, it is relevant in this thesis to discuss the phenomena which might cause such a loss of injectivity, even though we are considering a much shorter operation.

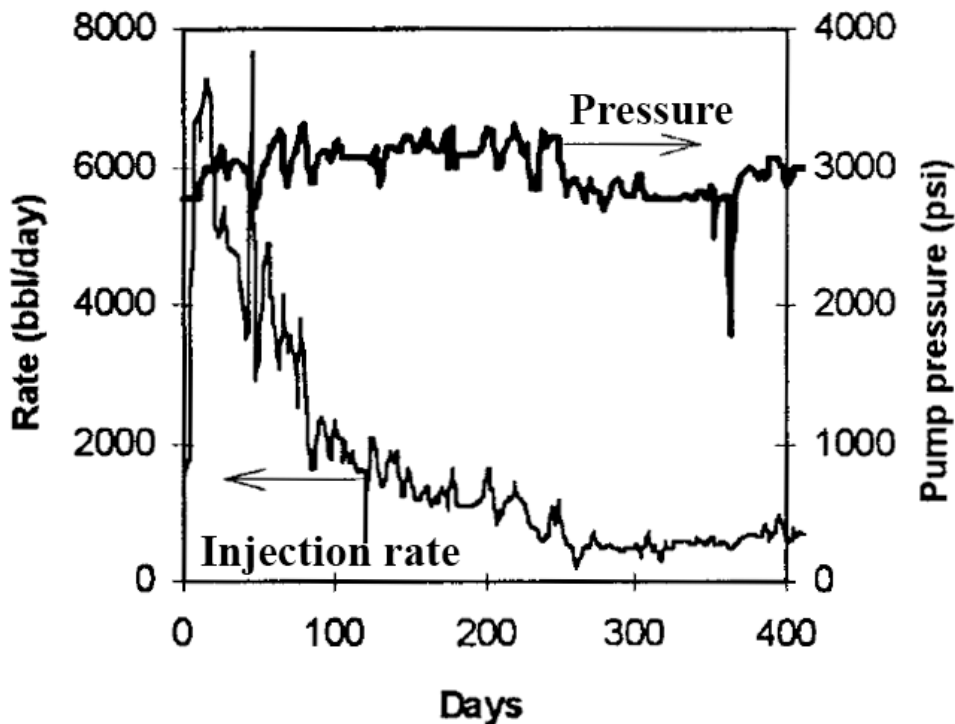


Figure 15 - Injection Rate and Pressure vs Time [32]

5.1.1 Pore Plugging

Injected fluids into a formation will to some certain degrees contain solid particles. The properties of such particles depend on the source. As the particles enter the formation, they might either in a physically or chemically way disturb the formation and cause a decrease in injection. Much depends on where the particles come to rest,

and how they will affect the permeability. Many formation parameters are important, such as pore size distribution and chemical composition of the formation. The properties of the injected fluid is also essential, such as velocity, density and viscosity. [30]

When the formation experiences a reduction in both porosity and permeability, the flow gets restricted and an increase in injection pressure is necessary to keep the injection rate at the desired level. If the pressure gets high enough it might cause a fracture in the formation, thus creating new flow paths and increase the injectivity. This cycle repeats through the injection process, but at a certain point a filtration cake may form and block the flow within the fracture. These effects however, are hard to analyze, as current models are not capable of predicting experimental data. [30]

One other interesting discussion in paper [30] is the use of injection to deposit cuttings in the formation. This is important for a PMCD operation, as all cuttings will be deposited into the formation. This is not something that will be simulated in this thesis, however it is worth mentioning when discussing injectivity.

5.1.2 Temperature Effects

When injecting fluids with low temperature into a formation, the temperature in the rocks will experience a gradually reduction. This will generate tensile stresses in the formation, between the low and high temperature rocks. Paper [30] states that this effect could be as much as 10-15 psi per degree Fahrenheit of cooling. This can ultimately result in a decreased fracture gradient in the formation. Because the well temperatures in the formation can be as high as 300°F (149°C), the large temperature differences can reduce the fracture gradient with up to 25% of the initial value.

5.2 Production Index

It is also desired to investigate production and injection flow rate models used in petroleum production. An inverted production model which correlates the relationship between the pressure difference and the flow rate, could be used in the transient model. One model is the PI-model, commonly used in production analysis.

The Production Index (PI) has been used to keep a measure of a wells potential to flow, or the ability of the well to produce liquids[33]. It is also used to measure formation damage, and how it affects the flow potential[34]. In the petroleum production industry, the production index is an important parameter when the inflow

performance relationship is estimated (IPR)[35]. By using this correlation, production field data can be used to evaluate and compare wells. The production index is normally written with the symbol J , and has the expression [33]:

$$J = \frac{q}{\bar{p} - p_{wf}} \quad (41)$$

where q is the reservoir flow rate in standard conditions [STB/day], \bar{p} is the average reservoir pressure and p_{wf} is pressure at the wellbore for a flowing well. There are several ways to calculate the value of PI. To use the expression above, the well must flow for a long time until it reaches pseudo steady-state flow [33]. Another way to calculate PI is through Darcys law. Paper [35] presents two equations to calculate PI, one for a Steady State scenario (Eq.(42)) and one for Pseudo Steady State (Eq.(43)). Both equations assume radial flow in a vertical well:

$$J = \frac{0,00708 k h}{\mu B \ln\left(\frac{r_e}{r_w}\right)} \quad (42)$$

$$J = \frac{0,00708 k h}{\mu B \ln\left(0,472 \frac{r_e}{r_w}\right)} \quad (43)$$

where k is the permeability, h is the injection height, μ is the viscosity of the fluid B is the formation volume factor of the fluid and r_e and r_w is the radius of the reservoir and the wellbore respectively.

Behavior of the PI value over a wide range of flow rates depends on the well, and is not the same for all. In some scenarios, the flow rate is directly proportional to the bottom hole pressure difference, causing the PI value to remain constant. However, in

some wells this is not the case and the PI value declines at higher flowrates, which is shown in figure 16 below.

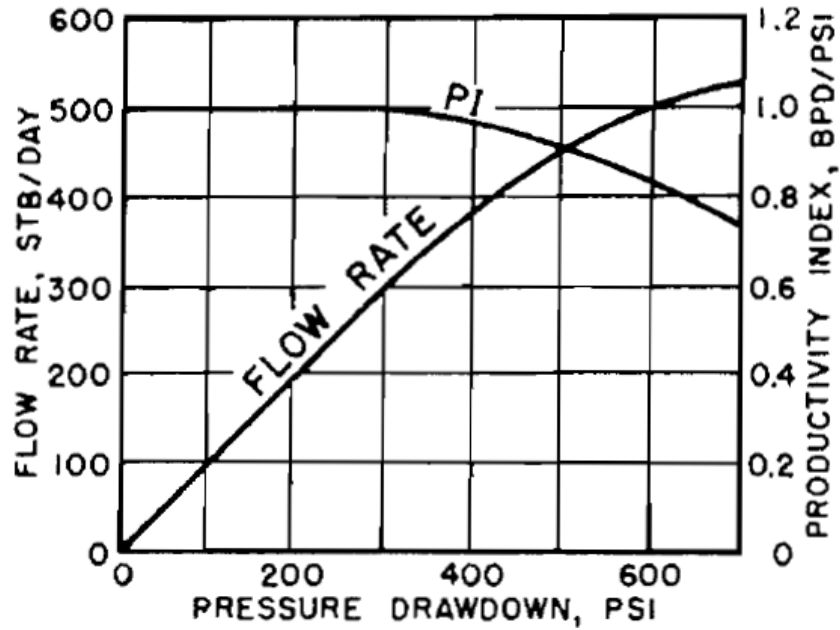


Figure 16 - Decline in productivity index at higher flow rates [8]

Presented in [33] and also in paper [36] is another variant of the production index, the injectivity index. Compared to the production index, it calculates the ratio of injection in STB per day to the pressure difference between reservoir and the flowing well. It is mainly used with salt water disposal wells and with injection wells for enhanced recovery with pressure maintenance[33]. The expression for the injectivity index is given as:

$$J_{injection} = \frac{q}{p_{wf} - \bar{p}} \quad (44)$$

Paper [36] also includes another variant of the equation, similar to equations (42) and (43), where it calculates the injectivity index based on Darcy's law.

$$J_{injection} = \frac{k_w h_i}{141.2 \mu_w B_w \cdot \left(\ln \left(\frac{r_e}{r_w} \right) + S \right)} \quad (45)$$

Where k_w is the permeability, h_i is the injection height, μ_w and B_w is the viscosity and the formation volume factor for water respectively, r_e and r_w is the radius of the reservoir and the wellbore respectively, and S is the skin factor.

This Darcy expression for injectivity relies on several assumptions [36]:

1. This expression only applies for one dimensional, radial flow. Fractures must be approximated for by the skin factor, and is only valid for a well in a pseudo-radial flow regime.
2. It assumes incompressible flow with a maintained pressure at the outside radius.
3. It assumes single phase flow.
4. Constant reservoir pressure.
5. The injection height might be lower than what is expected from reservoir characterization.

As note [36] states, equation (45) is flawed when used for fracture flow, and it is recommended to use equation (44).

5.3 Assumptions for Highly Fractured Injection

Since carbonate rocks and PMCD is associated with highly fractured formations, equation 44 is selected to model injection for the simulations in the next chapter. Some assumptions must be made for the PMCD bullheading operation, before the model can be used. In the next chapter with regards to injectivity the following assumptions is used:

- The fractures which is injected through is always in the bottom cell of the well.
- The injectivity index is constant through the entire operation. No loss in injectivity during simulation.
- There are no losses to other sections of the formations
- Only liquids will be injected using the model (except for case 5, where gas will be produced)
- Liquid injected in the well will have the similar physical properties as water. (Density, viscosity and speed of sound)

6. Implementation and Simulation of Injectivity Model in MATLAB

The AUSMV scheme has been written into a software called MATLAB, a numerical computing software which allows the user to perform calculations, matrix manipulations and plotting of data, using a programming language. As mentioned earlier, because this thesis is testing and suggesting improvements to the model presented in paper [8] and in thesis [9]. It is favorable to use the exact same code setup as in the references. This includes all fluid parameters, well geometry, boundary conditions and fluid input rates. By using the same setup, it is easy to compare the original simulation results with the results this thesis presents. The entire matlab code is given in the appendix, with all changes color coded.

This chapter is separated into six different cases, where each case will present the changes that have been done, explain the mathematics behind them, and new parameters in use. Also, each case will present the results from the simulations. To give a quick overview, this is a general description of the goal of each case:

- Case 1 & 2: Get the Injectivity Index model to work in the AUSMV scheme, by manipulating the flux boundary conditions of the code. In case 1 it will be done for the fluid injected during bullheading. In case 2 it will be done for the flowback into the reservoir when the kick migrates. Case 2 will adopt the ideas in [5], but with another way of doing it.
- Case 3 & 4: Move the injection model from the boundary conditions, and implement it in the source term. In case 2 it will be done for the fluid injected during bullheading. In case 4 it will be done for the flowback into the reservoir when the kick rises. Similar to case 2, case 4 will also adopt the ideas from [5], but with a third method of simulating the flowback.
- Case 5: Produce the kick into the well by using a reverse PI model.
- Case 6: Simulate two separate ways of handling the boundary cell with regards to slope limiters.
- Case 7: Simulate and compare two separate ways of handling boundary pressure calculations.

6.1 Matlab Code Configuration

This subsection presents all the data used in the original model to simulate for bullheading during PMCD drilling. All these values will be used in further simulations unless stated otherwise.

Geometry data of the well:

Well depth [m]	2000
Outer diameter of flow area [m]	0.2159
Inner diameter of flow area [m]	0.127

Table 2 - Well Geometry Data

Fluid data:

Liquid	
Density at standard conditions [kg/m^3]	1000
Viscosity [$Pa \cdot s$]	0.001
Sound velocity in fluid [m/s]	1500
Gas	
Density at standard conditions [kg/m^3]	1.0
Viscosity [$Pa \cdot s$]	0.0000182

Table 3 - Fluid Data

Well discretization:

Number of cells	25
Timestep	0.01

Table 4 - Well Discretization

Boundary conditions:

The boundary conditions of the code must be given for each phase of the operation. During this operation, three important conditions will determine how the well behaves. This includes if the well is open or closed, if the bullheading is started or not and if there is inlet of gas into the system. The simulation is set to run for 4000 seconds, but this will be changed later to get desired data output for separate times. During the first 10 seconds of the simulation, nothing happens. Then the kick is introduced into the system. By using an interpolation time of 10 seconds, the gas is given a gradually increasing flow rate, before it reaches its maximum value. The same interpolation is used to reduce the kick inflow rate. Then the well is closed and the kick rises through the well, before the bullheading starts at 1500 seconds. The inlet

maximum flowrates of both gas and liquid must be set in the code, and is given the values:

Inlet gas mass rate [kg/s]	8.0
Inlet liquid mass rate [kg/s]	25

Table 5- Inlet Fluid Rates

This is how the code will handle the boundary conditions through the simulation timesteps:

Time interval [s]	Conditions
0-10	Inlet liquid mass rate = 0.0 Inlet gas mass rate = 0.0 Well opening = 1.0 Bullheading = 0.0
10-20	Inlet gas mass rate = $8.0 * (time-10)/10$
20-110	Inlet gas mass rate = 8.0
110-120	Inlet gas mass rate = $8.0 - 8.0 * (time-110)/10$
120-130	Inlet gas mass rate = 0.0
130-1500	Well opening = 0.0
1500-1560	Inlet liquid mass rate = $-1.0 * 25 * (time-1500)/60$ Well opening = 1.0 Bullheading = 1.0
1560-4000	Inlet liquid mass rate = $-1.0 * 25$

Table 6 - Time vs Well Conditions

As stated in subchapter 5.3 one of the assumptions for the use of the injectivity index equation is that only one phase liquid is injected. Therefore, the code will only be simulated for 3000 seconds, as after 3000 seconds gas is also injected into the formation. To simulate two-phase injection, a more complex model is necessary.

The entire code is given in the appendix, and all changes will be color coded.

6.2 Case 1 - Injection Model During Bullheading in Boundary Conditions

The goal of case 1 is to implement and study how the injectivity index model works for simulation during the bullheading part of the simulation. For the original version of the code, the bottom hole pressure during the bullheading, was fixed to a constant value through the process. It was simply stated in the boundary conditions that BHP should be 200 bars. The figure below shows the bottom hole pressure of the well for the original code, with the constant bottomhole pressure.

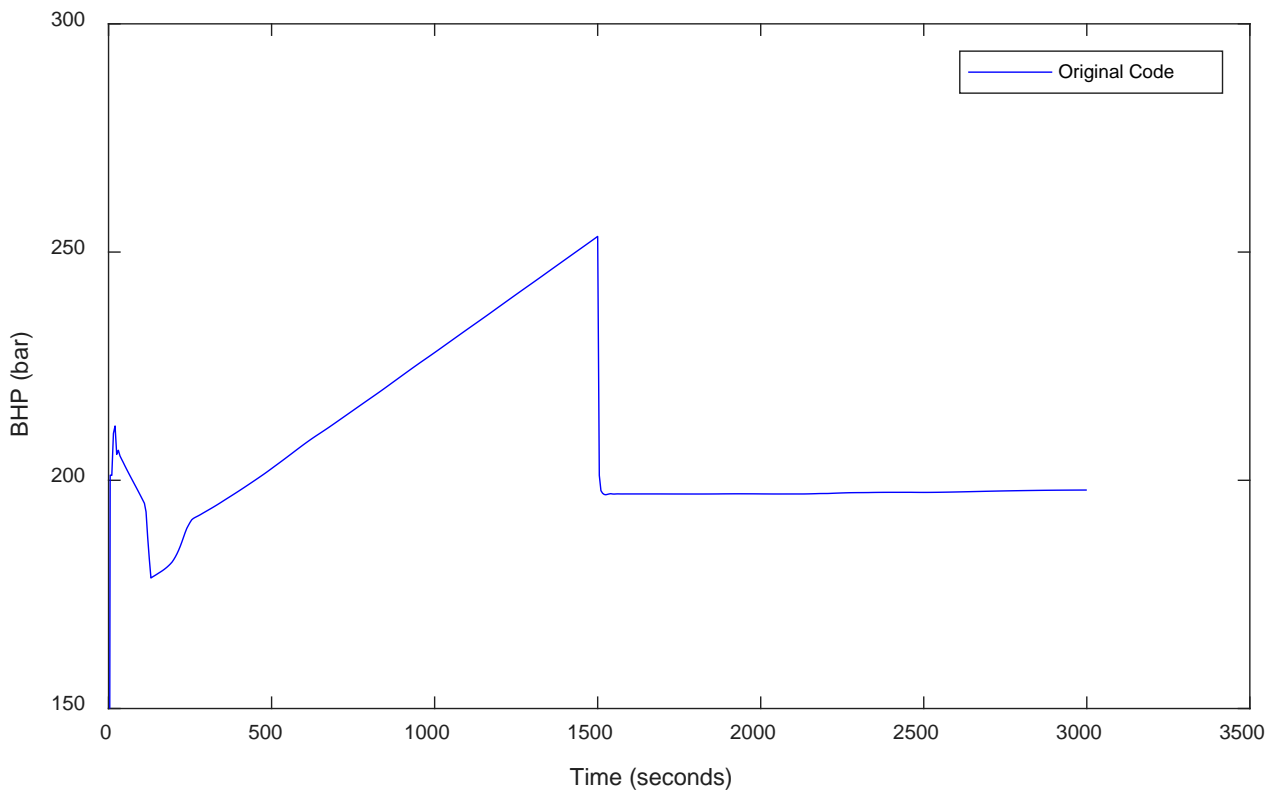


Figure 17- Bottom Hole Pressure vs Time for Original Model

6.2.1 Case 1 - Implementation and Preparation

This case will focus on the time interval from 1500 seconds till 3000 seconds. We want to end the simulation before gas reaches the bottom, because this model only handles injection of liquid. Ways to handle the injection of gas will be discussed later in the thesis.

To use the injectivity model, it is necessary to estimate a value for the injectivity index, set a value for the average reservoir pressure and consider how to handle the interpolation of the fluid out of the system. For the injectivity index, the symbol J will be used in the code.

First, a way to estimate a value for the injectivity index must be found. These are the assumptions made:

Average reservoir pressure [Pa]	$\bar{p} = 20000000$
Max liquid injection rate [kg/s]	$m_l = 25$
Ideal injection pressure difference [Pa]	$\Delta p = 1000000$

Table 7 - Values Used to Estimate Injectivity Index in Case 1

Ideal injection conditions will be assumed for the first simulation. By using the values above, inserted into equation 3, it is possible to create an expression to estimate a value for J:

$$J = \frac{m_l}{\Delta p \cdot \rho_{l,stc}} \quad (46)$$

With the assumed values, this expression says that for a 10-bar pressure difference between the reservoir and the wellbore, fluid will be injected into the formation at a 25 kg/s rate.

An expression to calculate the new volumetric flow rate is also necessary. The numerical mass liquid flux in the code has the units of $\left[\frac{kg/s}{m^2}\right]$, thus the new injection model must have the same units. By changing equation (44) the injection volumetric flow rate can be expressed as:

$$q_l = J \cdot (p_{wf} - \bar{p}) \quad (47)$$

By multiplying equation (47) with the density at standard conditions and dividing by the flow area, a new expression is created:

$$F_{c,l,1} = \frac{J \cdot (p_{wf} - \bar{p}) \cdot \rho_{l,stc}}{A} \quad (48)$$

The model must be inserted into the flux boundary conditions. In the boundary conditions of the original code, the convective fluid fluxes for the first cell during bullheading is calculated this way:

$$F_{c,l} = \begin{pmatrix} \alpha_l \rho_l v_l \\ 0 \\ \alpha_l \rho_l v_l^2 \end{pmatrix} \quad (49)$$

The new way to calculate the fluxes which is implemented into the code:

$$F_{c,l} = \begin{bmatrix} -\frac{J \cdot (p_{wf} - \bar{p}) \cdot \rho_{l,stc}}{A} \\ 0 \\ -\left(\frac{J \cdot (p_{wf} - \bar{p}) \cdot \rho_{l,stc}}{A}\right) \cdot v_l \end{bmatrix} \quad (50)$$

Also, the pressure fluxes must be changed. In the original code, it is given as:

$$F_p = \begin{pmatrix} 0 \\ 0 \\ 20000000 \end{pmatrix} \quad (51)$$

It is now possible to calculate a value for the pressure flux during the bullheading, and to do so equation (37) is used, which makes the new expression for pressure flux in the code:

$$F_p = \begin{pmatrix} 0 \\ 0 \\ p(1) + \frac{\Delta z}{2} \rho_{mix} g \cos \theta + \frac{\Delta z \Delta p_{fric}}{2 \Delta z} \end{pmatrix}$$

Finally, this is how interpolation of the Injection Index was handled:

Time interval [s]	Conditions
1500-1560	$J = J * (\text{time}-1500)/60$
1560-4000	$J = J$

Table 8 - Injection Index Interpolation

This was done to ensure a smooth transition when starting the bullheading process from closed in conditions.

All changes done in the matlab code is marked with red color in the Appendix.

6.2.2 Case 1 - Simulation Results

Simulation was performed with the new code, and is first plotted for pressure development vs time for top and bottom of the well. Results is shown in figure X and Y.

After that simulation was done for different values of J, to see how it affects the results. These values of J were used:

J =	J
J =	0.5 * J
J =	0.25 * J
J =	1.25 * J
J =	1.5 * J
J =	2 * J

Table 9 - Different Values of Injectivity Used in Simulation

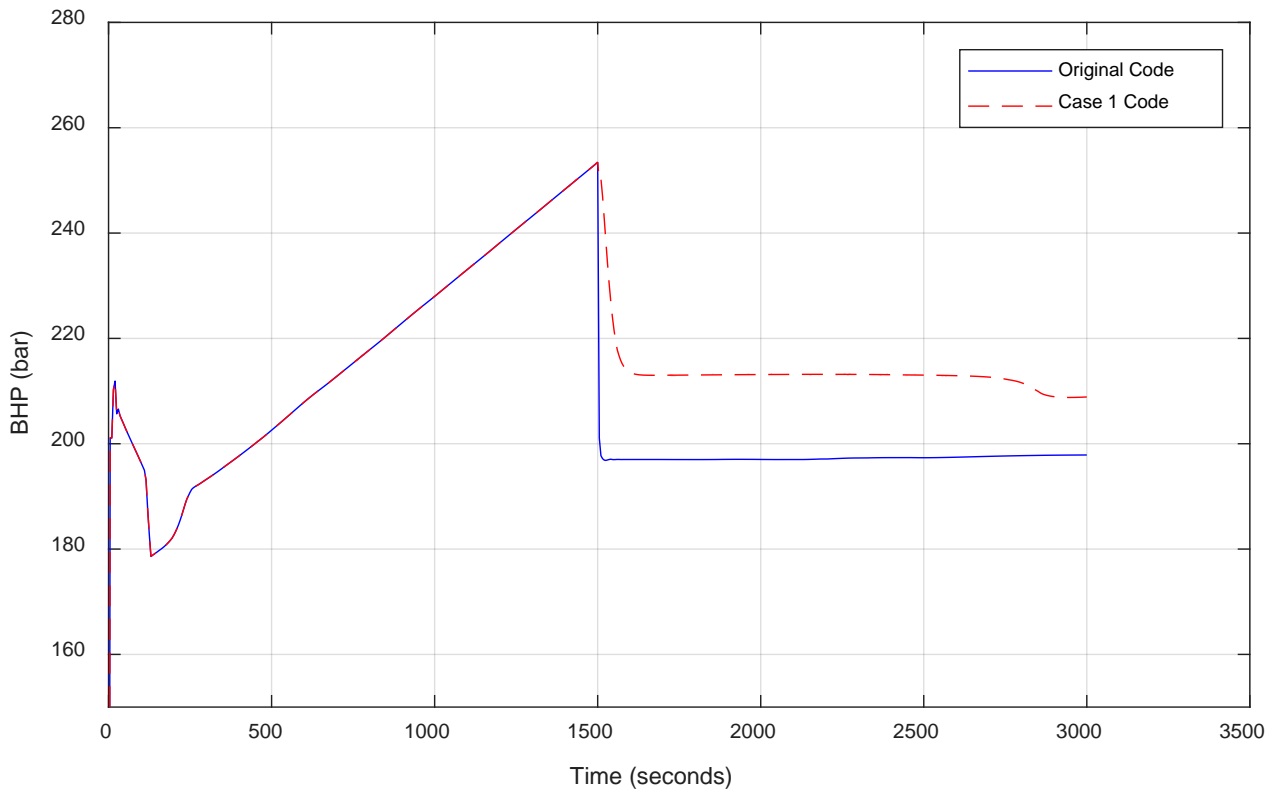


Figure 18 - Bottom Hole Pressure vs Time for Case 1

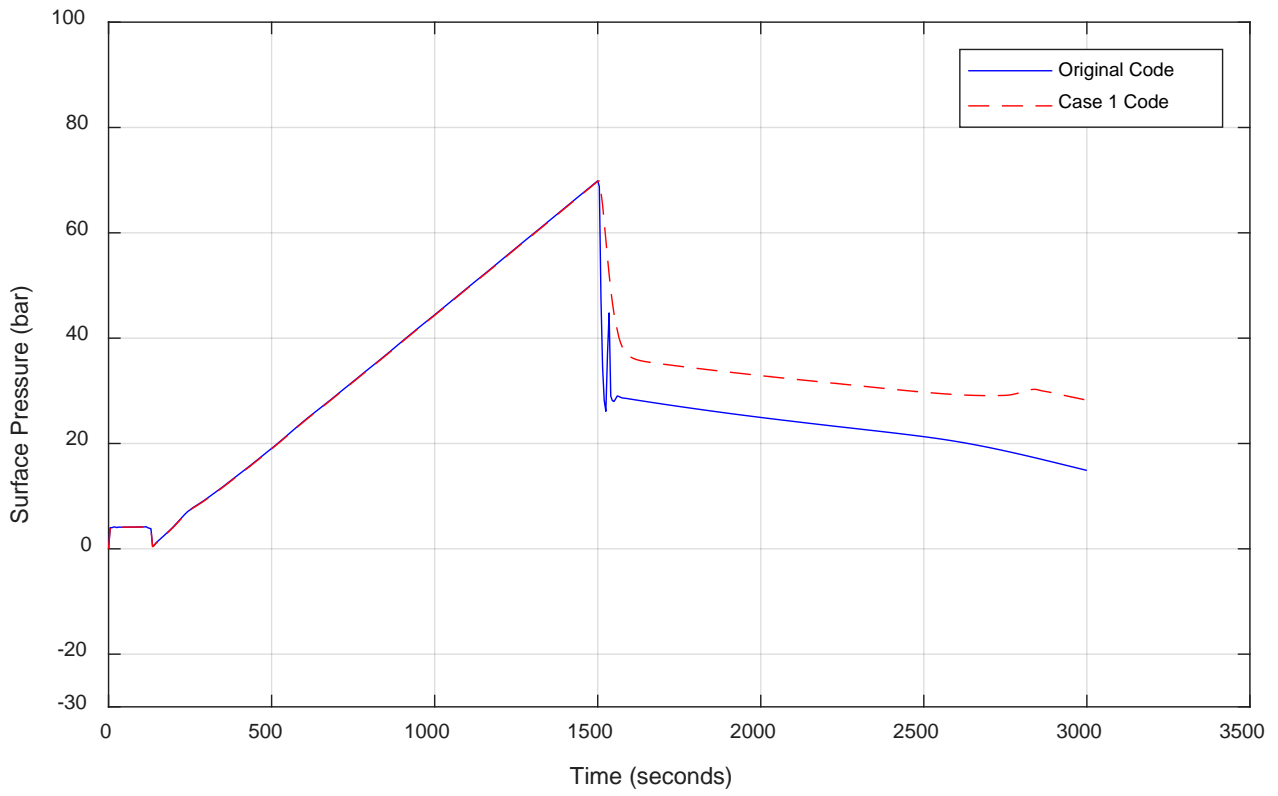


Figure 19 - Surface Pressure vs Time for Case 1

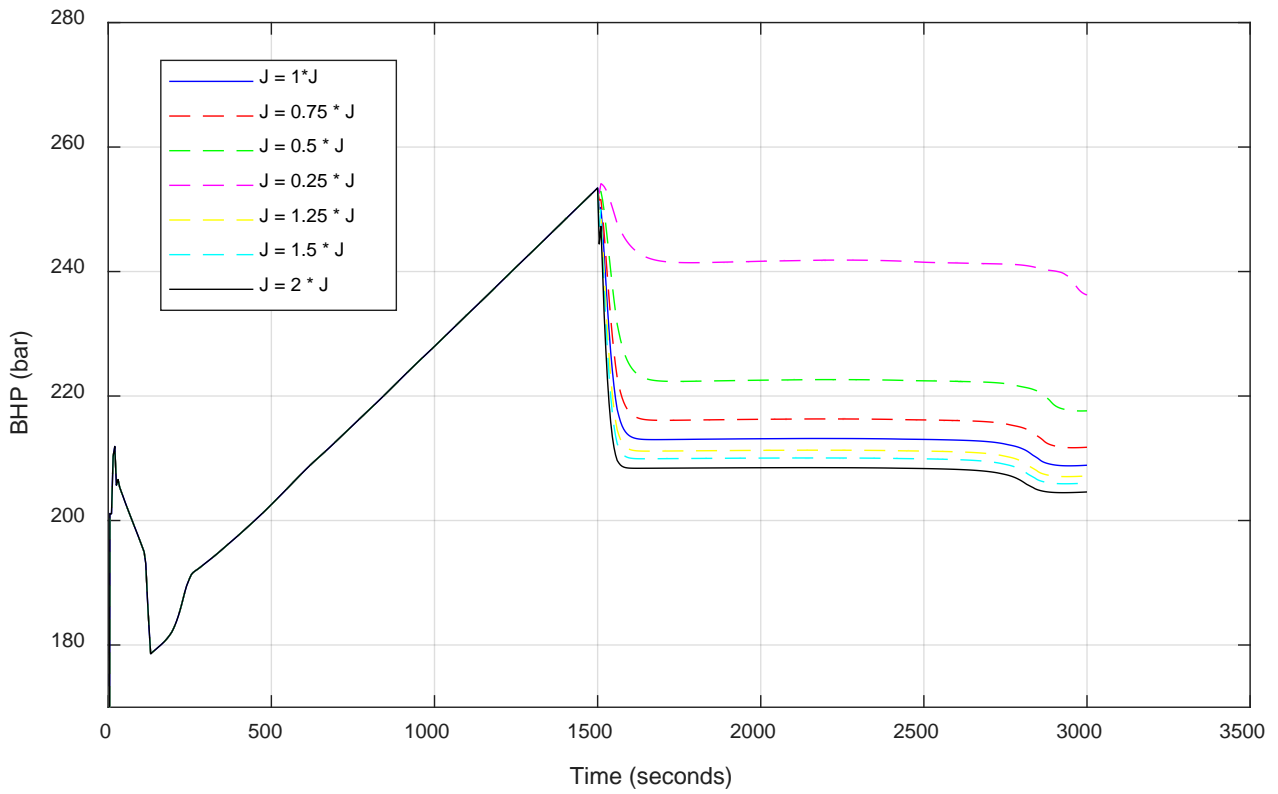


Figure 20 - Bottom Hole Pressure vs Time for Different Injectivities for Case 1

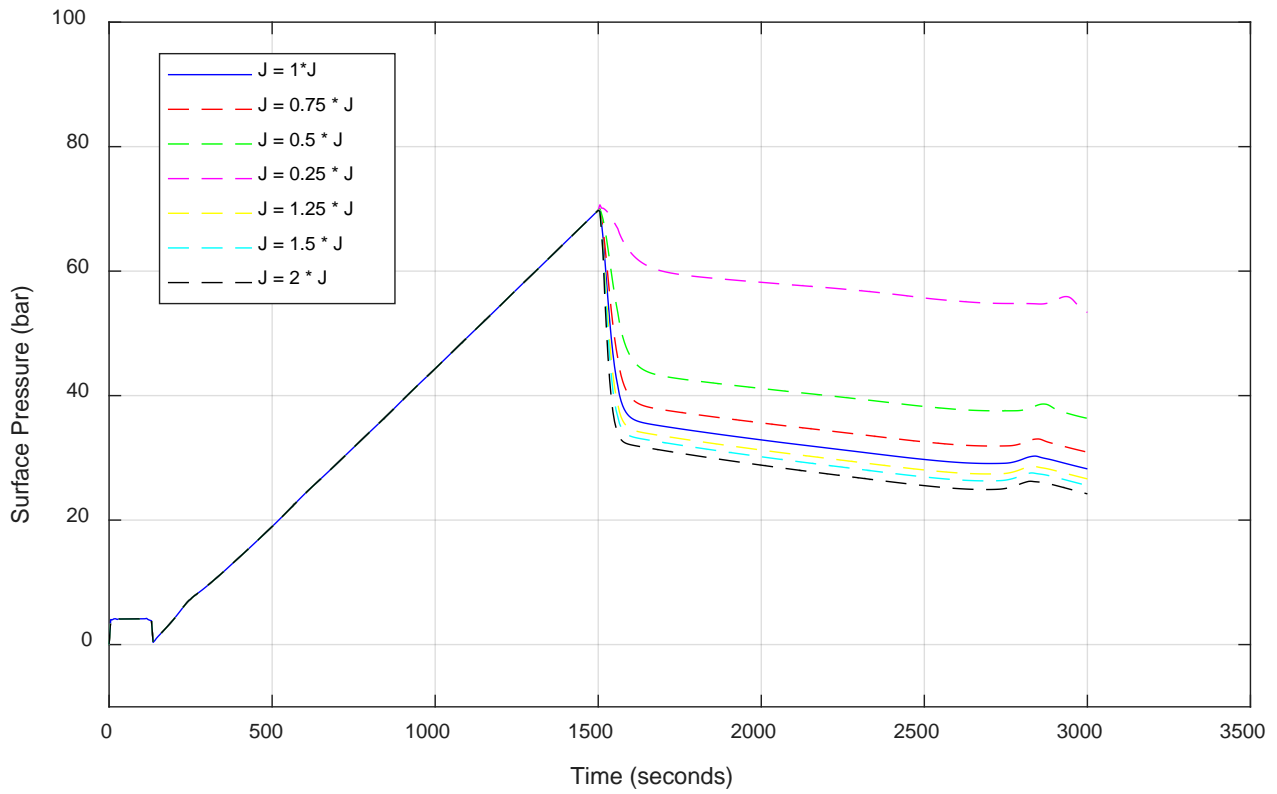


Figure 21 - Surface Pressure vs Time for Different Injectivities for Case 1

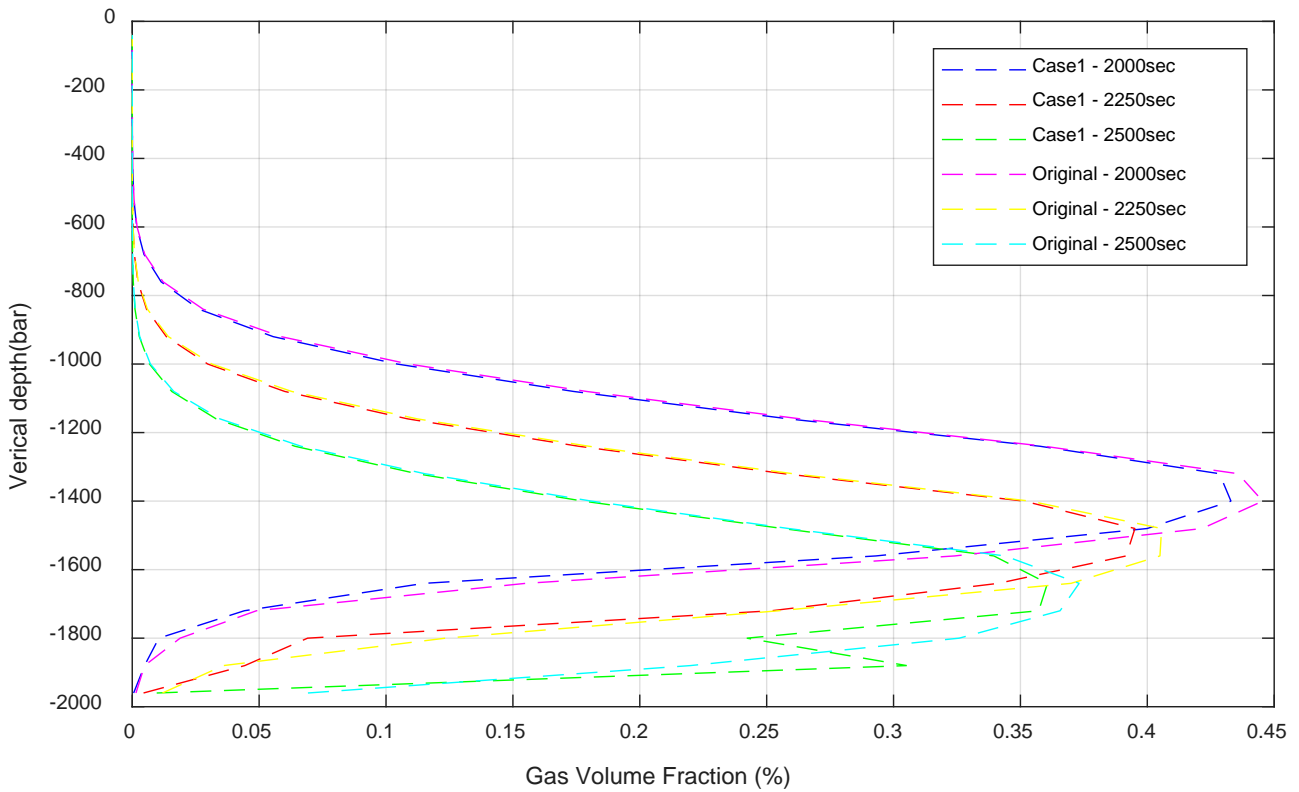


Figure 22 - Gas Volume Fraction vs Depth for Case 1

6.3 Case 2 – Flowback to Reservoir During Kick Rise in Boundary Conditions

In case 2, the goal is to put the injectivity model in use during the time the kick rises through the well, and the well is closed. From figure 17, in the time interval 250 – 1500 seconds, the pressure is increasing linearly as the gas rises. In this scenario, the pressure rises in the bottom of the well, but the code has no way for the liquid to go back into the reservoir to even out the pressure. In reality, there is a limit for how much the BHP can increase since fluid will be forced into the formation as the pressure rises. This was considered in paper [5]

6.3.1 Case 2 - Implementation and Preparation

The same model as derived in case 1 is used in this case, the new equation for the mass and momentum fluxes:

$$F_{c,l} = \begin{bmatrix} -\frac{J \cdot (p_{wf} - \bar{p}) \cdot \rho_{l,stc}}{A} \\ 0 \\ -\left(\frac{J \cdot (p_{wf} - \bar{p}) \cdot \rho_{l,stc}}{A}\right) \cdot v_l \end{bmatrix} \quad (52)$$

This time the equation is inserted into the boundary conditions when the well is closed in, which requires to make a condition in the code (wellopening = 0). When this condition is met, equation 52 is used. But it is also necessary to prevent the model from becoming negative, and adding liquid into the well. This happens if the reservoir pressure becomes larger than the well pressure. To do this, another condition is made in the code: if the liquid flux get larger than 0, all liquid fluxes is set to 0:

$$F_{cl} = \begin{bmatrix} 0 \\ 0 \\ 0 \end{bmatrix}$$

To estimate a value for J, the same assumptions are made for this scenario as for case 1:

Average reservoir pressure [Pa]	$\bar{p} = 20000000$
Max liquid flowback rate [kg/s]	$m_l = 25$
Ideal injection pressure difference [Pa]	$\Delta p = 1000000$

All changes done to the code is marked in Appendix with brown color.

6.3.2 Case 2 - Simulation Results

For case 2 simulation was done for bottom hole pressure and surface pressure, compared to original. Liquid velocity and gas volume fraction vs depth is also below:

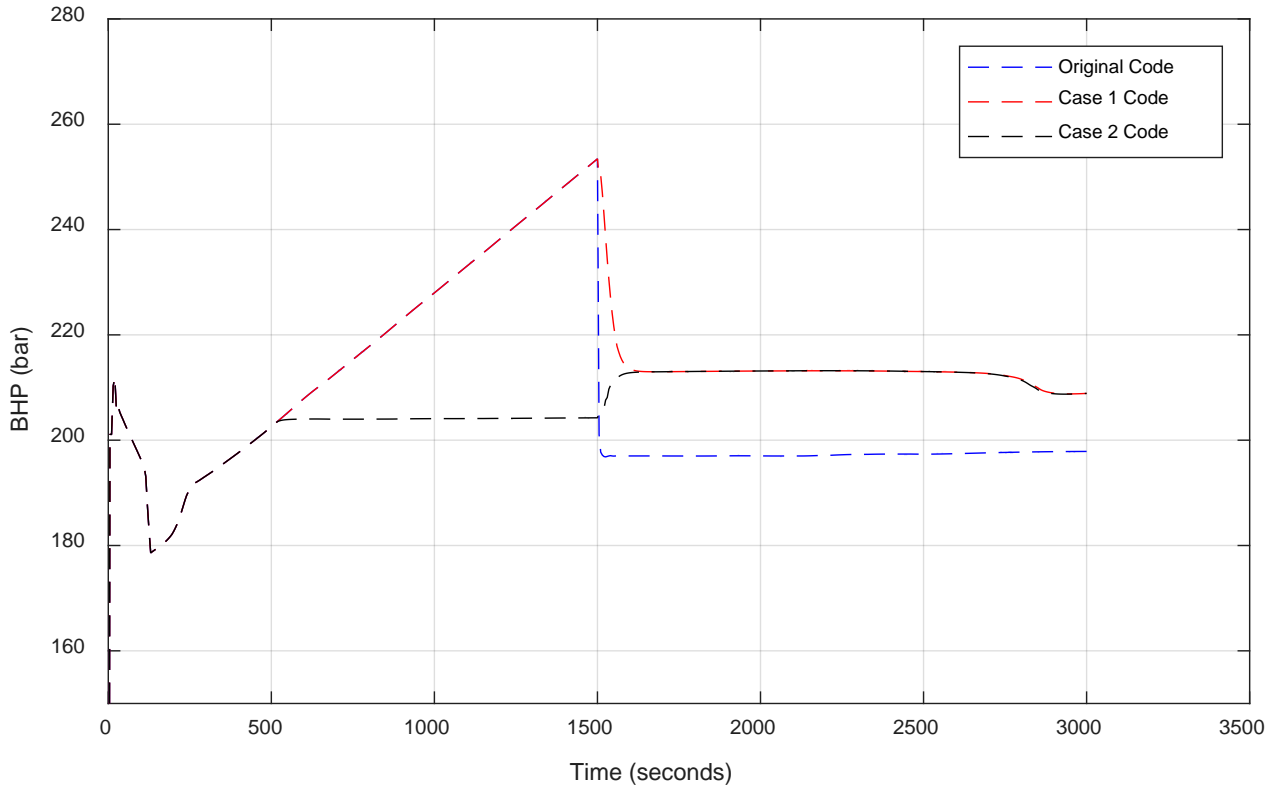


Figure 24 - Bottom Hole Pressure vs Time for Case 2

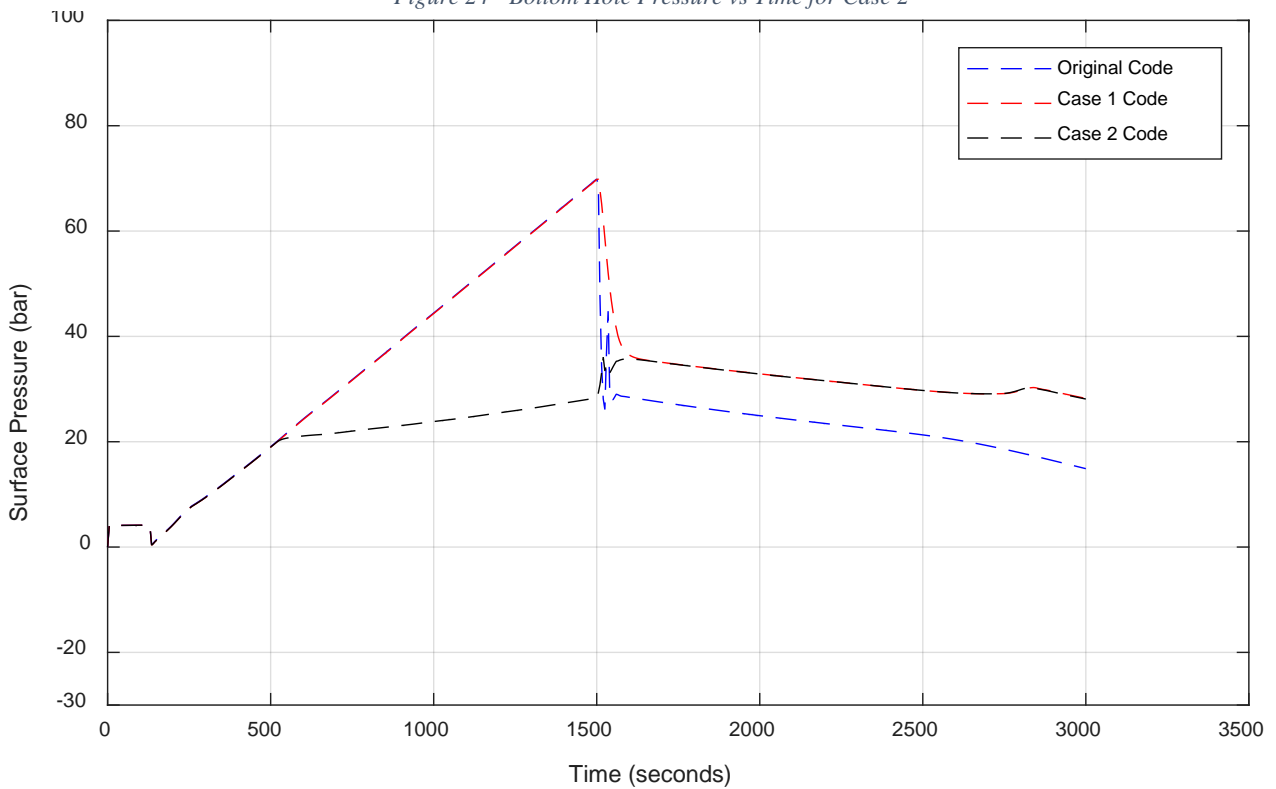


Figure 23 - Surface Pressure vs Time for Case 2

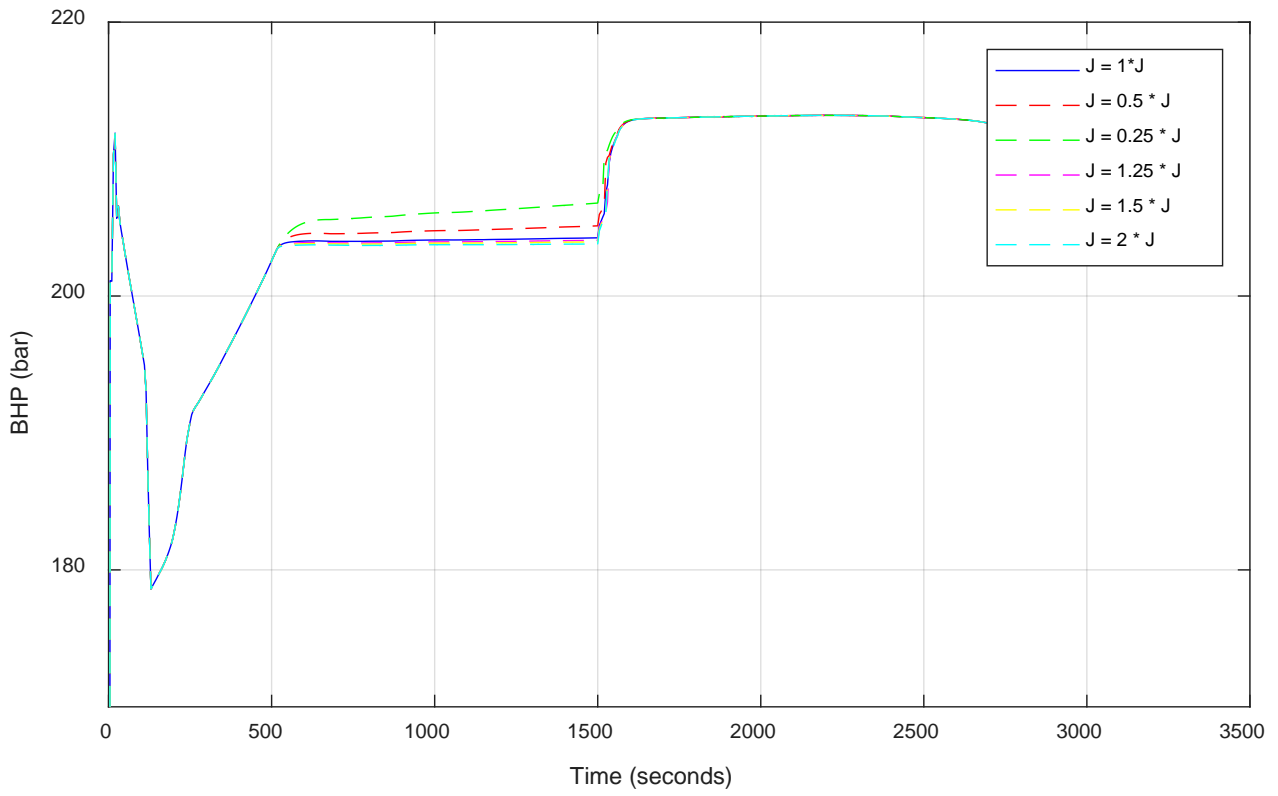


Figure 25 - Bottom Hole Pressure vs Time for Different Injectivities for Case 2

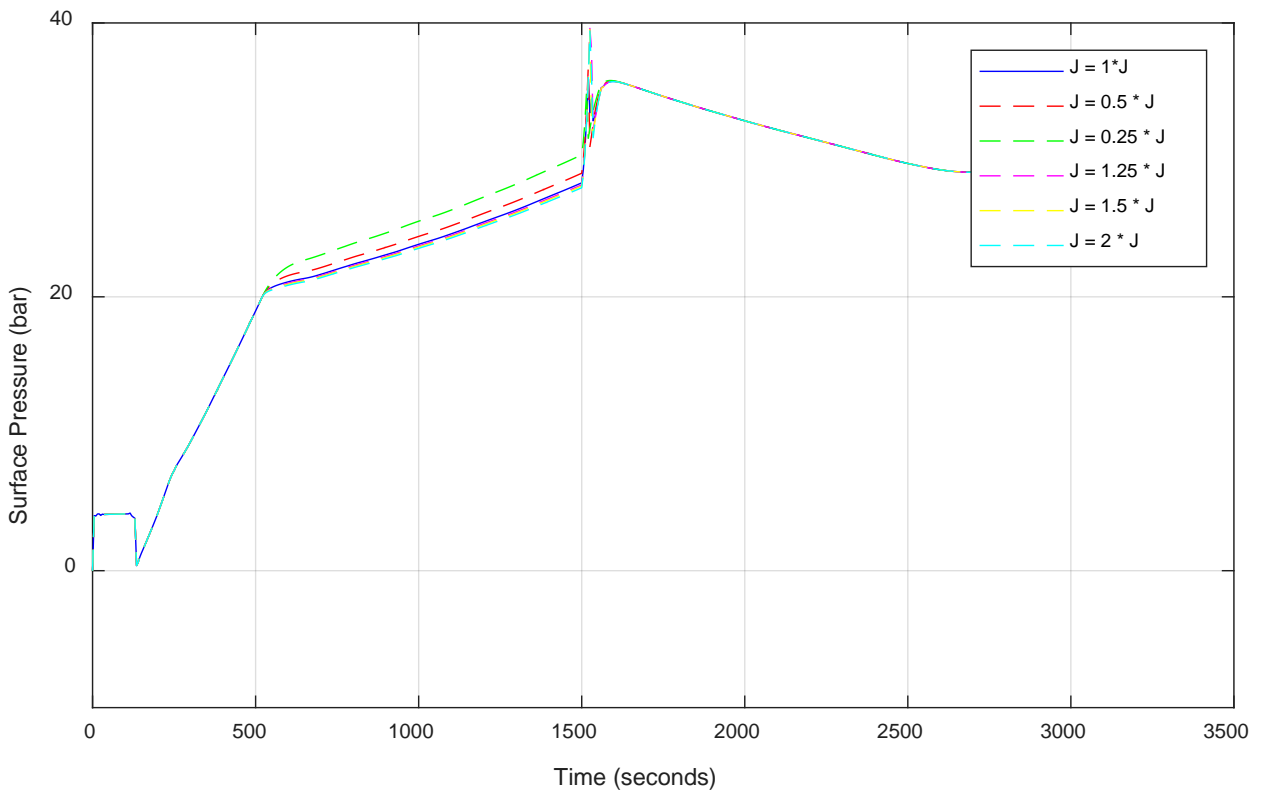


Figure 26 - Surface Pressure vs Time for Different Injectivities for Case 2

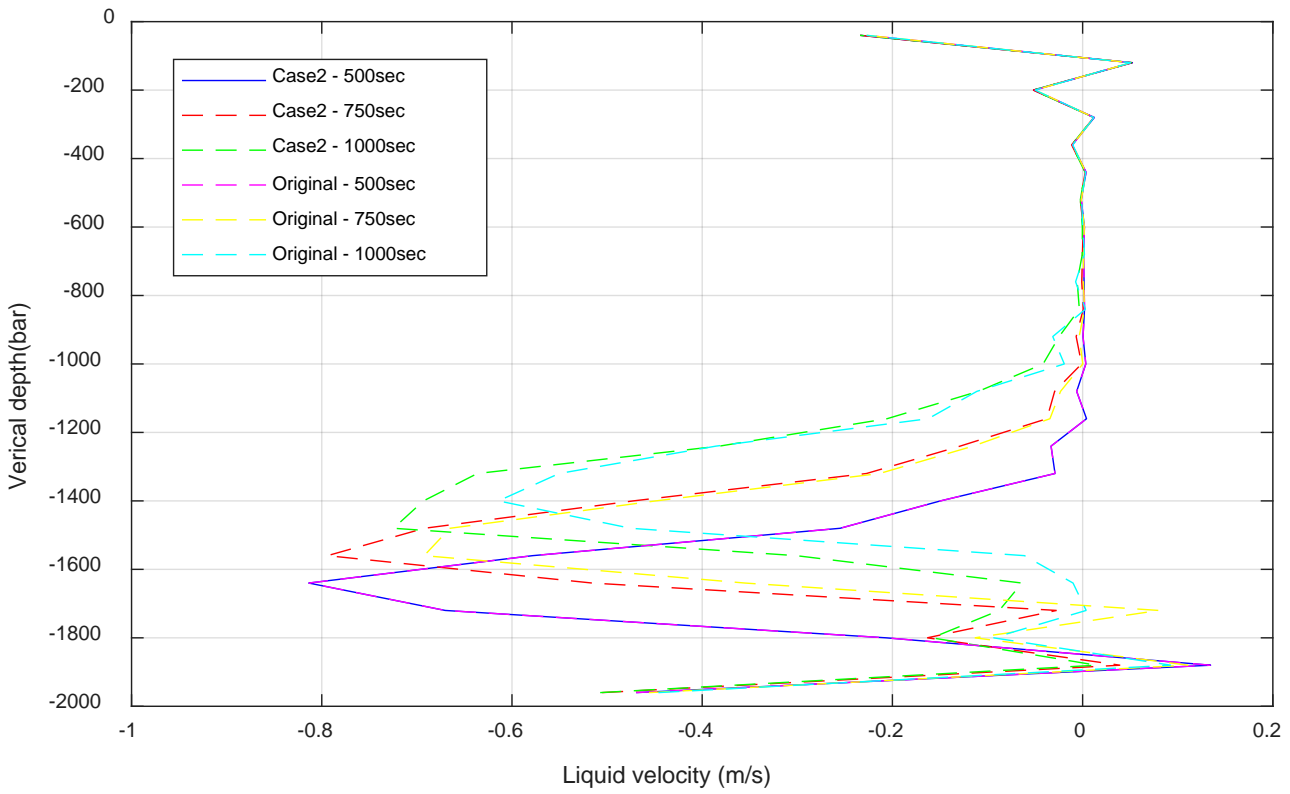


Figure 27 - Liquid Velocity vs Depth for Case 2

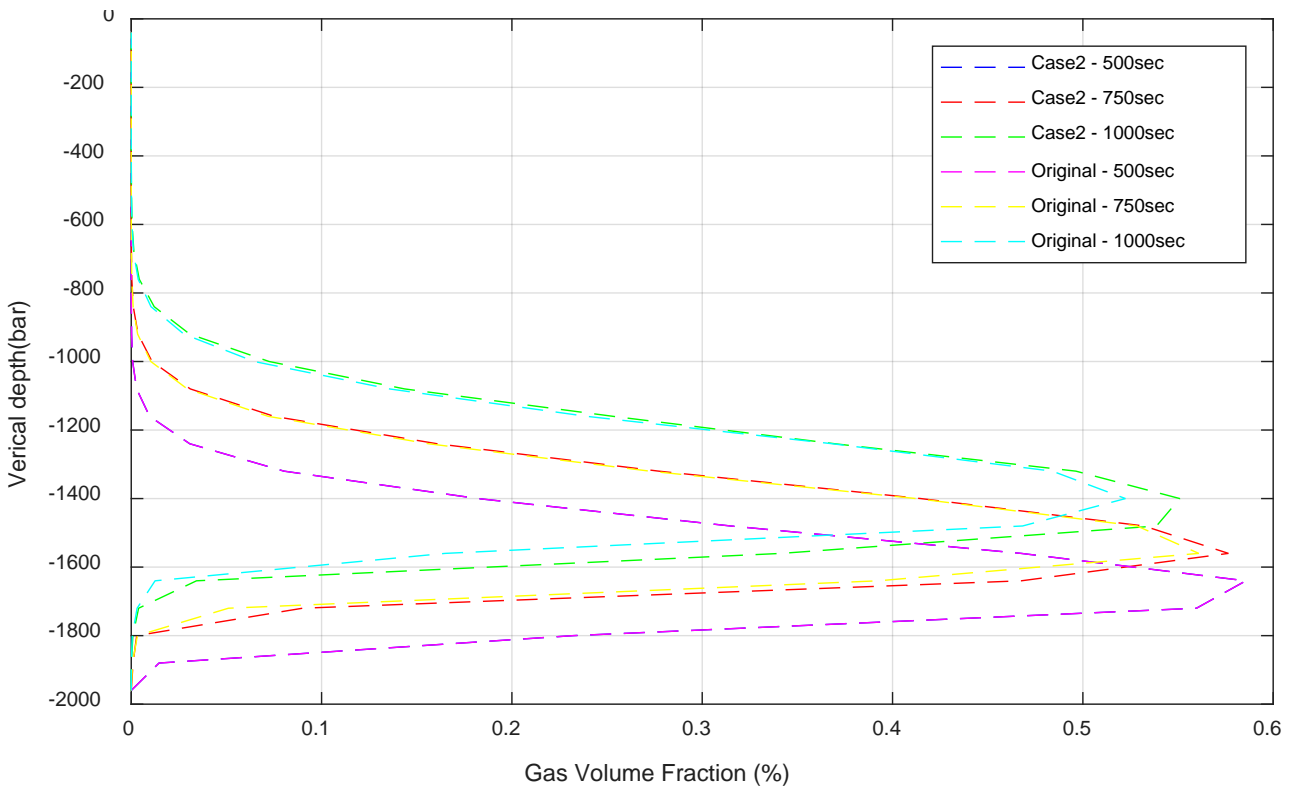


Figure 28 - Gas Volume Fraction vs Depth

6.4 Case 3 – Injection Model During Bullheading in Source Term.

The goal of case 3 is very similar to case 1. We want to make the injectivity index model work during the bullheading phase of the simulation, but this time by implementing it as a part of the source term. The main difference between these two ways is how the model is treated in the first cell. As an influx boundary condition, the injectivity will force the fluid out of the cell at the first boundary flux, but when implemented in the source term, the fluid will leave in the middle of the cell. In the previous simulations, a well discretization of 25 cells was used, and with a total well length of 2000 meters, this means that each cell has a length of 80 meters. This makes a 40-m difference between the two methods, with respect to where the fluid is physically injected. Figure 29 below illustrates the difference between the two in the bottom boundary cell, where the red arrows represent the flux injection and the blue arrows represent source term injection.

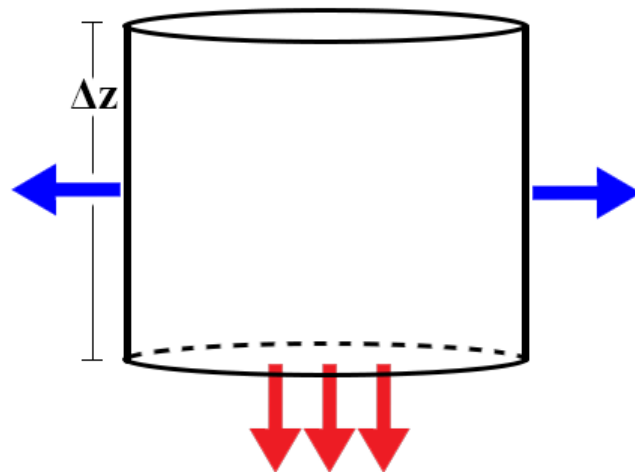


Figure 29 - Physical Difference Between Source Term and Boundary Flux Injection in Bottom Cell

6.4.1 Case 3 - Implementation and Preparation

Same as for case 1, the changes will be performed for the operation in the 1500 – 3000 seconds interval. The same way of assuming an ideal value for the injectivity index is also used, with the same values:

Average reservoir pressure [Pa]	$\bar{p} = 20000000$
Max liquid flowback rate [kg/s]	$m_l = 25$
Ideal injection pressure difference [Pa]	$\Delta p = 1000000$

Table 10 - Values Used to Estimate Injectivity Index in Case 3

The equation that is to be modified now is the timestep update equation, equation 34, which calculates new variables for each timelevel. It is described in more detail in subchapter ‘4.3 The AUSMV Scheme’ in this thesis.

$$U_j^{n+1} = U_j^n - \frac{\Delta t}{\Delta z} (F_{j+1/2}^{AUSMV} - F_{j-1/2}^{AUSMV})^n - \Delta t Q_j^n$$

In this expression Q_j^n represents the source term which will be updated to include the injection model. By using equation (47) we can write the source term as:

$$\Delta t Q_j^n = \Delta t \cdot \frac{J \cdot (p_{wf} - \bar{p}) \cdot \rho_{l, stc}}{A \cdot \Delta z} \quad (53)$$

which has the units of $[kg/m^3]$. The expression will only be calculated for $j=1$, the first cell and used in the mass conservation laws for liquid. In the code version of the equation the area, A , is not included because the area has already been included in the conservative variables. Two conditions are set for the new model. The first says that the model can only be used during the bullheading part of the simulation, hence $Bullheading = 1$ in the code. The second is related to the fact that the source term is a part of the timestep update equation, which is located outside the boundary condition part of the code. That is why it is necessary to set a condition which only allows the new source term to be used for cell nr. 1 in the discretization.

Because the model is now implemented in the source term, it is necessary to stop injection of fluid through the boundary flux, hence the convective liquid fluxes for bullheading is set to 0:

$$F_{cl} = \begin{bmatrix} 0 \\ 0 \\ 0 \end{bmatrix}$$

The estimated injection index in the code is interpolated the same way as in case 1. All changes written in the code is marked in purple.

6.4.2 Case 3 - Simulation Results

The Simulation results will be compared with the original code and case 1 for bottom hole pressure and surface pressure. Also, it will be simulated for different values of J.

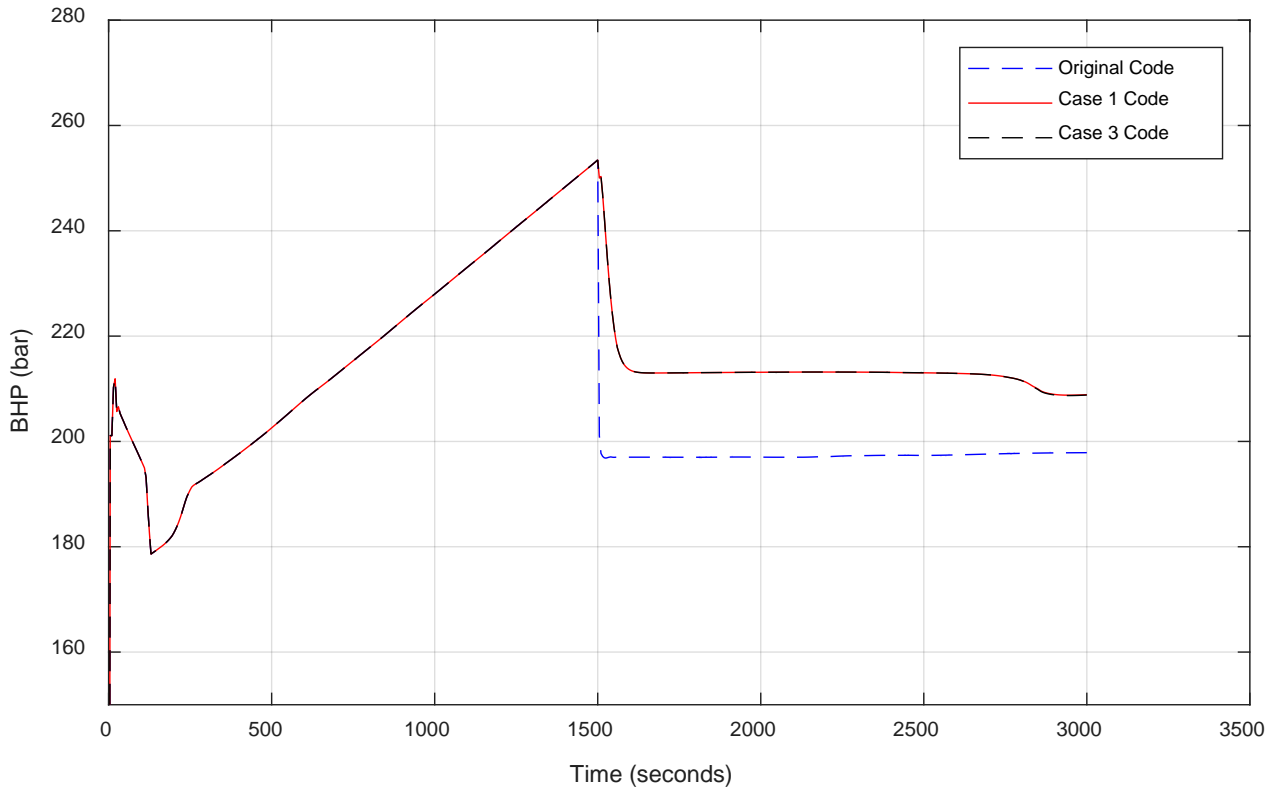


Figure 30- Bottom Hole Pressure vs Time for Case 3

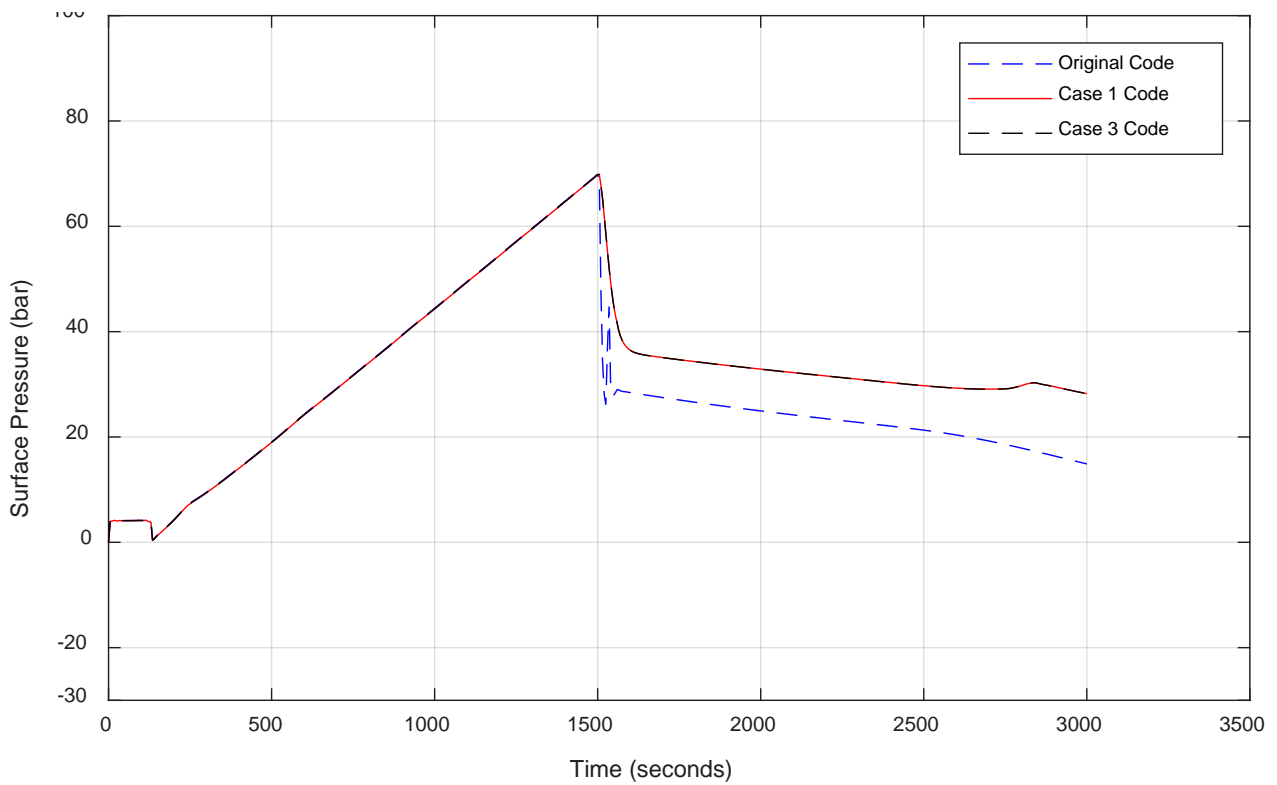


Figure 31 - Surface Pressure vs Time for Case 3

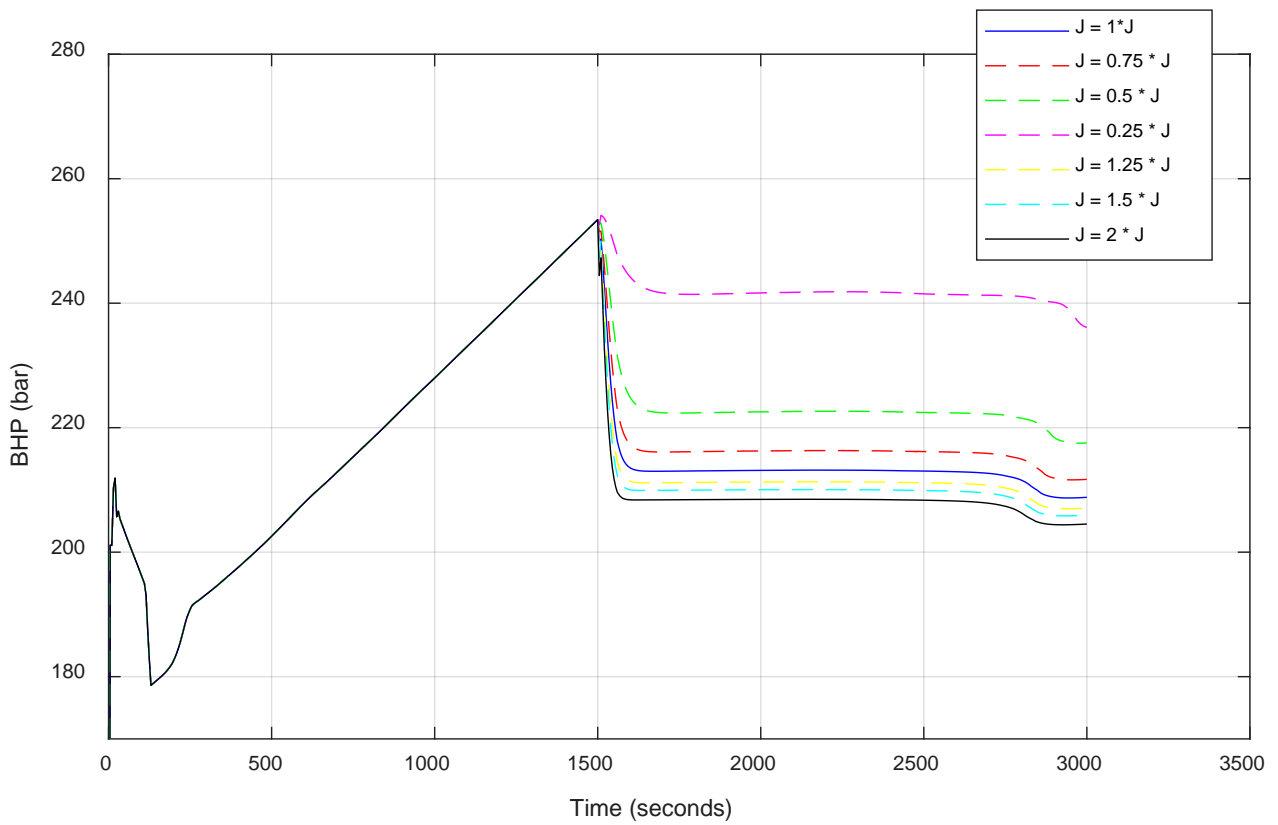


Figure 32 - Bottom Hole Pressure vs Time for Case 3

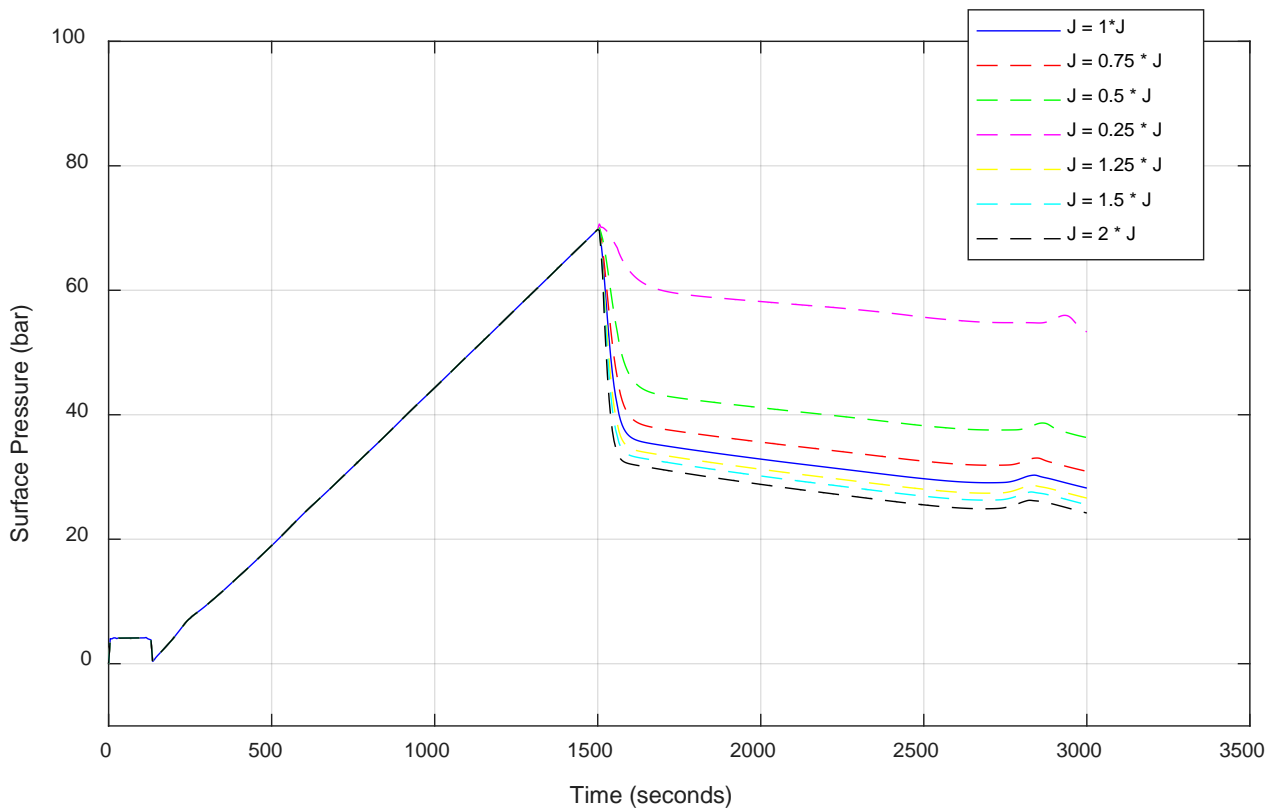


Figure 33 - Surface Pressure vs Time for Case 3

6.5 Case 4 – Flowback to Reservoir During Kick Rise in Source Term.

In case 4 the objective is to combine what is done in case 2 and case 3. The goal is to use the new source term equation to handle the fluid injection caused by the kick. As described in case 2, the pressure will increase at the bottom of the well as the kick rises through the well. In the original version of the code this is shown in the bottomhole pressure plot. But as described, this pressure buildup will cause an injection of fluid.

6.5.1 Case 4 - Implementation and Preparation

The same source term equation as derived in case 3 will be used, but it is important to define new conditions for when the expression will be used. Because the expression is outside the boundary condition section of the code, the first condition must be to only use the equation for the first cell ($j=1$). The next condition is to only use the expression when the well is closed, which is the time interval when the kick rises. Finally, a condition must also be made to make sure the equation don't produce liquid into the well if the reservoir pressure should be larger than the wellbore pressure. When all three conditions are met the equation will be used and inject well fluid into the reservoir as the pressure rises.

The same assumptions to calculate an ideal injection index is used for this case:

Average reservoir pressure [Pa]	$\bar{p} = 20000000$
Max liquid flowback rate [kg/s]	$m_l = 25$
Ideal injection pressure difference [Pa]	$\Delta p = 1000000$

Table 11 - Values Used to Estimate Injectivity Index in Case 4

All changes made is highlighted with pink and white font in the code.

6.5.2 Case 4 - Simulation Results

The Simulation results will be compared with the original code, case 2 and case 3 for bottom hole pressure and surface pressure. Also, it will be simulated for different values of J.

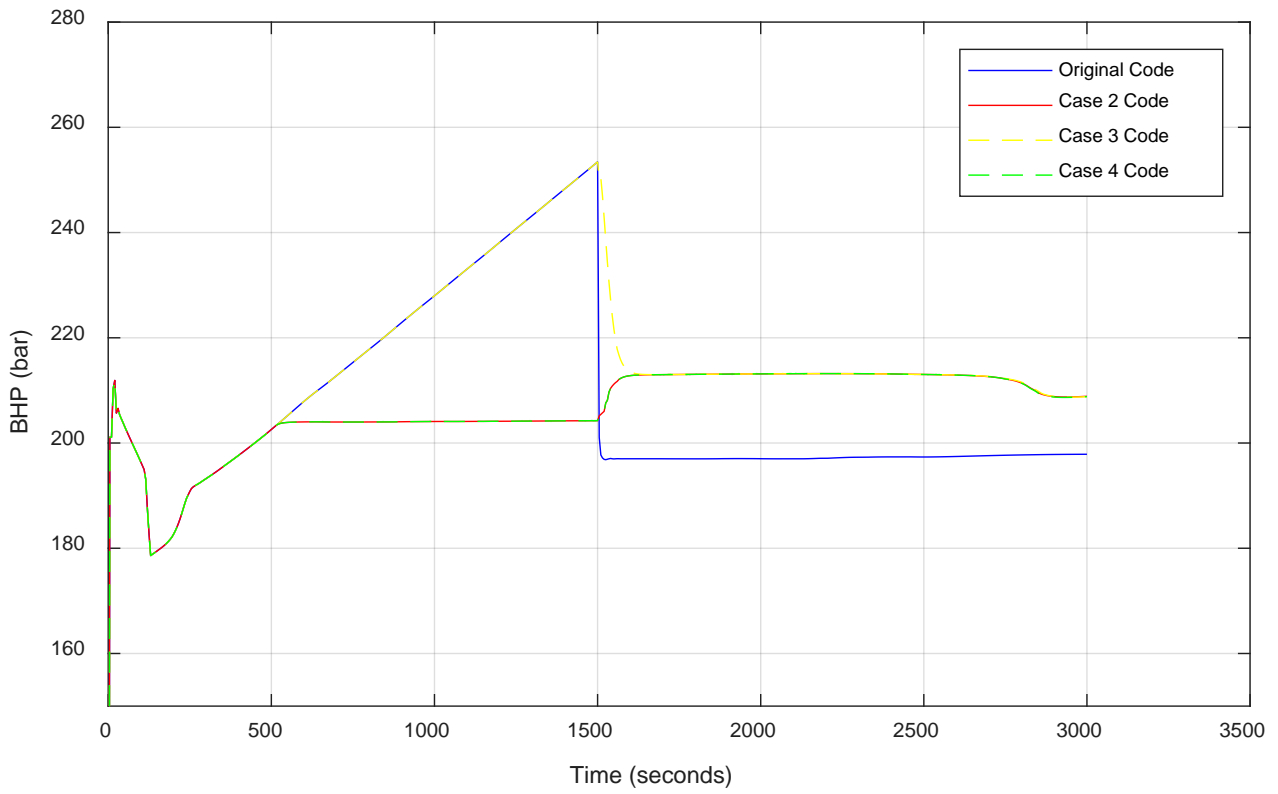


Figure 34 - Bottom Hole Pressure vs Time for Case 4

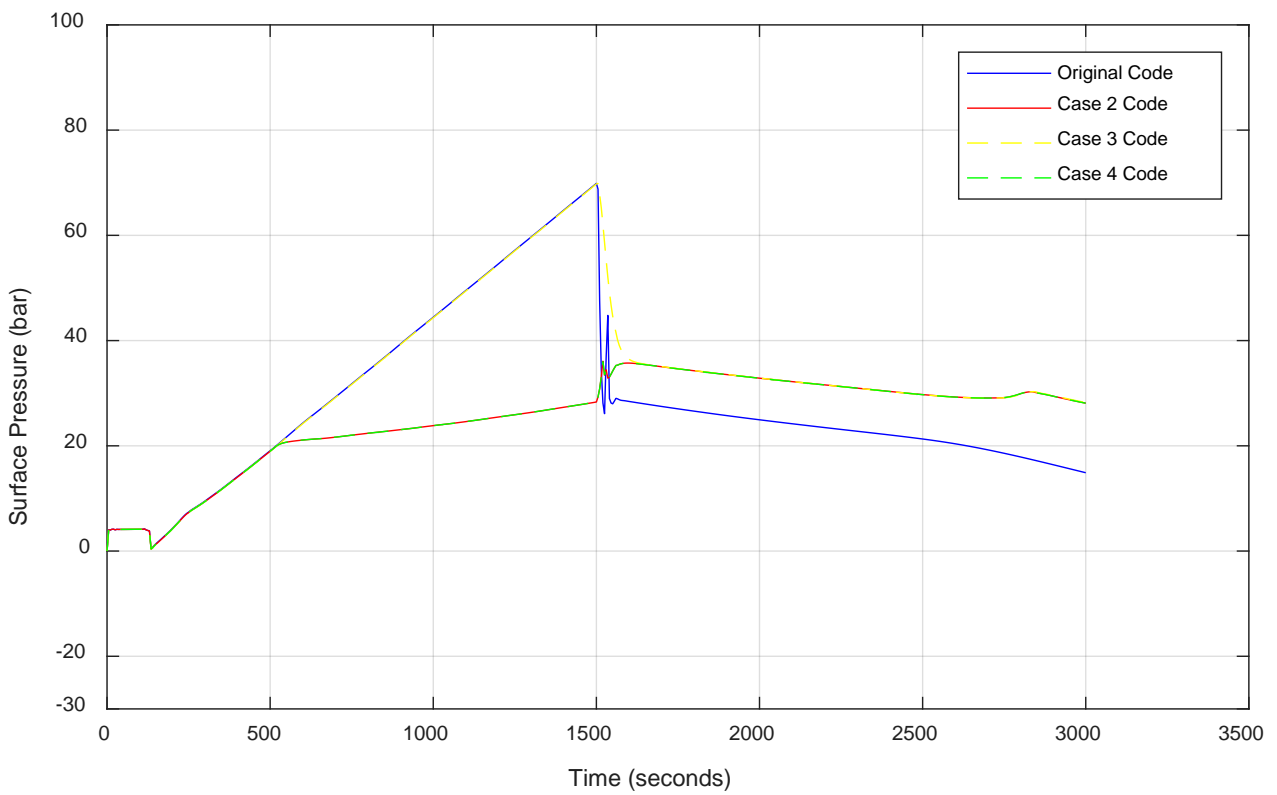


Figure 35 - Surface Pressure vs Time for Case 4

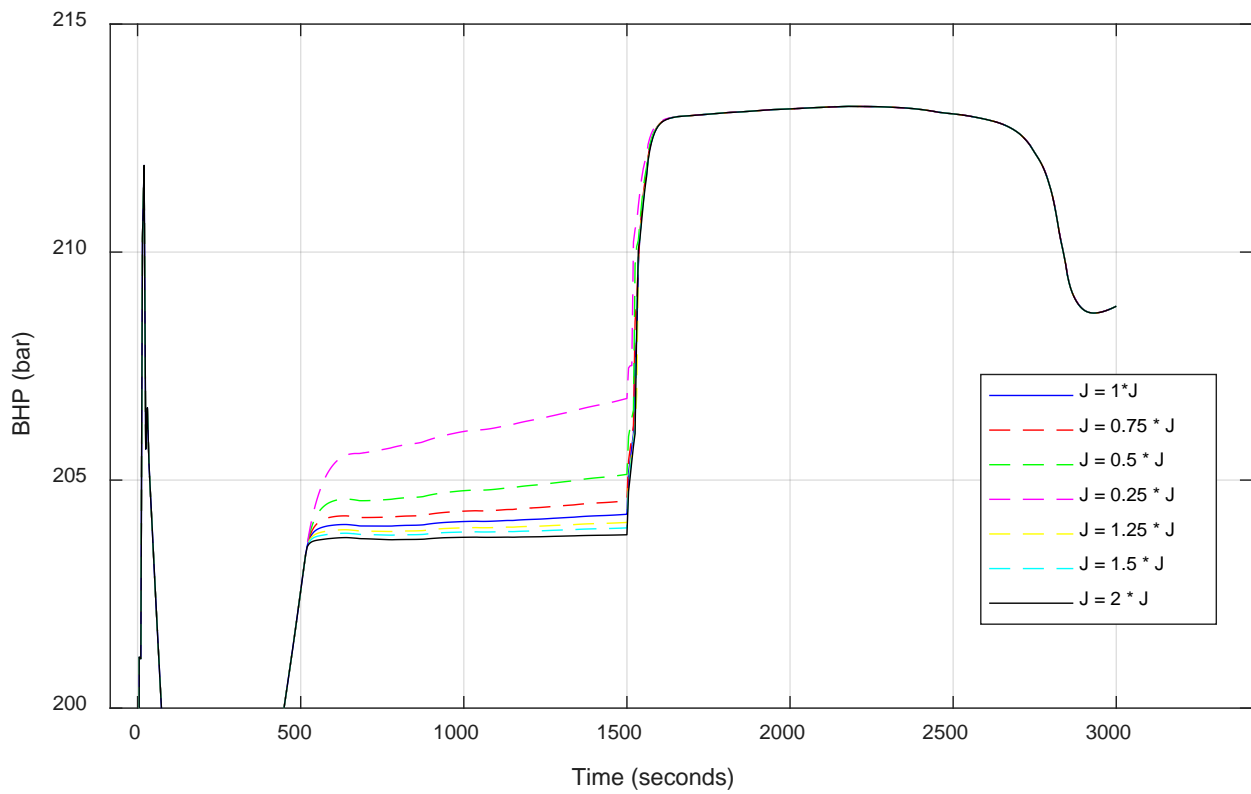


Figure 36 - Bottom Hole Pressure vs Time for Different Injectivities for Case 4

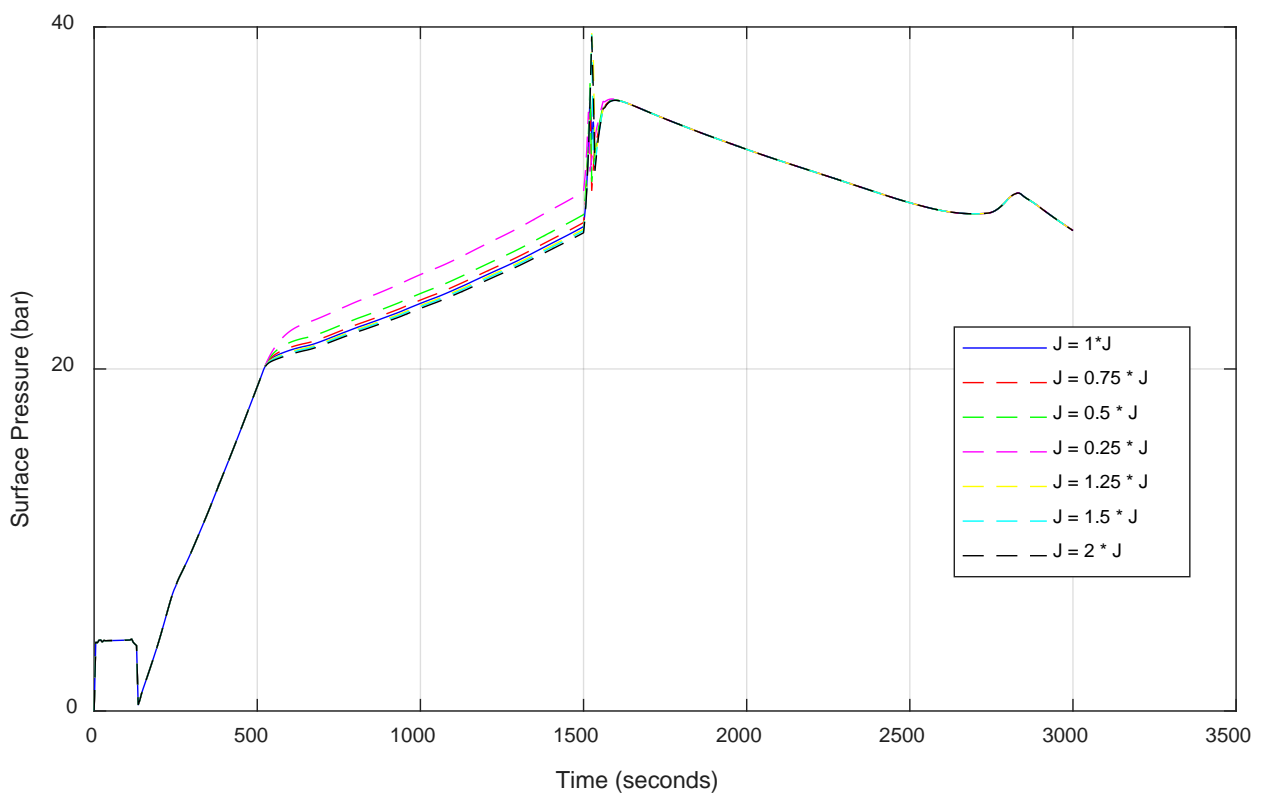


Figure 37 - Surface Pressure vs Time for Different Injectivities for Case 4

6.6 Case 5 –Taking the Kick with The Injectivity Model.

In this case, we want to use a PI model produce the kick into the well instead of specifying a gas mass rate in the flux at the bottom cell. The case is much more experimental than the previous cases, as the injectivity model is only defined for liquids. Simulating a realistic gas kick scenario would take a more complex model, considering the ideal gas law, compressibility and other variables. However, we found it interesting to see how the code would handle a simplified scenario, and how the results would be affected. In the following simulation, changes will be applied to the case 4 code, where all liquid injections are done with the source term injectivity model. Instead of using the injectivity model, we will use a production model. A Production Index (PI) model for gas is used in the source term of the gas mass conservation law. One must make sure that the total sign of the source term is positive. This new PI model for gas, will be implemented alongside the changes from case 4 with injection during shut-in well and bullheading in source term. Simulation will also be done with the original code, where no injection model.

6.6.1 Case 5 - Implementation and Preparation

To make the source term expression produce gas, a certain set of conditions must be made in the code. First, like case 1 and 3, the well must be open ($wellopening = 1.0$). Also, the code will only be valid for the first cell. To produce the kick in the right time interval, a condition for time is made. The expression is only used between 10 seconds and 120 seconds. Interpolation is also used, and is done in the boundary condition section of the code. A final condition is made, to make sure no gas leaves the well at the bottom. Only when the reservoir pressure is larger than the wellbore pressures the code will be active. This will change the sign of the pressure value from positive to negative, and thus make the gas volume be produced into well.

To calculate an ideal production index, these values is used:

Average reservoir pressure [Pa]	$\bar{p} = 20000000$
Gas injection rate [kg/s]	$m_g = 8$
Ideal injection pressure difference [Pa]	$\Delta p = 1000000$

Table 12 - Values Used to Estimate Production Index in Case 5

All changes in the code are marked with dark turquoise font.

6.6.2 Case 5 - Simulation Results

For this case, it is interesting to see how much mass of gas is taken into the system, as well as the volume. The pressure results from the simulation will be compared to case 4 results, as it includes the code from case 3 as well, and the results from the original code.

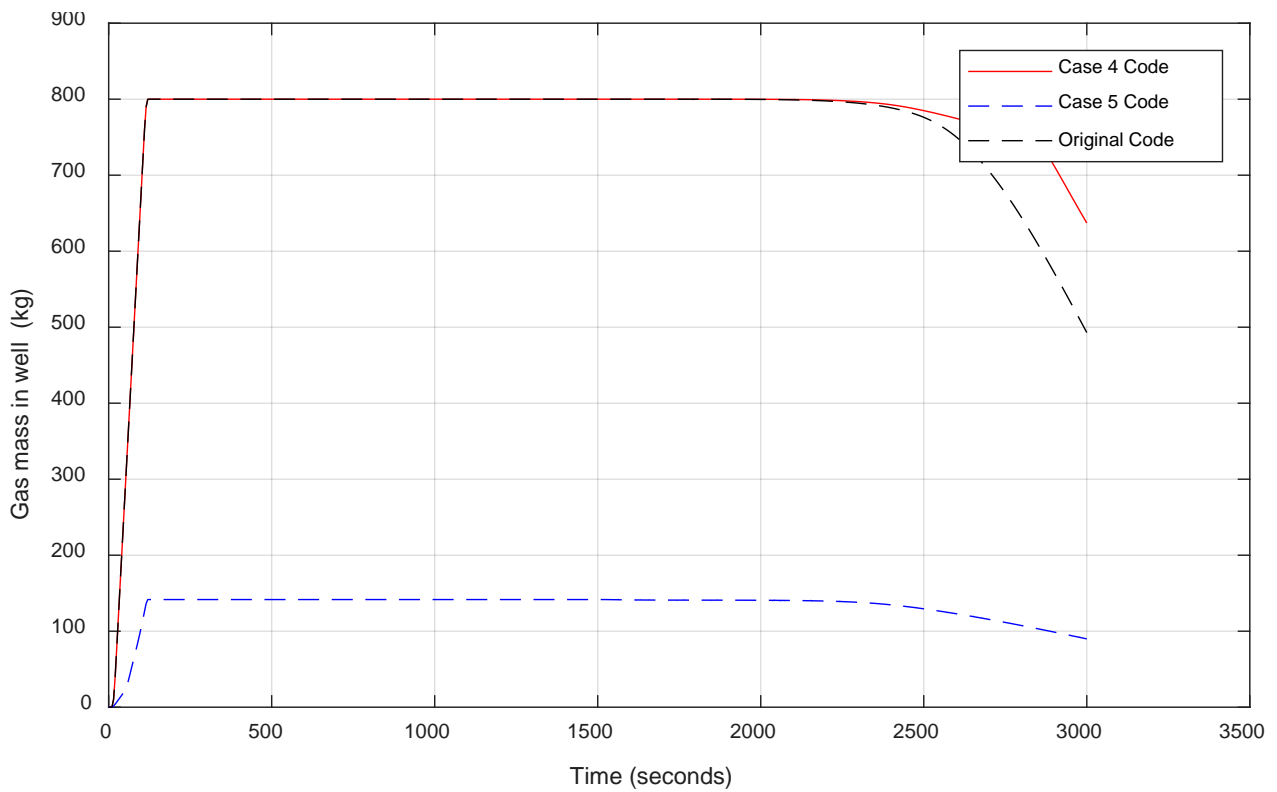


Figure 38 - Gas Mass vs Time for Case 5

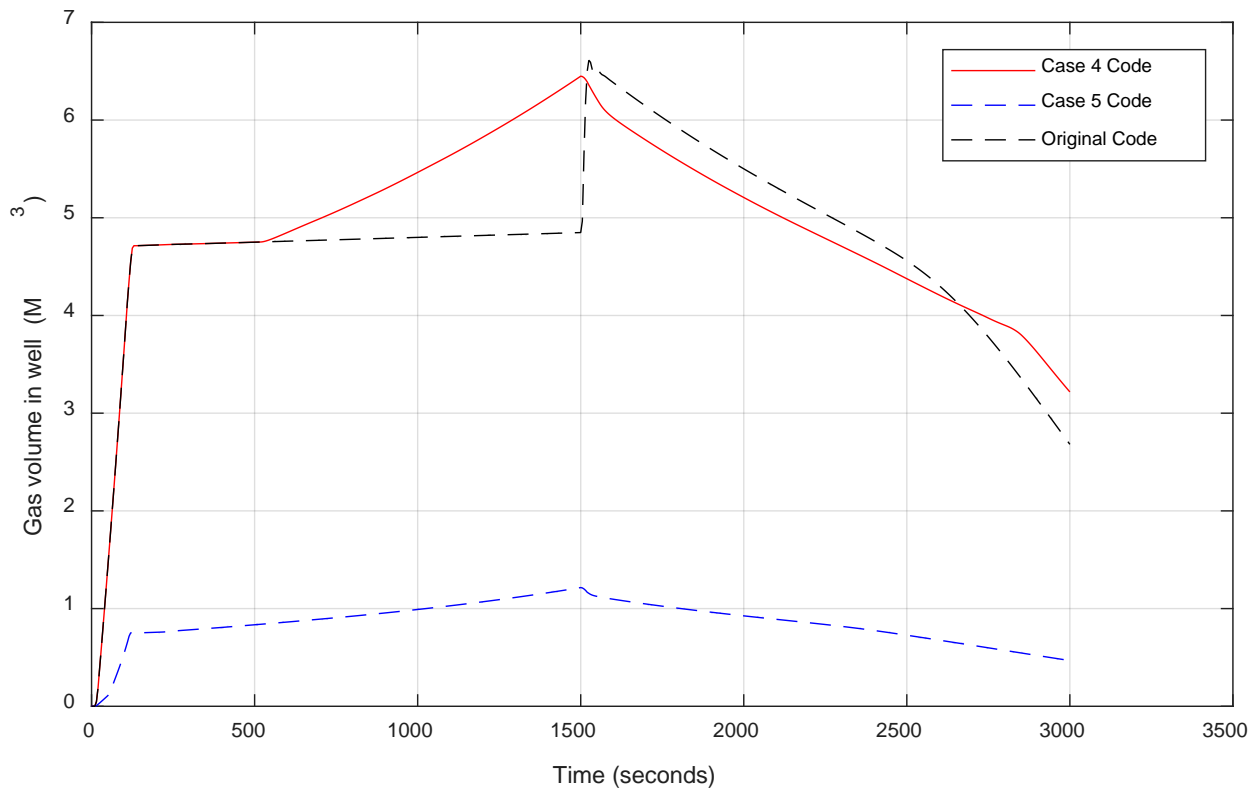


Figure 40 - Gas Volume vs Time for Case 5

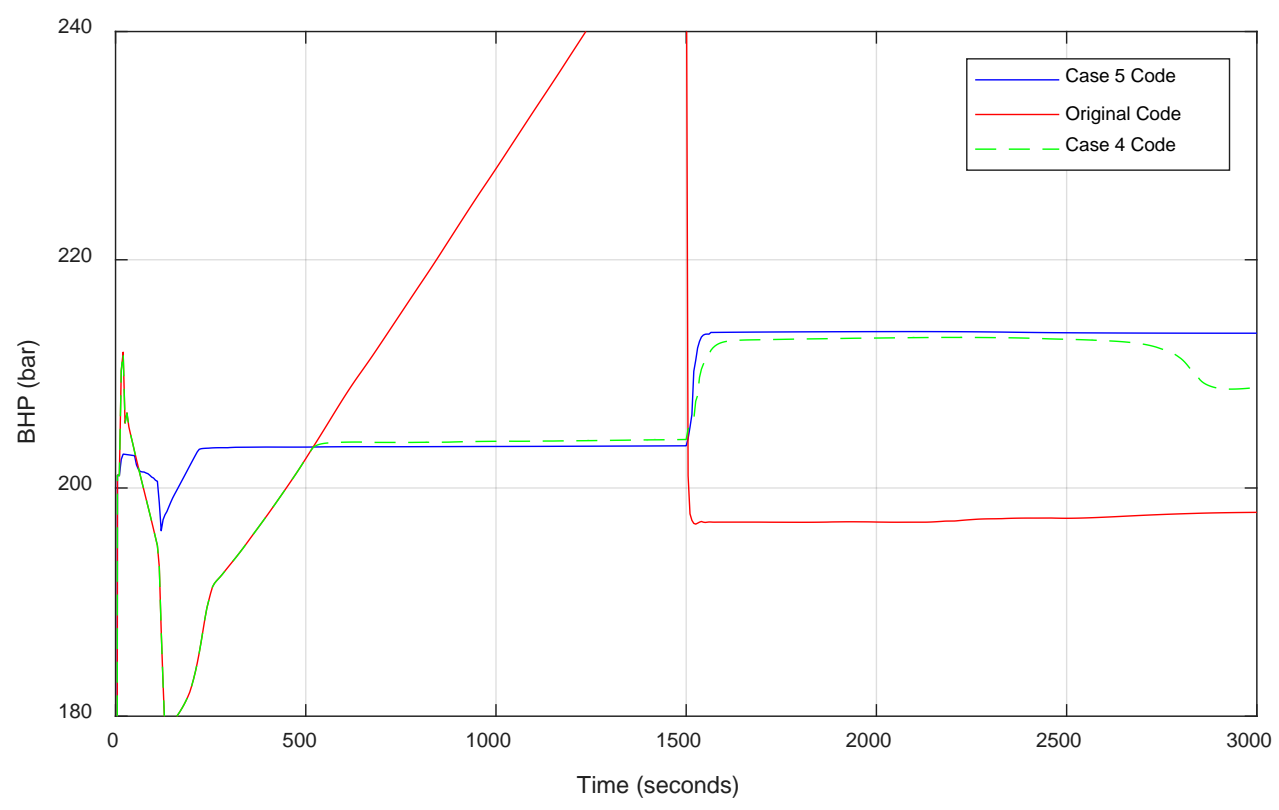


Figure 39 - Bottom Hole Pressure vs Time for Case 5

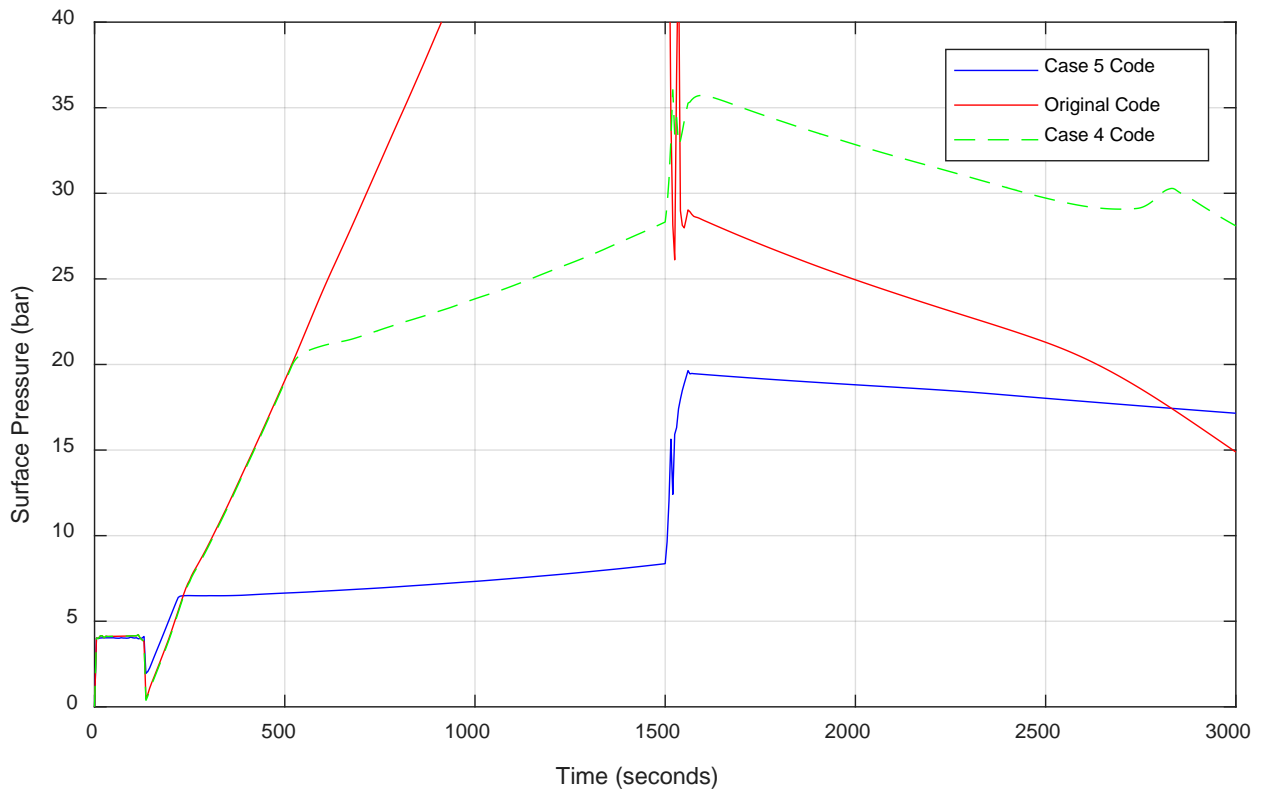


Figure 41 - Surface Pressure vs Time for Case 5

6.7 Case 6 – Effect of Different Boundary Conditions for Slope Limiters

As described in subchapter 4.5 , the AUMSV was upgraded from first to second order to improve on the numerical diffusion which occurs between interfaces in the flow. The concept is to calculate boundary values between all cells in the discretization, instead of using a constant value for each cell. These boundary values are then used to calculate the numerical fluxes. This makes it necessary to define the conditions for the boundary cells, which can be done in two ways. We found it interesting in this thesis to simulate for the two separate ways of handling them, and see how the number of cells and length of timestep affects the results. There is one slope limiter for each cell variable in the system, for a total of 6 slope limiter variables. The variables that are used in the code includes liquid density, pressure, liquid velocity, gas velocity, gas volume fraction and gas density.

6.7.1 Case 6 - Implementation and Preparation

The two methods of calculating slope limiters for the boundary cells was already included in the original code, and still a matter of discussion. We will simply switch between the two pieces of code and simulate for each.

- One method is to first calculate all slope limiters for all cells except the first and last cell. Then the boundary cells are set to be equal to their closest neighbor cells. For instance, pressure slope in cell 1 is set equal to the pressure slope in cell 2.
- The other method is simply to set all boundary cell slope limiters to zero.

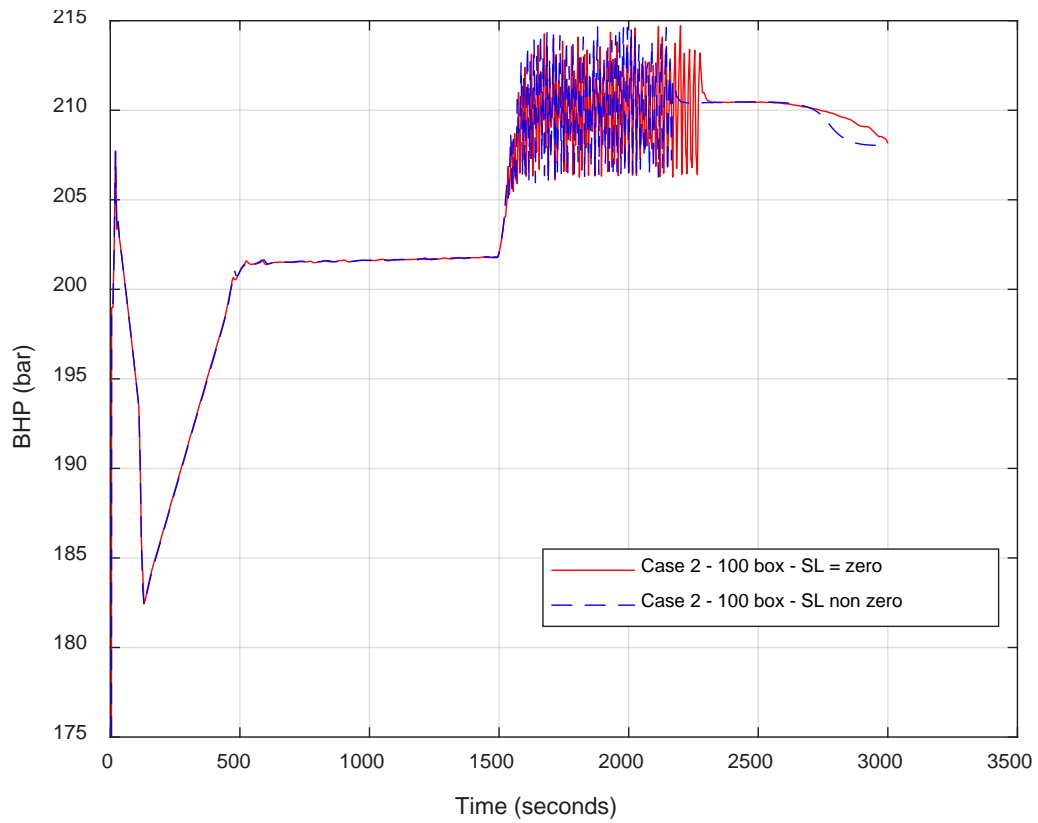
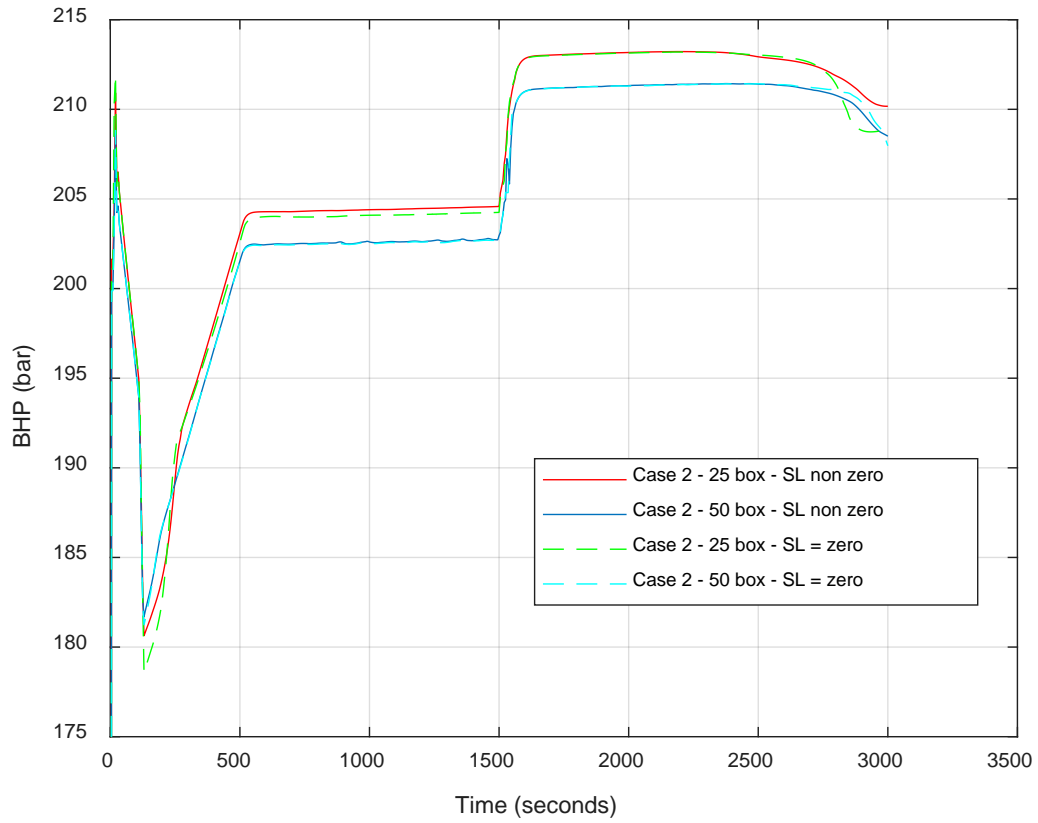
Because these two simulations are related to the discretization of the well, it is also interesting to see effects from number of boxes. Simulations will be run for these different values:

Number of boxes	Timestep	Slope Limiter Condition
25 boxes	0,01	Zero
50 boxes	0,005	Zero
100 boxes	0,0025	Zero
25 boxes	0,01	Extrapolation
50 boxes	0,005	Extrapolation
100 boxes	0,0025	Extrapolation

Table 13 - Slope Limiter Condition vs Number of Boxes and Timestep

All changes made is marked with light blue color in the Appendix.

6.7.2 Case 6 - Simulation Results



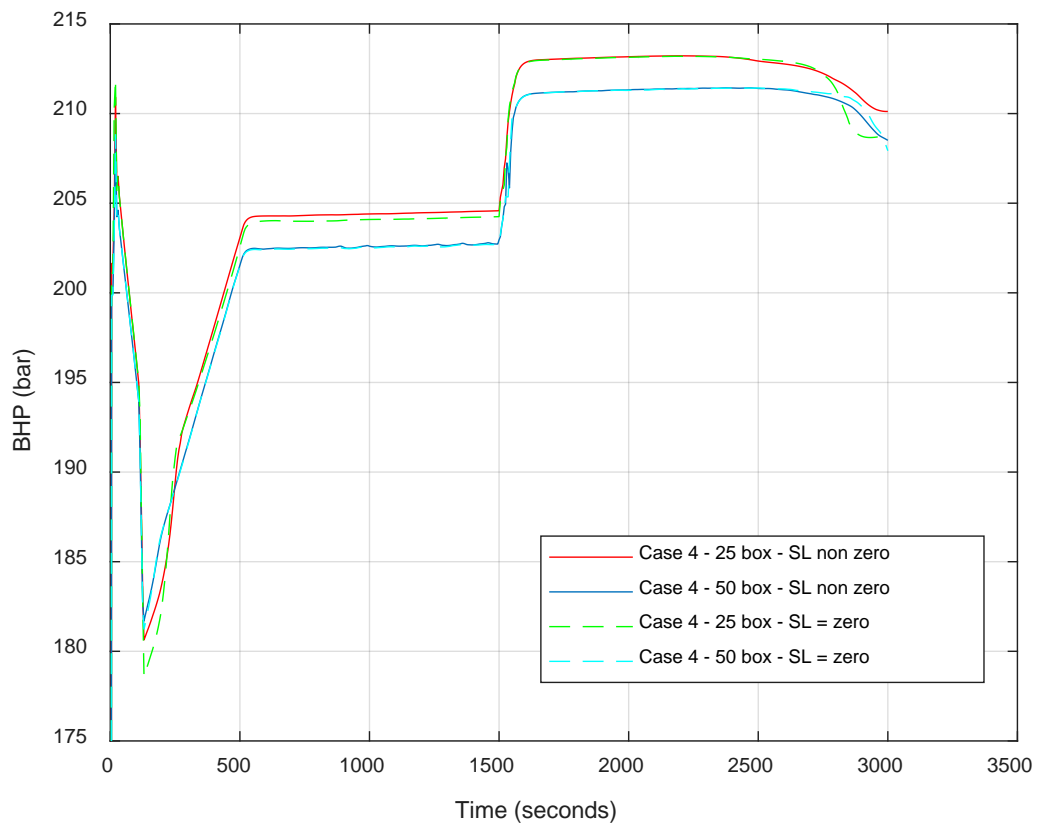


Figure 44 – Bottom Hole Pressure vs Time for Case 6

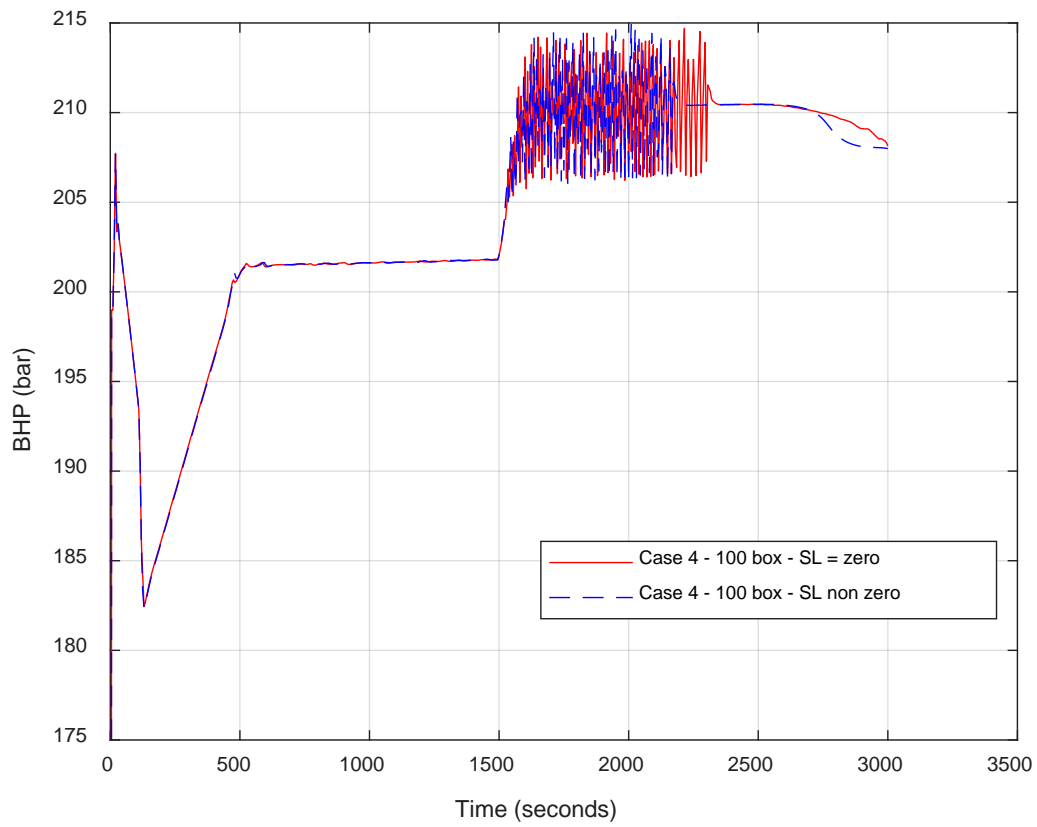


Figure 45 – Bottom Hole Pressure vs Time for Case 6

6.8 Case 7 – Effect of Different Boundary Conditions for Inlet Pressure

In case 7 we wanted to see the how the choice of inlet and outlet pressure boundary condition affected the results. As described in subchapter 4.4 , the original code was presented with two different methods of doing the calculation. The first is an interpolation of the neighbor cells, and the second calculates by using the equation for pressure, which on its most basic form is written as:

$$P = \rho gh + friction$$

6.8.1 Case 7 - Implementation and Preparation

Necessary code to change between the two models was already written in the code, but turned off. All previously simulation was done by using equation 37 and 39, and to get results with the interpolation method, equation 38 and 40, the code had to be activated. All changes made in the code is marked in dark green color.

6.8.2 Case 7 - Simulation Results

Simulations will be done for the original code, the case 2 code and the case 4 code. This way the three different codes can be compared. In the figure, the text legend hydrostatic refers to the use of eq. 37 and 39, and the legend interpolation refers to use of eq. 38 and 40 .

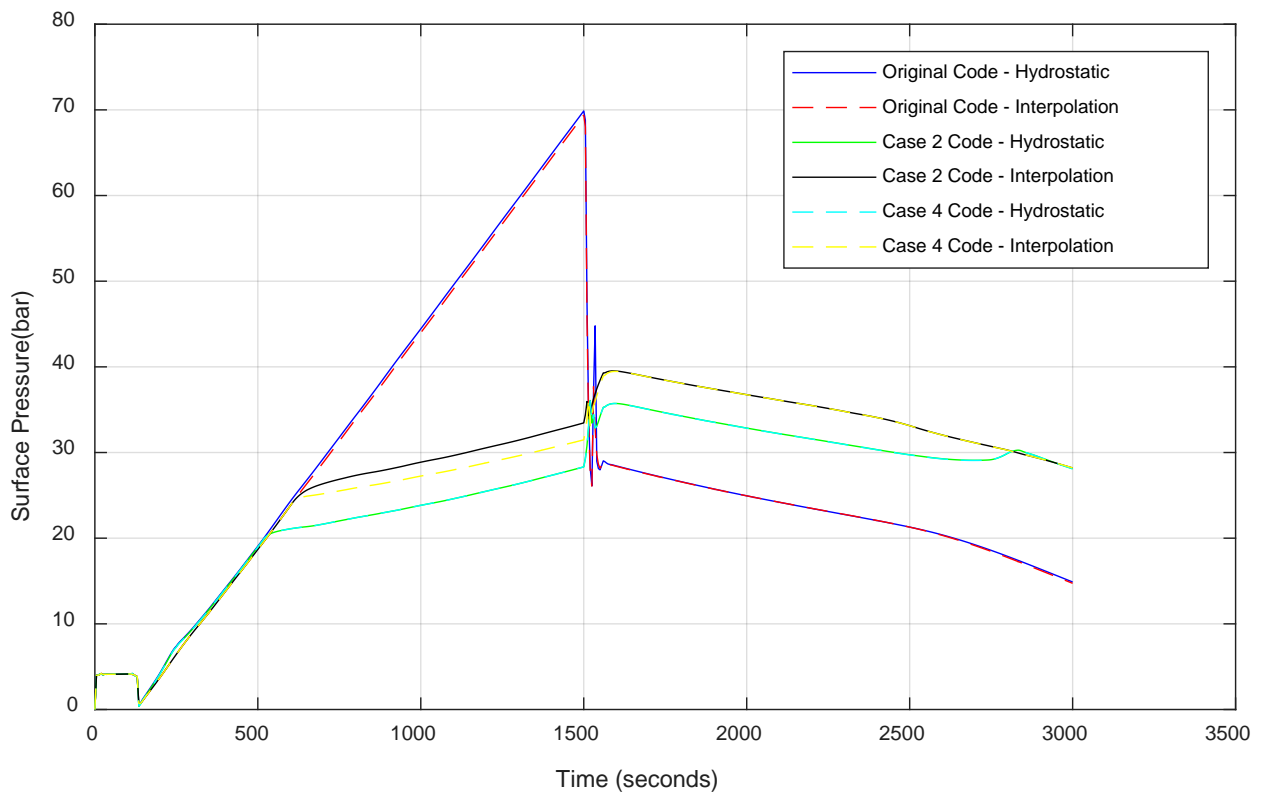


Figure 46 – Surface Pressure vs Time for case 7

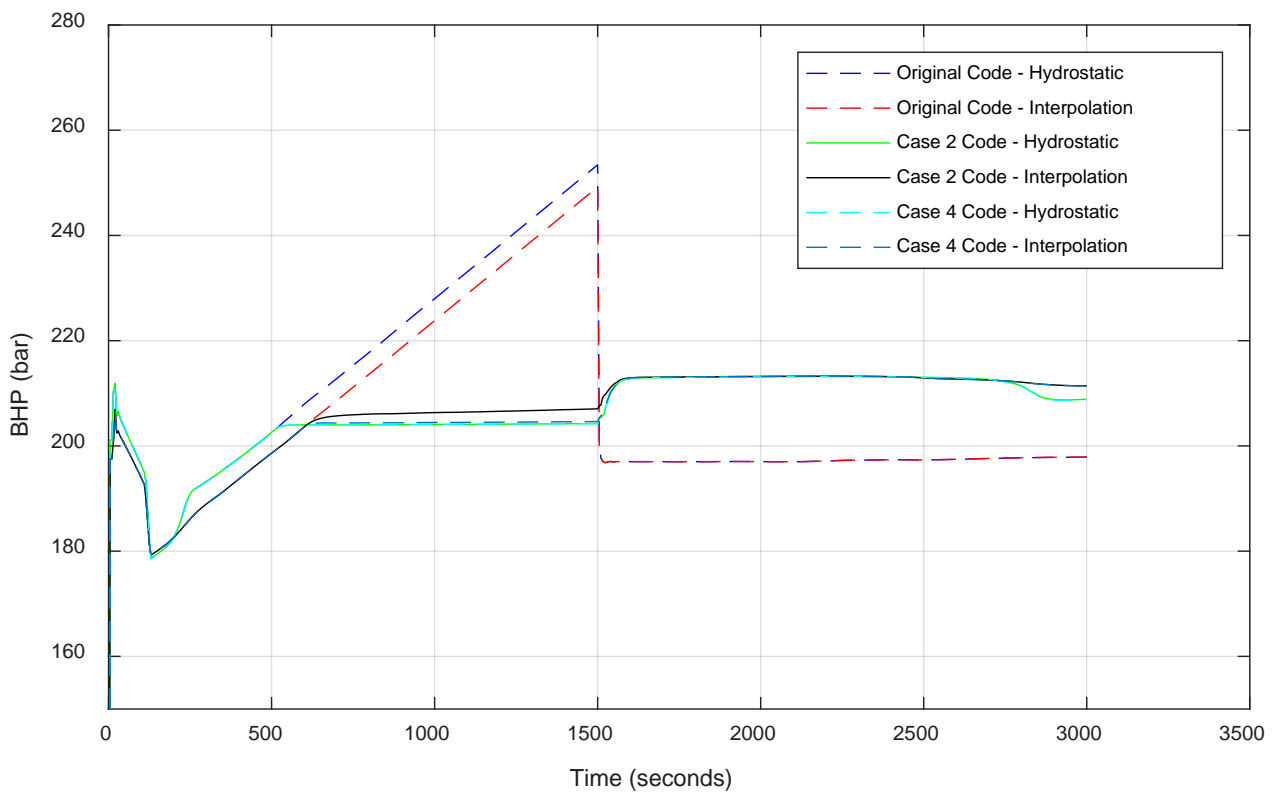


Figure 47 – Bottom Hole Pressure vs Time for Case 7

7. Observations, Conclusions and Future Work

In this chapter, the results from each case will be described and discussed. Then conclusions will be drawn based on each case, and the main findings will be presented. Suggestions for future work will also be made.

7.1 Observations

Case 1

The goal in case 1 was to make the injectivity index model work in the boundary treatment of the fluxes, and to see how it affected the pressure development through time. It was only implemented for the bullheading part of the simulation, which means the time interval of interest is from 1500 seconds to 3000 seconds. These are the observations made from the simulations:

- Figure 18 & figure 19: The bottomhole pressure during bullheading is higher for this case compared to the original code where we assumed the pressure to be 200bar. This goes for both in the bottom of the well and at the surface. When the bullheading is initiated the expanded gas in the well becomes compressed, which increases the hydrostatic pressure. This increase in hydrostatic pressure reduces the surface pressure. Towards 3000 seconds, the bottom pressure drops slightly, because the bullheaded gas has reached the bottom and is starting to go back into the formation. In the code, the gas can freely leave the well without any increase in pressure.
- Figure 20 & figure 21: The different values of the injectivity index, J , creates very different results. Good injectivity (larger values of J) makes a slightly lower pressure in the well, but bad injectivity (lower values of J) causes a significant increase in pressure. Same trend is seen for both surface and bottom pressure.
- Figure 22: The gas volume fraction profiles give an indication of where the gas is situated, and the results indicates that the gas is moving downwards. For case 1, the gas is slightly more compressed for all times compared to the original code. This is because of the increased bottomhole pressure due to injection resistance.

Case 2

Case 2 has a similar goal as case 1, implementing the injectivity index model in the boundary treatment, but now during the closed well gas migration. For the old code results, the bottomhole pressure increased through the entire shut-in well period, which is unrealistic for a PMCD situation. A more realistic way of doing this was introduced by paper [5], and is an important improvement to the code. The expected effect was to see a constant bottomhole pressure and an increasing surface pressure. For this case, the time interval of interest is 130 seconds to 1500 seconds. The same injectivity model as for case 1 is used during bullheading.

- Figure 24 & figure 23: The pressure at the bottom of the well rises at the same rate as the original code, until 500 seconds. Then it stabilizes at around 205 bars, for the rest of shut in period. Now, the pressure has increased to a sufficient level, such that the liquid that is forced downwards in the well by the kick will be injected into the reservoir. Surface pressure also rises with the same rate as before, until 500 seconds. Then the rate increases at a much lower rate from 20 bars to 30 bars.
- Figure 25 & figure 26: The effects from better injectivities (larger value of J) does not affect the bottom injection pressure much. For worse injectivity, the pressure increases to a slightly higher pressure. At the surface, the same is seen. Worse injectivity causes a slight increase in injection pressure, which corresponds to the increase at the bottom. Better injectivity has no effect.
- Figure 27 & figure 28: From the gas volume fraction plot it can be seen that the kick is moving upwards in the well. Initially the gas has the same position for case 2 and the original code, but as the kick moves further up, the case 2 kick expands more. This is because of the lower pressure due to flowback into the formation at the bottom. The velocity profile indicates the position of the kick in the well, and shows that the liquid is moving faster downwards because it has to pass a larger gas bubble (because the case 2 kick has expanded).

Case 3

The goal of case 3 was to make the injectivity index model to work in the source term for the bullheading procedure. As illustrated in figure 29, moving the model from the flux boundary conditions to the source term, represents moving the injection from the

bottom of the cell to the middle of cell. The same time interval as case 1 is in focus for this case.

- Figure 30 & figure 31: The results from the simulation is almost identical to the results from the simulation of case 1. However, the data is not precisely the same but has a trivial difference of 50 pascals. The same is observed for the surface pressure.
- Figure 32 & figure 33: Effects from different degree of injectivity has the same behavior as in case 1, for both surface pressure and bottomhole pressure.

Case 4

With case 4 the objective was to use the source term injectivity equation to handle the flowback when the well is closed, which is a combination of the work done in case 3 and case 2. The time interval of discussion is from 130 seconds till 1500 seconds.

- Figure 34 & figure 35: The results is equal to the model in the boundary conditions (case 2), with exact same behavior. For bottomhole pressure, a rapid increase in pressure until 500 seconds, then it stabilizes. The surface pressure increases in the same manner in the beginning, but the rate changes and becomes much slower after 500 seconds.
- Figure 36 & figure 37 : These plots also show the same results as boundary treatment model (case 2). Good injectivity does not affect the pressure development much, but bad injectivity makes the pressure increase.

Case 5

Case 5 was more of an experimental study, where the goal was to see if the source term model could be used to take the gas kick into the well. The model was changed to only be valid when reservoir pressure was higher than the well pressure, which would then induce a gas flow into the well.

- Figure 38 & figure 40: Kick volume and mass taken varies a lot compared to the previous way of taking the kick. The total mass difference in gas is nearly 650 kg, with a volume difference of 4 m³(at 130 seconds before gas has expanded). In order to take a larger kick, a higher PI value has to be used. It is easier to control the kick size taken in a simulation by specifying the gas mass rate in kg/s directly, compared to taking the kick by using a PI model. In case 5 the kick volume taken will depend on the PI value and the pressure difference

between reservoir and bottomhole. The pressure difference varies through time and makes it much harder to control how much gas is taken.

- Figure 39 & figure 41: The bottomhole pressure shows that the pressure does not drop as low as before when the kick enters, and stabilizes much faster after the kick is produced into the well. The surface pressure shows very different pressures. The overall surface pressure for case 5 is much lower than for the original and case 4 simulation, which is caused by the much smaller amount of gas taken. This is mainly because the hydrostatic column has less gas and the bottomhole pressure is the same, hence the hydrostatic pressure is higher ($P_{Surf} = P_{Bot} - \rho gh - \Delta P_{friction}$).

Case 6

In case 6 the goal was to study the effects of slope limiters boundary treatment on the boundary injection model, and the source term injection model. It was tested for case 2 and 4, since they include the changes made in case 1 and case 3 respectively. Also, different number of boxes in the discretization was tested, and the timestep was changed accordingly.

- Figure 43 & figure 42: This was simulations done with the case 2 code. Difference in results between number of boxes is much larger than the difference between choice of slope limiter boundary treatment. When increasing the box number, the bottomhole pressure drops with around 2 bars for the whole simulation. By increasing number of boxes the simulation becomes more accurate. Problems occur during bullheading with 100 boxes, where the pressure oscillates during the first half of the interval (1500 – 3000 seconds). This happens for both slope limiters treatments, but lasts about 150 seconds longer for the slope limiters set to 0.
- Figure 44 & figure 45: The case 4 results is very similar to the case 2 simulation, with the same oscillation when using 100 boxes.

Case 7

Case 7 was a study of two different methods of modeling the inlet and outlet pressure at the boundaries. Both models were given in the code, so it was only necessary to turn on the alternative model.

- Figure 46: For the original code, the pressure model using equation 37 and 39, gave a slightly higher bottomhole pressure during the closed well time interval. There was no difference between the hydrostatic model and the interpolation model for case 4, except a deviation from 250 seconds till 500 seconds. For case 2, the pressure was slightly higher during the closed well with the interpolation model. All results were equal during the bullheading.
- Figure 47: For case 2 and 4, the surface pressure plot shows a much bigger difference between the pressure model (using equation 37 and 39), and the interpolation model. After 500 seconds the interpolation model gives a slightly higher pressure for the rest of the simulation. The original code shows very little difference between the two models.

7.2 Conclusions

7.2.1 – Case 1 & 2 conclusion

The results from case 1 and 2 shows clearly that the implemented injection model works as intended. Originally the pressure was fixed to 200 bars through the entire bullheading injection, and all fluid were assumed to be injected into the formation at this pressure. Resistance from the formation was not considered at all. The results from case 1 shows that the bottom hole pressure will increase to slightly above 210 bars, which is a 10-bar overpressure relative to the fixed 200 bar reservoir pressure. This seems reasonable, as a 10-bar overpressure was selected to calculate an ideal injectivity index. For this bottomhole pressure, all fluids will be injected at the selected 25 kg/s rate. Simulation does show that the well pressures are heavily dependent on how injective the formation is. Case 2 showed a significant improvement for the pressure development during the shut-in well gas migration. It was interesting to see how much lower the surface and bottom hole pressure became when fluids were allowed to go back into the formation. These results are in line with the results shown in paper [5]. Hence, this is a more realistic representation of what will happen during a shut-in period, of a well in a carbonate formation. This is a much more realistic result, as the pressure increase at the bottom will force fluids into the formation and not keep increasing without injection.

7.2.2 – Case 3 & 4 conclusion

The simulations show that there is insignificant difference between the source term model and modelling injectivity through the boundary conditions. As stated in paper [5], a source term solution could be a more effective approach to handle fluid losses to the fractures, than the virtual cell method they used. The simulations done in this thesis shows no sign of a difference between a boundary treatment model and a source term model when injection is done in the bottom of the well. However, the source term model provides more flexibility with regards to the location of the injection, since the injection zone can be placed in any cell (or multiple cells) through the discretization, while the boundary condition model only applies to the bottom cell. For bottom cell simulation, the same conclusions can be made for case 3 and 4, as for case 1 and 2.

7.2.2 – Case 5 conclusion

The results from case 5 indicates that a much lower amount of gas mass has been produced into the well. Because the injectivity model needs a pressure difference to take fluids, it will only produce fluids into the well when the well pressure is below 200 bars. The surface pressure also indicates a much smaller kick, as the pressure increase at top is much smaller. When using the Productivity Index model to produce the kick into the well, it will depend on the PI value (J) and the pressure difference, $\Delta P = P_{Res} - P_{Well}$. In order to take a larger kick, a larger J must be used. Anyway, it is not easy control the kick size in this simulating approach because ΔP will vary. One should also investigate what a good production model could be for gas.

7.2.3 – Case 6 conclusion

The simulations done for different slope limiters, shows that there is a minor difference between the two treatments, but not a significant. More interesting and unexpected was that the two models had problems with simulation for 100 boxes and a 0.0025 second timestep, which is the same CFL conditions as the two other simulations. This was only during the first half of the bullheading. Because of this unexpected result, two additional simulations were done for both case 2 and case 4 code, this time with an even smaller timestep (0.001), but the results were the same. Since both variants of the injectivity model suffered from this, boundary condition model and the source term model, it is not a problem with the implementation of either of the models, but might be related to the injection model itself, as it seems they are alternating between injecting too much and too little in an oscillating manner.

7.2.4 – Case 7 conclusion

Case 7 was a look at the two different ways of doing pressure boundary calculations. There is some difference between the two models. It's not so clear in the bottom of the well, but the difference really shows in the surface pressure plot. It is hard to determine which model of the two that is more correct, even though it would seem that the pressure model from equation 37 and 39 is more accurate because it is based on physical properties of the well and the fluid.

7.3 The Main Findings & Future Work.

- Changed boundary conditions at the bottom of the well from a fixed pressure to a boundary condition injection model that depends on the injectivity of the formation. The injection model was also successfully implemented in the source term. Well pressure will be affected by the formations injectivity.
- Injectivity Index model during shut-in well for a PMCD operation was successfully implemented in boundary conditions and in the source term, same as was done in paper [5] by using another method. The source term approach seems more flexible because it can handle multiple injection zones at different locations in the well.
- A challenge that remains is how to define the injection model for mud, since this thesis assumed that the liquid had water properties.
- This thesis has proven that the injectivity model can be used to get more realistic results for PMCD bullheading with the AUSMV scheme. It can be implemented in the boundary conditions of the code or in the source term of the partial differential equations, and give very similar results. However, the simulations were done with an ideally calculated value for the injectivity index. It was tested how the code would handle different injectivities, but it remains to find a good way to estimate a realistic J based on reservoir properties.
- A gas production model is necessary to correctly model how the reservoir pressure would force a kick into the well. More work is needed to define a good model to how gas enters the well from a fractured carbonate system. At the same time, there should be a model for how liquids simultaneous possible are forced out of the well.
- The focus of the thesis was to make sure the code could handle one phase injection of liquid. We only simulated for the time interval of the bullheading before gas had reached the bottom, which meant only liquids was forced into the formations. It remains to find a proper injection model for gas, implement it and correctly model two-phase injection and its effect on the bottomhole pressure.

- Simulations done for case 6 showed unexpected results related to the discretization and number of boxes. More work should be done to identify the cause of the oscillations and how it can be prevented.

8. References

- [1] P. Oudeman, D. t. Avest, E. O. Grodal, H. A. Asheim, and R. J. H. Meissner. 1994. Bull Heading to Kill Live Gas Wells. SPE 28896.
- [2] W. L. Koedertiz. 1995. Gas Kick Behavior During Bullheading Operations in Vertical Wells.
http://digitalcommons.lsu.edu/cgi/viewcontent.cgi?article=6962&context=gradschool_disstheses <02.06.2017>
- [3] A. Farahat, A. Dahab, and A. H. El-Sayed. 2017. A Successful Application of MPD with CBHP Technique in Temsah Field - A Case History. Paper OMC-2017-534 presented at Offshore Mediterranean Conference and Exhibition, Ravenna, Italy, 29-31 March.
- [4] B. Goodwin, S. Nauduri, and G. Medley. 2014. MudCap Drilling: New Variations, Drivers, Limitations, and Lessons Learned - Case Histories. Paper SPE/IADC-168956-MS presented at SPE/IADC Managed Pressure Drilling & Underbalanced Operations Conference & Exhibition, Madrid, Spain, 8-9 April.
- [5] F. d. S. Terra, A. C. V. M. Lage, K. K. Fjelde, M. F. Naccache, and S. Stuckenbruck. 2017. Prediction Model for Gas Migration in Well During PMCD Operation. Paper SPE-185276-MS presented at IADC/SPE Managed Pressure Drilling & Underbalanced Operations Conference & Exhibition, Rio de Janeiro, Brazil, 28-29 March.
- [6] Benny, A. M. Hidayat, A. Karnugroho, J. Sosa, and J. S. S. Toralde. 2013. Combining Pressurized Mud Cap Drilling (PMCD) and Early Kick Detection (EKD) Techniques for Fractured Formations Overlying a High Pressure Reservoir in Offshore Kalimantan. Paper SPE-165893-MS presented at SPE Asia Pacific Oil & Gas Conference and Exhibition, Jakarta, Indonesia, 22-24 October.
- [7] R. Ho, D. Moore, D. Pirie, and J. Kozicz. 2014. Drilling Deepwater Carbonates Using Managed Pressure Drilling on a Dynamically Positioned Drillship. Paper SPE-167995-MS presented at IADC/SPE Drilling Conference and Exhibition, Fort Worth, Texas, USA, 4-6 March.
- [8] A. A. Ghauri, K. K. Fjelde, and J. Frøyen. 2016. A Transient Model for Hydraulic Simulation of Bullheading and Pressurized Mud Cap Drilling. Paper OMAE2016-54293 presented at International Conference on Ocean, Offshore and Arctic Engineering, Busan, South Korea, June 19-24.
- [9] A. A. Ghauri, "Use of the AUSMV scheme for simulation of gas migration, bullheading and Pressurized Mud Cap Drilling," Master Thesis, Faculty of Science and Technology, Univesity of Stavanger, Stavanger, 2014.
- [10] S. Evje and K. K. Fjelde. 2002. Hybrid Flux-Splitting Schemes for a Two-Phase Flow Model. *Journal of Computational Physics* 175. p. 674–701.
- [11] 2014. Bullheading Well Control Method.
<http://www.drillingformulas.com/bullheading-well-control-method/>
<06.05.2017>
- [12] Well Control - Bullheading. <http://www.wipertrip.com/well-control/secondary-control/191-well-control-bullheading.html> <08.05.2017>
- [13] R. D. Grace, *Advanced Blowout & Well Control*. Texas: Gulf Publishing Company, 1994.
- [14] K. P. Malloy, C. R. Stone, J. George H. Medley, and e. al. 2009. Managed-Pressure Drilling: What It Is and What It Is Not. Paper IADC/SPE 122281

- presented at IADC/SPE Managed Pressure Drilling and Underbalanced Operations Conference & Exhibition, San Antonio, Texas, 12-13 February.
- [15] B. Gedge, H. K. D. Singh, E. Refugio, B. T. Quoc, and N. B. Bot.2013. Managed Pressure Drilling - A Solution for Drilling the Challenging and Un-Drillable Wells in Vietnam and South East Asia. Paper SPE-165775-MS presented at SPE Asia Pacific Oil and Gas Conference and Exhibition, Jakarta, Indonesia, 22-24 October.
- [16] D. B. Bennion, F. B. THomas, R. F. Bietz, and D. W. Bennion.1996. Underbalanced Drilling, Praises and Perils. Paper SPE-35242-MS presented at Permian Basin Oil and Gas Recovery Conference, Midland, Texas, 27-29 March.
- [17] B. Hilts.2013. Managed Pressure Drilling. Paper SPE 167621-STU presented at SPE Annual Technical Conference and Exhibition, New Orleans, Louisiana, USA, 30 September-2 October.
- [18] R. Urselmann, J. Cummins, R. N. Worrall, and G. House.1999. Pressured Mud Cap Drilling: Efficient Drilling of High-Pressure Fractured Reservoirs. Paper SPE-52828-MS presented at SPE/IADC Drilling Conference, Amsterdam, Netherlands, 9-11 March.
- [19] J. E. L. d. Guevaram *et al.*2012. Mud Cap Application Solves Chronic Drilling Problem in a Highly Fractured , Low Pressure Reservoir. Paper SPE-151085-MS presented at IADC/SPE Drilling Conference and Exhibition, San Diego, California, USA, 6-8 March.
- [20] B. Rehm, J. Schubert, A. Haghshenas, A. S. Paknejad, and J. Hughes, *Managed Pressure Drilling*. Houston, Texas: Gulf Publishing Company, 2008.
- [21] M. Runtuwene, S. Suprihono, D. Rizka, A. E. Prasetya, J. S. Toralde, and S. Nas.2009. Pressurized Mud Cap Drilling Drastically Reduces Non-Productive Time in Soka Field, South Sumatera. Paper SPE/IADC 125311 presented at Middle East Drilling Technology Conference & Exhibition, Manama, Bahrain, 26-28 October.
- [22] G. T. Teixeira, F. Fabri, L. S. d. Almeida, P. H. P. d. Silva, and R. B. Vadinal.2017. Lessons Learned in Drilling Fluids Projects during MPD and MCD Operations in Brazil's Offshore Wells, SPE/IADC-185277-MS. Paper SPE-185277-MS presented at Operations Conference & Exhibition, Rio de Janeiro, Brazil, 28-29 March.
- [23] M. N. Jayah, I. A. A. Aziz, T. Mathews, A. Voshall, and F. R. Rodriguez.2013. Implementation of PMCD to Explore Carbonate Reservoirs from Semi-Submerible Rigs in Malaysia results in Safe and Economical Drilling Operations. Paper SPE-163479-MS presented at SPE/IADC Drilling Conference, Amsterdam, The Netherlands, 5-7 March.
- [24] K. Muir. Managed Pressure Drilling (MPD) - Systems & Applications. http://www.drillsafe.org.au/06-08_pres/DrillSafe_Forum_Jun08_KEEP_DRILLING_Ken_Muir_Managed_Pressure_Drilling_Talk.pdf <10.06.2017>
- [25] S. A. Nelson. 2013. Carbonates & Other Rocks. <http://www.tulane.edu/~sanelson/eens212/carbonates.htm> <06.05.2017>
- [26] N. H. Houg, I. Rubianto, A. R. Abuelaish, and M. A. B. Abdullah.2016. Successful PMCD Application Significantly Improved Drilling Efficiency on Carbonate Drilling. Paper SPE-180658-MS presented at IADC/SPE Asia Pacific Drilling Technology Conference, Singapore, 22-24 August.

- [27] K. K. Fjelde and S. Evje, "The AUSMV Scheme - A Simple But Robust Model for Analyzing Two-Phase Flow," University of Stavanger 2010.
- [28] J. E. Udegbunam, K. K. Fjelde, S. Evje, and G. Nygaard. 2014. A Simple Transient Flow Model for MPD and UBD Applications. Paper SPE/IADC 168960 presented at SPE/IADC Managed Pressure Drilling & Underbalanced Operations Conference & Exhibition, Madrid, Spain, 8-9 April.
- [29] K. K. Fjelde, J. Frøyen, and A. A. Ghauri. 2016. A Numerical Study of Gas Kick Migration and Uncertainty. Paper SPE-180053-MS presented at SPE Bergen One Day Seminar, Bergen, 20 April.
- [30] J. F. Bautista and A. D. Taleghani. 2016. The State Of The Art And Challenges in Geomechanical Modeling Of Injector Wells; A Review Paper. Paper OMAE2016-54383 presented at ASME 2016 35th International Conference on Ocean, Offshore and Arctic Engineering, Busan, South Korea, June 19-24.
- [31] Material Balance Analysis Theory.
http://www.fekete.com/SAN/WebHelp/FeketeHarmony/Harmony_WebHelp/Content/HTML_Files/Reference_Material/Analysis_Method_Theory/Material_Balance_Theory.htm <29.05.2017>
- [32] M. M. Sharma, S. Pang, K. E. Wennberg, and L. N. Morgenthaler. 2000. Injectivity Decline in Water-Injection Wells: An Offshore Gulf of Mexico Case Study SPE-60901-PA.
- [33] B. C. Craft and M. F. Hawkins, *Applied Petroleum Reservoir Engineering - 2. Edition*. United States of America: Englewood Cliffs, N.J., Prentice-Hall, 1991.
- [34] A. A. Gahtani, K. Fahd, and Dhahran. 2011. A New Productivity Index Formula for ESP-Lifted Wells. Paper SPE-141984-MS presented at SPE Middle East Oil and Gas Show and Conference, Manama, Bahrain, 25-28 September.
- [35] S. Alarifi, S. AlNuaim, and A. Abdulraheem. 2015. Productivity Index Prediction for Oil Horizontal Wells Using Different Artificial Intelligence Techniques. Paper SPE-172729-MS presented at SPE Middle East Oil & Gas Show and Conference, Manama, Bahrain, 8-11 March.
- [36] A. Settari. 2000. TAURUS Reservoir Solutions. Note on the Calculation of PWRI Well Injectivity Index.
http://www.advntk.com/pwrijip2003/pwri/toolbox/documents/minutes_12_00/note_calc_PWRI_injectivity.doc <05.04.2017>

9. Appendix

Below is all color codes for changes in the code illustrated:

Case 1, Case2, Case3, Case4, Case5, Case6 and Case7

```
% Transient two-phase code based on AUSMV scheme: Gas and Water
% The code can handle area changes. The area changes are defined
inside
% the cells such that the where the fluxes are calculated, the
geometry is
% uniform.

clear;
t = cputime
tic,

% Geometry data/ Must be specified
welldepth = 2000;
nobox = 25; %Number of boxes in the well
nofluxes = nobox+1;
dx = welldepth/nobox; % Boxlength
%dt = 0.005;

% Welldepth array
x(1)= -1.0*welldepth+0.5*dx;
for i=1:nobox-1
    x(i+1)=x(i)+ dx;
end

dt= 0.01; % Timestep
dtdx = dt/dx;
time = 0.0;
endtime=3000; % Rime for end of simulation
nosteps = endtime/dt; %Number of total timesteps
timebetweensavingtimedata = 5; % How often in s we save data vs
time for plotting.
nostepsbeforesavingtimedata = timebetweensavingtimedata/dt;

% Slip parameters used in the gas slip relation. vg =Kvmix+S
k = 1.2;
s = 0.55;

% Viscosities (Pa*s)/Used in the frictional pressure loss model.
viscl = 0.001; % Liquid phase
viscg = 0.0000182; % Gas phase

% Density parameters. These parameters are used when finding the
% primitive variables pressure, densities in an analytical manner.
% Changing parameters here, you must also change parameters inside
the
% density routines roliq and rogas.

% liquid density at stc and speed of sound in liquid
dstc = 1000.0; %Base density of liquid, See also roliq.
pstc = 100000.0; % Pressure at standard conditions, 100000 Pascal
```

```

    al = 1500; % Speed of sound/compressibility of liquid phase.
    t1 = dstc-pstc/(al*al); % Help variable for calc primitive
variables from
    % conservative variables
% Ideal gas law constant
    rt = 100000;

% Gravity constant

    grav = 9.81;
% grav = 0;

% Well opening. opening = 1, fully open well, opening = 0 (<0.01),
the well
% is fully closed. This variable will control what boundary
conditions that
% will apply at the outlet (both physical and numerical): We must
change
% this further below in the code if we want to change status on
this.

    wellopening = 1.0;
    bullheading = 0.0;

% Specify if the primitive variables shall be found either by
% a numerical or analytical approach. If analytical = 1, analytical
% solution is used. If analytical = 0. The numerical approach is
used.
% using the itsolver subroutine where the bisection numerical method
% is used.

    analytical = 1;

% Define and initialize flow variables

% Here we specify the outer and inner diameter and the flow area

    for i = 1:nobox
% do(i) = 0.3112;
        do(i)=0.2159
        di(i) = 0.127;
        area(i) = 3.14/4*(do(i)*do(i)- di(i)*di(i));
        fricgrad(i)=0;
% ang(i)=3.14/2;
    end

```

```

% Initialization of slope limiters.
for i = 1:nobox
    sl1(i)=0;
    sl2(i)=0;
    sl3(i)=0;
    sl4(i)=0;
    sl5(i)=0;
    sl6(i)=0;
end

% Now comes the initialization of the physical variables in the well.
% First primitive variables, then the conservative ones.

% Below we initialize pressure and fluid densities. We start from top
of
% the well and calculated downwards. The calculation is done twice
with
% updated values to get better approximation. Only hydrostatic
% considerations.

p(nobox)= 100000.0+0.5*dx*9.81*dstc; % Pressure
dl(nobox)=rholiq(p(nobox)); % Liquid density
dg(nobox)=rogas(p(nobox)); % Gas density

for i=nobox-1:-1:1
    p(i)=p(i+1)+dx*9.81*dl(i+1);
    dl(i)=rholiq(p(i));
    dg(i)=rogas(p(i));
end

for i=nobox-1:-1:1
    p(i)=p(i+1)+dx*9.81*(dl(i+1)+dl(i))*0.5;
    dl(i)=rholiq(p(i));
    dg(i)=rogas(p(i));
end

% Initialize phase velocities, volume fractions, conservative
variables
% The basic assumption is static fluid, one phase liquid.

for i = 1:nobox
    vl(i)=0; % Liquid velocity new time level.
    vg(i)=0; % Gas velocity at new time level
    eg(i)=0; % Gas volume fraction
    ev(i)=1-eg(i); % Liquid volume fraction
    qv(i,1)=dl(i)*ev(i)*area(i);
    qv(i,2)=dg(i)*eg(i)*area(i);
    qv(i,3)=(dl(i)*ev(i)*vl(i)+dg(i)*eg(i)*vg(i))*area(i);
end

```

```

source = zeros(nobox,3);

% Section where we also initialize values at old time level

for i=1:nobox
    dlo(i)=dl(i);
    dgo(i)=dg(i);
    po(i)=p(i);
    ego(i)=eg(i);
    evo(i)=ev(i);
    vlo(i)=vl(i);
    vgo(i)=vg(i);
    qvo(i,1)=qv(i,1);
    qvo(i,2)=qv(i,2);
    qvo(i,3)=qv(i,3);
end

% Intialize fluxes between the cells/boxes

for i = 1:nofluxes
    for j =1:3
        flc(i,j)=0.0; % Flux of liquid over box boundary
        fgc(i,j)=0.0; % Flux of gas over box boundary
        fp(i,j)= 0.0; % Pressure flux over box boundary
    end
end

% Main program. Here we will progress in time. First som
intializations
% and definitions to take out results. The for loop below runs until
the
% simulation is finished.

countsteps = 0;
counter=0;
printcounter = 1;
pbot(printcounter) = p(1);
pchoke(printcounter)= p(nobox);
liquidmassrateout(printcounter) = 0;
gasmassrateout(printcounter)=0;
timeplot(printcounter)=time;
kickvolume=0;

for i = 1:nosteps
    countsteps=countsteps+1;
    counter=counter+1;
    time = time+dt;

    g = grav;

% Then a section where specify the boundary conditions.
% Here we specify the inlet rates of the different phases at the

```

```

% bottom of the pipe in kg/s. We interpolate to make things smooth.
% It is also possible to change the outlet boundary status of the
well
% here. First we specify rates at the bottom and the pressure at the
outlet
% in case we have an open well. This is a place where we can change
the
% code.

```

```

XX = 8;
YY =25;

```

```

ZZ1= 25;
J1 = (ZZ1/dstc)/1000000;
pres = 20000000;

```

```

ZZ2 = 25;
J2 = (ZZ2/dstc)/1000000
pres = 20000000;

```

```

ZZ3= 25;
J3 = (ZZ3/dstc)/1000000;
pres = 20000000;

```

```

ZZ4= 25;
J4 = (ZZ4/dstc)/1000000;
pres = 20000000

```

```

ZZ5 = 8;
JG = (ZZ5/dgstc)/1000000;
pres = 20000000;

```

```

if (time < 10)
    inletligmassrate=0.0;
    inletgasmassrate=0.0;
    JG = 0;

elseif ((time>=10) & (time < 20))
    inletligmassrate = 0*(time-10)/10;
    inletgasmassrate = XX*(time-10)/10;
    JG = JG*(time-10)/10;

elseif ((time >=20) & (time<110))
    inletligmassrate = 0;
    inletgasmassrate = XX;
    JG = JG;

elseif ((time>=110)& (time<120))
    inletligmassrate = 0;
    inletgasmassrate = XX-XX*(time-110)/10;
    JG = JG-JG*(time-110)/10;

elseif ((time>=120&time<130))
    inletligmassrate =0;

```



```

inletgasmassrate =0;

elseif ((time>=130)&(time<1500))
    inletligmassrate =0;
    inletgasmassrate =0;
    wellopening = 0;

elseif ((time>=1500)&(time<1560))
    wellopening = 1.0;
    bullheading = 1.0;
    inletligmassrate=-1.0*YY*(time-1500)/60;
    inletgasmassrate =0;
    xint = (time-1500)/60;
    k = 1.2*(1-xint)+xint*1.12;
    J1 = J1*(time-1500)/60;
    J3 = J3*(time-1500)/60;

elseif((time>=1560)&(time<4000))
    wellopening = 1.0;
    bullheading = 1.0;
    inletligmassrate=-1.0*YY;
    inletgasmassrate =0;
    k = 1.12;
    J1 = J1;
    J3 = J3;

else
    wellopening = 1.0;
    bullheading = 1.0;
    inletligmassrate=-1.0*YY;
    inletgasmassrate =0;
    k = 1.12;
    J1 = J1;
    J3 = J3;

end

kickvolume = kickvolume+inletgasmassrate/dgo(1)*dt;
% specify the outlet pressure /Physical. Here we have given the
pressure as
% constant. It would be possible to adjust it during openwell
conditions
% either by giving the wanted pressure directly (in the command
lines
% above) or by finding it indirectly through a chokemodel where the
wellopening
% would be an input parameter. The wellopening variable would
equally had
% to be adjusted inside the command line structure given right
above.

pressureoutlet = 100000.0;

% Based on these boundary values combined with use of extrapolations
techniques
% for the remaining unknowns at the boundaries, we will define the
mass and
% momentum fluxes at the boundaries (inlet and outlet of pipe).

% inlet fluxes first.

```

```

if (bullheading<=0)
    flc(1,1)= inletligmassrate/area(1);
    flc(1,2)= 0.0;
    flc(1,3)= flc(1,1)*vlo(1);
% flc(1,3)=0;

    fgc(1,1)= 0.0;
    fgc(1,2)= inletgasmassrate/area(1);
    fgc(1,3)= fgc(1,2)*vgo(1);

    fp(1,1)= 0.0;
    fp(1,2)= 0.0;
    fp(1,3)= po(1)+0.5*(po(1)-po(2));
    fp(1,3)=po(1)+0.5*(dlo(1)*evo(1)+dgo(1)*ego(1))*g+...
        0.5*dx*fricgrad(1);

    if (wellopening==0)

        flc(1,1) = -(1.0)*J2*(po(1)-pres)*dstc/area(1);
        flc(1,2) = 0.0;
        flc(1,3) = flc(1,1)*vlo(1);

        if (flc(1,1)>0)

            flc(1,1) = 0.0;
            flc(1,2) = 0.0;
            flc(1,3) = flc(1,1)*vlo(1);
        end
    end

else
    flc(1,1)=dlo(1)*evo(1)*vlo(1);
    flc(1,2)=0.0;
    flc(1,3)=flc(1,1)*vlo(1);

    flc(1,1)=(-1.0)*J1*(po(1)-pres)*dstc/area(1);
    flc(1,2)=0.0;
    flc(1,3)=flc(1,1)*vlo(1);

    flc(1,1)=0.0;
    flc(1,2)=0.0;
    flc(1,3)=flc(1,1)*vlo(1);

    fgc(1,1)=0.0;
    fgc(1,2)=dgo(1)*ego(1)*vgo(1);
    fgc(1,3)=fgc(1,2)*vgo(1);

    fp(1,1)=0.0;
    fp(1,2)=0.0;
    fp(1,3)=20000000;

    fp(1,1)=0.0;
    fp(1,2)=0.0;
    fp(1,3)=po(1)+0.5*(dlo(1)*evo(1)+dgo(1)*ego(1))*g+...
        0.5*dx*fricgrad(1);
    fp(1,3)= po(1)+0.5*(po(1)-po(2));
end

```

```

% Outlet fluxes (open & closed conditions)

    if (wellopening>0.01)

% Here open end condtions are given

        if (bullheading<=0)
            flc(nofluxes,1)= dlo(nobox)*evo(nobox)*vlo(nobox);

            flc(nofluxes,2)= 0.0;
            flc(nofluxes,3)= flc(nofluxes,1)*vlo(nobox);
%         flc(nofluxes,3)=0;

            fgc(nofluxes,1)= 0.0;
            fgc(nofluxes,2)= dgo(nobox)*ego(nobox)*vgo(nobox);
            fgc(nofluxes,3)= fgc(nofluxes,2)*vgo(nobox);

            fp(nofluxes,1)= 0.0;
            fp(nofluxes,2)= 0.0;
            fp(nofluxes,3)= pressureoutlet;
        else
            flc(nofluxes,1)= inletligmassrate/area(nobox);
            flc(nofluxes,2)= 0.0;
            flc(nofluxes,3)= flc(nofluxes,1)*vlo(nobox);

            fgc(nofluxes,1)=0.0;
            fgc(nofluxes,2)=0.0;
            fgc(nofluxes,3)=0.0;

            fp(nofluxes,1)=0.0;
            fp(nofluxes,2)=0.0;
            fp(nofluxes,3)= po(nobox)-0.5*(po(nobox-1)-po(nobox));
            fp(nofluxes,3)= po(nobox)...
            -0.5*dx*(dlo(nobox)*evo(nobox)+dgo(nobox)*ego(nobox))*g;
            -0.5*dx*fricgrad(nobox);

        end
    else

% Here closed end conditions are given

        flc(nofluxes,1)= 0.0;
        flc(nofluxes,2)= 0.0;
        flc(nofluxes,3)= 0.0;

        fgc(nofluxes,1)= 0.0;
        fgc(nofluxes,2)= 0.0;
        fgc(nofluxes,3)= 0.0;

        fp(nofluxes,1)=0.0;
        fp(nofluxes,2)=0.0;
        fp(nofluxes,3)= po(nobox)-0.5*(po(nobox-1)-po(nobox));
        fp(nofluxes,3)= po(nobox)...
        -0.5*dx*(dlo(nobox)*evo(nobox)+dgo(nobox)*ego(nobox))*g;
        -0.5*dx*fricgrad(nobox);
    end
end

```

end

```
% Implementasjon av slopelimitere
s11(1)=0;
s11(nobox)=0;
s12(1)=0;
s12(nobox)=0;
s13(1)=0;
s13(nobox)=0;

for i=2:nobox-1
    s11(i)=minmod(dlo(i-1),dlo(i),dlo(i+1),dx);
    s12(i)=minmod(po(i-1),po(i),po(i+1),dx);
    s13(i)=minmod(vlo(i-1),vlo(i),vlo(i+1),dx);
    s14(i)=minmod(vgo(i-1),vgo(i),vgo(i+1),dx);
    s15(i)=minmod(ego(i-1),ego(i),ego(i+1),dx);
    s16(i)=minmod(dgo(i-1),dgo(i),dgo(i+1),dx);
end
s11(1)=s11(2);
s11(nobox)=s11(nobox-1);
s12(1)=s12(2);
s12(nobox)=s12(nobox-1);
s13(1)=s13(2);
s13(nobox)=s13(nobox-1);
s14(1)=s14(2);
s14(nobox)=s14(nobox-1);
s15(1)=s15(2);
s15(1)=0;
s15(nobox)=s15(nobox-1);
s16(1)=s16(2);
s16(nobox)=s16(nobox-1);

s11(nobox)=0;
s12(nobox)=0;
s13(nobox)=0;
s14(nobox)=0;
s15(nobox)=0;
s16(nobox)=0;

% Ny Kode 11/11-15
s11(1)=0;
s12(1)=0;
s13(1)=0;
s14(1)=0;
s15(1)=0;
s16(1)=0;

% s11(nobox)=0;
% s12(nobox)=0;
% s13(nobox)=0;
% s14(nobox)=0;
% s15(nobox)=0;
% s16(nobox)=0;

% Ny Kode 11/11-15
% s11(1)=0;
% s12(1)=0;
% s13(1)=0;
```

```

% s14(1)=0;
% s15(1)=0;
% s16(1)=0;

% Now we will find the fluxes between the different cells.
% NB - IMPORTANT - Note that if we change the
compressibilities/sound velocities of
% the fluids involved, we need to do changes inside the csound
function.

for j = 2:nofluxes-1

%      cl = csound(ego(j-1),po(j-1),dlo(j-1),k);
%      cr = csound(ego(j),po(j),dlo(j),k);
%      c = max(cl,cr);
%      pll = psip(vlo(j-1),c,evo(j));
%      plr = psim(vlo(j),c,evo(j-1));
%      pgl = psip(vgo(j-1),c,ego(j));
%      pgr = psim(vgo(j),c,ego(j-1));
%      vmixr = vlo(j)*evo(j)+vgo(j)*ego(j);
%      vmixl = vlo(j-1)*evo(j-1)+vgo(j-1)*ego(j-1);
% %
%      pl = pp(vmixl,c);
%      pr = pm(vmixr,c);
%      mll= evo(j-1)*dlo(j-1);
%      mlr= evo(j)*dlo(j);
%      mgl= ego(j-1)*dgo(j-1);
%      mgr= ego(j)*dgo(j);
% %
%      flc(j,1)= mll*pll+mlr*plr;
%      flc(j,2)= 0.0;
%      flc(j,3)= mll*pll*vlo(j-1)+mlr*plr*vlo(j);
% %
%      fgc(j,1)=0.0;
%      fgc(j,2)= mgl*pgl+mgr*pgr;
%      fgc(j,3)= mgl*pgl*vgo(j-1)+mgr*pgr*vgo(j);
% %
%      fp(j,1)= 0.0;
%      fp(j,2)= 0.0;
%      fp(j,3)= pl*po(j-1)+pr*po(j);

% Her legges kode inn for å få med slopelimitere (på tetthet og
trykk, enfase)

%      psll = po(j-1)+dx/2*s12(j-1);
%      pslr = po(j)-dx/2*s12(j);
%      dsll = dlo(j-1)+dx/2*s11(j-1);
%      dslr = dlo(j)-dx/2*s11(j);
%
%      cl = csound(ego(j-1),psll,dsll,k);
%      cr = csound(ego(j),pslr,dslr,k);
%      c = max(cl,cr);
%
%      pll = psip(vlor(j-1),c,evo(j));
%      plr = psim(vlol(j),c,evo(j-1));
%      pgl = psip(vgor(j-1),c,ego(j));
%      pgr = psim(vgol(j),c,ego(j-1));
%      vmixr = vlol(j)*evo(j)+vgol(j)*ego(j);
%      vmixl = vlor(j-1)*evo(j-1)+vgor(j-1)*ego(j-1);

```



```

%      mll= lvv*dsll;
%      mlr= lvh*dslr;
%      mgl= gvv*dgll;
%      mgr= gvh*dglr;
%
%      flc(j,1)= mll*pll+mlr*plr;
%      flc(j,2)= 0.0;
%      flc(j,3)= mll*pll*vlv+mlr*plr*vlh;
%
%
%      fgc(j,1)=0.0;
%      fgc(j,2)= mgl*pgl+mgr*pgr;
%      fgc(j,3)= mgl*pgl*vgv+mgr*pgr*vgh;
%
%      fp(j,1)= 0.0;
%      fp(j,2)= 0.0;
%      fp(j,3)= pl*psll+pr*pslr;

end

% Fluxes have now been calculated. We will now update the
conservative
% variables in each of the numerical cells.

      hydgrad = g*(dlo.*evo+dgo.*ego);
      fricgrad =
dpfric1(vlo,vgo,evo,ego,dlo,dgo,po,do,di,viscl,viscg);
      %      source(1:nobox,3) = hydgrad+fricgrad;

sumfric = 0;
sumhyd= 0;

for j=1:nobox
%
%
%      ar = area(j);
%
%      pressure=p(j);

%      We calculate the frictional gradient by calling upon the
dpfric function.
%      fricgrad(j) =
dpfric(vlo(j),vgo(j),evo(j),ego(j),dlo(j),dgo(j),pressure,do(j),di(j)
),viscl,viscg);
%      hydgrad(j)=g*(dlo(j)*evo(j)+dgo(j)*ego(j));

%      source(1:nobox,3) = hydgrad+fricgrad;

%      qv(j,:)=qvo(j,:)-dtdx*ar*((flc(j+1,:)-flc(j,:))...
%                               +(fgc(j+1,:)-fgc(j,:))...
%                               +(fp(j+1,:)-fp(j,:)))...
%                               -dt*ar*source(j,:);

qv(j,1)=qvo(j,1)-dtdx*((ar*flc(j+1,1)-ar*flc(j,1))...
+(ar*fgc(j+1,1)-ar*fgc(j,1))...

```



```

        +(ar*fp(j+1,1)-ar*fp(j,1)));

qv(j,2)=qvo(j,2)-dtdx*((ar*flc(j+1,2)-ar*flc(j,2))...
        +(ar*fgc(j+1,2)-ar*fgc(j,2))...
        +(ar*fp(j+1,2)-ar*fp(j,2)));

qv(j,3)=qvo(j,3)-dtdx*((ar*flc(j+1,3)-ar*flc(j,3))...
        +(ar*fgc(j+1,3)-ar*fgc(j,3))...
        +(ar*fp(j+1,3)-ar*fp(j,3)))...
        -dt*ar*(fricgrad(j)+hydgrad(j));

if (j==1)&&(wellopening ==1.0)
    if(p(1)<pres)
        if (time>=10) & (time<120)

            qv(1,2) = qv(1,2)+(dt*(JG*(pres-po(1)))*dgstc/dx);
            kickvolume = kickvolume + JG*(po(1)-pres)*dt/dg(1);

        end
    end
end

if (j==1)&&(bullheading==1.0)

    qv(1,1) = qv(1,1)-((1.0)*dt*(J3*(po(1)-pres))*dstc/dx);

end

if (j==1)&&(wellopening==0)
    if p(1)>pres

        qv(1,1) = qv(1,1)-((1.0)*dt*(J4*(po(1)-pres))*dstc/dx);

    end
end

%
sumfric=sumfric+fricgrad(j)*dx;
sumhyd=sumhyd+hydgrad(j)*dx;

end

% Section where we find the physical variables (pressures, densities
etc)
% from the conservative variables. Some trickes to ensure stability.
These
% are induced to avoid negative masses.

qv(:,1)=qv(:,1)./area';
qv(:,2)=qv(:,2)./area';

```

```

    gasmass=0;
    liqmass=0;

    for j=1:nobox

% Remove the area from the conservative variables to find the
% the primitive variables from the conservative ones.

%     qv(j,1)= qv(j,1)/area(j);
%     qv(j,2)= qv(j,2)/area(j);

    if (qv(j,1)<0.00000001)
        qv(j,1)=0.00000001;
    end

    if (qv(j,2)< 0.00000001)
        qv(j,2)=0.00000001;
    end

    gasmass = gasmass+qv(j,2)*area(j)*dx;
    liqmass = liqmass+qv(j,1)*area(j)*dx;

    end % end of fix loop

% Below, we find the primitive variables pressure and densities
% based on
% the conservative variables q1,q2. One can choose between getting
% them by
% analytical or numerical solution approach specified in the
% beginning of
% the program.

    if (analytical == 1)
        % Coefficients:
        a = 1/(al*al);
        b = t1-qv(:,1) '-rt*qv(:,2) '/(al*al);
        c = -1.0*t1*rt*qv(:,2) ' ;

        % Analytical solution:
        p=(-b+sqrt(b.*b-4*a.*c))/(2*a); % Pressure
        dl= (dstc + (p-pstc)/(al*al)); % Density of liquid
        dg = (p/rt); % Density of gas
    else
        % Numerical Solution:
        % [p(j),error]=itsolver(po(j),qv(j,1),qv(j,2)); % Pressure
        % dl(j)=rholiq(p(j)); % Density of liquid
        % dg(j)=rogas(p(j)); % Density of gas
        %
        % % In case a numerical solution is not found, the program will
        write out "error":
        %     if error > 0
        %         error
        %     end
    end

```

```

end

%
%   if (analytical == 1)
%       % Coefficients:
%       a = 1/(al*al);
%       b = t1-qv(j,1)-rt*qv(j,2)/(al*al);
%       c = -1.0*t1*rt*qv(j,2);
%
%       % Analytical solution:
%       p(j)=(-b+sqrt(b*b-4*a*c))/(2*a); % Pressure
%       dl(j)= dstc + (p(j)-pstc)/(al*al); % Density of liquid
%       dg(j) = p(j)/rt; % Density of gas
%   else
%       %Numerical Solution:
%       [p(j),error]=itsolver(po(j),qv(j,1),qv(j,2)); % Pressure
%       dl(j)=rholiq(p(j)); % Density of liquid
%       dg(j)=rogas(p(j)); % Density of gas
%
%       % Incase a numerical solution is not found, the program will
write out "error":
%       if error > 0
%           error
%       end
%   end

% Find the phase volume fractions based on new conservative
variables and
% updated densities.

%   eg(j)= qv(j,2)/dg(j);
%   ev(j)=1-eg(j);

%
%   eg=qv(:,2)'./dg;
%   ev=1-eg;

%   Reset average conservative variables in cells with area changes
inside.

%   qv(j,1)=qv(j,1)*area(j);
%   qv(j,2)=qv(j,2)*area(j);

%
%   qv(:,1)=qv(:,1).*area';
%   qv(:,2)=qv(:,2).*area';

%   The section below is used to find the primitive variables
vg,vl
%   (phase velocities) based on the updated conservative variable
q3 and
%   the slip relation.

% Part where we interpolate in the slip parameters to avoid a
% singularities when approaching one phase gas flow.

```

```
% In the transition to one-phase gas flow, we need to
% have a smooth transition to no-slip conditions.
```

```
gasvol=0;
```

```
for j=1:nobox
```

```
% Implementer cutoff
```

```
%   if (eg(j)<0.03)
%       ktemp = 1.0;
%       stemp = 0;
%   elseif ((eg(j)>=0.03)&(eg(j)<=0.07))
%       xinttemp = (eg(j)-0.03)/0.04;
%       ktemp = xinttemp*k+(1-xinttemp)*1;
%       stemp = xinttemp*s+(1-xinttemp)*0;
%   else
%       ktemp=k;
%       stemp=s;
%   end
```

```
%   if (eg(j)<0.08)
%       ktemp = 1.0;
%       stemp = 0;
%   elseif ((eg(j)>=0.08)&(eg(j)<=0.12))
%       xinttemp = (eg(j)-0.08)/0.04;
%       ktemp = xinttemp*k+(1-xinttemp)*1;
%       stemp = xinttemp*s+(1-xinttemp)*0;
%   else
%       ktemp=k;
%       stemp=s;
%   end
```

```
ktemp=k;
stemp=s;
```

```
k0(j) = ktemp;
s0(j) = stemp;
if ((eg(j)>=0.7) & (eg(j)<=0.8))
    xint = (eg(j)-0.7)/0.1;
    k0(j) = 1.0*xint+k*(1-xint);
%    s0(j) = 0.0*xint+s*(1-xint);
elseif(eg(j)>0.8)
    k0(j)=1.0;
end
```

```
if ((eg(j)>=0.9) & (eg(j)<=1.0))
    xint = (eg(j)-0.9)/0.1;
    s0(j) = 0.0*xint+s*(1-xint);
end
```

```
if (eg(j)>=0.999999)
    k1(j) = 1.0;
    s1(j) = 0.0;
else
    k1(j) = (1-k0(j)*eg(j))/(1-eg(j));
    s1(j) = -1.0*s0(j)*eg(j)/(1-eg(j));
end
```

```
%    k0(j) = k;
%    s0(j) = s;
```

```

%      if ((eg(j)>=0.75) & (eg(j)<=1.0))
%          xint = (eg(j)-0.75)/0.25;
%          k0(j) = 1.0*xint+k*(1-xint);
%          s0(j) = 0.0*xint+s*(1-xint);
%      end
%
%      if (eg(j)>=0.999999)
%          k1(j) = 1.0;
%          s1(j) = 0.0;
%      else
%          k1(j) = (1-k0(j)*eg(j))/(1-eg(j));
%          s1(j) = -1.0*s0(j)*eg(j)/(1-eg(j));
%      end

```

```

%      k0(j) = k;
%      s0(j) = s;
%      if ((eg(j)>=0.7) & (eg(j)<=0.8))
%          xint = (eg(j)-0.7)/0.1;
%          k0(j) = 1.0*xint+k*(1-xint);
%      %      s0(j) = 0.0*xint+s*(1-xint);
%      end
%
%      if (eg(j)>=0.999999)
%          k1(j) = 1.0;
%          s1(j) = 0.0;
%      else
%          k1(j) = (1-k0(j)*eg(j))/(1-eg(j));
%          s1(j) = -1.0*s0(j)*eg(j)/(1-eg(j));
%      end

```

```

gasvol=gasvol+eg(j)*area(j)*dx;

```

```

end

```

```

%      Below we operate with gas vg and liquid vl velocities
specified
%      both in the right part and left part inside a box. (since we
have
%      area changes inside a box these can be different. vgl is gas
velocity
%      to the left of the disconinuity. vgr is gas velocity to the
right of
%      the discontinuity.
%

```

```

%      help1 = dl(j)*ev(j)*k1+dg(j)*eg(j)*k0;
%      help2 = dl(j)*ev(j)*s1+dg(j)*eg(j)*s0;
%
%      vmixhelp1 = (qv(j,3)/area(j)-help2)/help1;
%      vg(j)=k0*vmixhelp1+s0;
%      vl(j)=k1*vmixhelp1+s1;

```

```

help1 = dl.*ev.*k1+dg.*eg.*k0;

```

```

help2 = dl.*ev.*s1+dg.*eg.*s0;

vmixhelp1 = (qv(:,3)'./area-help2)./help1;
vg=k0.*vmixhelp1+s0;
vl=k1.*vmixhelp1+s1;

% Old values are now set equal to new values in order to prepare
% computation of next time level.

%   for j = 1:nobox
%       po(j)=p(j);
%       dlo(j)=dl(j); %Liquid density
%       dgo(j)=dg(j); %Gas density
%       vlo(j)=vl(j); %Liquid velocity
%       vgo(j)=vg(j); %Gas velocity
%       ego(j)=eg(j); %Gas fration
%       evo(j)=ev(j); %Liquid fraction.
%
%
%       for m =1:3
%           qvo(j,m)=qv(j,m);
%       end
%   end

po=p;
dlo=dl;
dgo=dg;
vlo=vl;
vgo=vg;
ego=eg;
evo=ev;
qvo=qv;

% Section where we save some timedependent variables in arrays.
% e.g. the bottomhole pressure. They will be saved for certain
% timeintervalls defined in the start of the program in order to
ensure
% that the arrays do not get to long!

if (counter>=nostepsbeforesavingtimedata)
    printcounter=printcounter+1;
    time
    pbot(printcounter)= p(1);
    pchoke(printcounter)=p(nobox);
    pcasingshoe(printcounter)=p(25); %NB THIS MUST BE DEFINED IN
CORRECT BOX

```

```

liquidmassrateout(printcounter)=dl(nobox)*ev(nobox)*vl(nobox)*area(nobox);

gasmassrateout(printcounter)=dg(nobox)*eg(nobox)*vg(nobox)*area(nobox);
hyd(printcounter)=sumhyd/100000;
fric(printcounter)=sumfric/100000;
volgas(printcounter)=gasvol;
massgas(printcounter)=gasmass;
massliq(printcounter)=liqmass;
pout(printcounter)=p(nobox)-0.5*dx*...
(dlo(nobox)*evo(nobox)+dgo(nobox)*ego(nobox))*g-
dx*0.5*fricgrad(nobox);
pin(printcounter)=
p(1)+0.5*dx*(dlo(1)*evo(1)+dgo(1)*ego(1))*g+0.5*dx*fricgrad(1);
timeplot(printcounter)=time;

massrate(printcounter) = dl(nobox-2)*ev(nobox-2)*vl(nobox-2)*area(nobox-2);

counter = 0;

end
end

% end of stepping forward in time.

% Printing of resultssection

countsteps % Marks number of simulation steps.

% Plot commands for variables vs time. The commands can also
% be copied to command screen where program is run for plotting
other
% variables.

toc,
e = cputime-t
plot(timeplot,pbot/100000)

disp('cfl')
cfl = al*dt/dx

%plot(timeplot,pchoke/100000)
%plot(timeplot,liquidmassrateout)
%plot(timeplot,gasmassrateout)
%plot(vg)

%Plot commands for variables vs depth/Only the last simulated
%values/endtime is visualised

```

```
%plot(vl,x);  
%plot(vg,x);  
%plot(eg,x);  
%plot(p,x);  
%plot(dl,x);  
%plot(dg,x);
```